University of Southern Queensland

Faculty of Health, Engineering and Sciences

Design and Analysis of a Wearable Arduino IOT Health Monitoring Device for Mining Workers

A dissertation submitted by

Joshua Naumann

In the fulfilment of

ENG4111 & ENG4112 Research Project

Towards the degree of

Bachelor of Engineering (Honours) (Mechatronics)

Submitted October 2023

Abstract

Mining workers experience harsh environmental conditions during their working shifts which impacts the health and safety of the workforce. Due to the high risks involved coupled with poor safety measure execution, many existing and future employees are opting out of this line of work creating an inaccessibility issue for employers (Porselvi et al., 2021). Traditional health monitoring methods have been proven to be difficult to install and challenging to power due to the dynamic changing environment and busy operations (Rudrawar et al., 2022).

A review of the current literature was performed to find the current development surrounding health monitoring systems in the mining space. From the review, it was found that health monitoring systems have been designed in the past, however, minimal experimentation has been conducted to determine the effects of harsh environmental conditions on the system and systems that are wearable are marginal.

Potential options for the sensor selection and battery setup were explored and then analysed to turn the concept design into a prototype. The methodology consisted of conducting several experiments on the prototyped design to determine the effects of high temperature, high humidity, and varying dust concentrations on the sensor readings. The sensor readings were also compared to commercial-grade sensor readings to determine the accuracy of the prototype system.

The project found that the prototype performs well under high temperature and high humidity conditions, however, is affected by high concentrations of dust. The developed health monitoring device has potential as an early warning detection system. However, if a high precision of accuracy is required, the system would provide inadequate output for such a purpose.

University of Southern Queensland

Faculty of Health, Engineering and Sciences

ENG4111 & ENG4112 Research Project

Limitations of Use

The Council of the University of Southern Queensland, its Faculty of Health, Engineering and Sciences, and the staff of the University of Southern Queensland do not accept any responsibility for the truth, accuracy or completeness of material contained within or associated with this dissertation.

Persons using all or any part of this material do so at their own risk, and not at the risk of the Council of the University of Southern Queensland, its Faculty of Health, Engineering and Sciences or the staff of the University of Southern Queensland.

This dissertation reports an educational exercise and has no purpose or validity beyond this exercise. The sole purpose of the course pair entitled "Research Project" is to contribute to the overall education within the student's chosen degree program. This document, the associated hardware, software, drawings, and any other material set out in the associated appendices should not be used for any other purpose: if they are so used, it is entirely at the risk of the user.

Certification

I certify that the ideas, designs and experimental work, results, analyses, and conclusions set out in this dissertation are entirely my own effort, except where otherwise indicated and acknowledged.

I further certify that the work is original and has not been previously submitted for assessment in any other course or institution, except where specifically stated.

Joshua Naumann

Table of Contents

Chapter 1 – Introduction

1.1 Background

The Australian mining industry contributes to a large portion of economic gain through exporting and is continually growing and expanding to the current day. Australia is the fourth largest coal producer in the world with Queensland being the primary coal mining state (Cortes-Ramirez et al., 2022). The mining sector is responsible for a significant contribution to the Australian workforce and the issue around health and safety is a concern that must be addressed.

Workers in the mines, particularly underground mines, experience a range of environmental condition changes consisting of but not limited to exposure to toxic gases, temperature change and fire incidents. The safety risks experienced by employees increase as the distance from the ground level increases. These risks arise from the nature and process of extracting materials from the mining sites. Due to the high risks involved coupled with poor safety measure execution, many existing and future employees are opting out of this line of work creating an inaccessibility issue for employers (Porselvi et al., 2021).

Safety detection plays a very major role in the safety and efficacy of mining situations where workers are exposed to harsh environmental conditions. The ability to detect changes in conditions such as airborne contaminants, gas outbursts, temperature and humidity is important as they may cause serious harm to people working in these environments.

1.2 IoT Smart Technology

“The Internet of Things (IoT) is often referred to as a collection of objects connected to the Internet using wireless networks,” (The Arduino Team, 2023). These objects have the task of collecting and exchanging information from their surroundings by enabling a connection between the physical and digital worlds (The Arduino Team, 2023). IoT devices often called “smart” devices work by machine-to-machine (M2M) communication across other related devices apart of the network.

In the past, Cable Monitoring Systems (CMS) technology has been used for the monitoring of mining workers' health. This solution is highly costly due to the required layout of cables and potential damage from human and environmental conditions. CMS has high power and time consumption due to the structure of the system (Maheswari et al., 2019). Traditional monitoring systems for mining operations are challenging to power and difficult to install due to the dynamic changing environment and busy operations (Rudrawar et al., 2022). Monitoring the position and health parameters of workers deep in the mines is important to increase the efficiency of the operation and hold safety protocols to a high standard.

Manual methods used to monitor and analyse environmental conditions are difficult due to the frequent dynamic changes and wide range of parameters to monitor. Fortunately, this job can be achieved using wireless communication devices and complementary electronic units. The adoption of smart technology within mining scenarios is minimal due to the technology application being relatively new. Although the technology is being used within some companies, the experimental data from testing is lacking and should be investigated. The need for smart technology implementation in mining sites is high and will streamline the process creating a more manageable and safer environment.

With the advancement in smart technology over the years, a system may be designed and implemented to address these issues beneficially. Arduino is an open-source, C programming language-based electronics platform that integrates software and hardware. The Arduino platform is an inexpensive, cross-platform method that can be utilised to perform various tasks based on inputs and outputs (The Arduino Team, 2018).

1.3 Wearable Devices

Recently there has been a considerable increase in the wearable technology consumer market and has proven significant in many different industries. Studies relating to the construction industry have been conducted along the lines of health and safety monitoring with the use of proximity detection and physiological monitoring of workers in the field to combat issues in the line of work (Mardonova & Choi, 2018). In some cases, wearable technology has been used recently to assist in environmental quality monitoring in industrial mines, coal mines and process control in hard rock mines. An intelligent piece of technology was created to warn employees in underground coal mines about the level of hazardous gases with the use of sensors (Mardonova & Choi, 2018). However, there has been limited research into the experimental data and testing of the supposed systems in the harsh environments of working practice.

1.4 Project Brief

The idea for the project came from researching the importance of health monitoring in underground mining scenarios where the safety of workers is at the most risk and the environmental conditions are unforgiving. A problem faced by the mining industry is the ability to monitor health parameters in real-time with a cost-effective method without infringing on performance. By designing and creating a system capable of doing so, accidents and health risks may be mitigated.

The project investigates and proposes a design for a smart technology device used to monitor mining workers' health under harsh conditions. The process to achieve this resulted in the selection of various electronic components and supporting software to collect and analyse data to provide an understanding of the efficiency and usefulness of the device under mining conditions.

1.5 Research Objectives

To successfully fulfil the project outcome, several objectives must be completed to ensure the project is progressing through the processes mentioned in the project timeline.

These objectives are:

1. Research the issues in mining scenarios regarding effects on health and safety.
2. Conduct a literature review on existing technologies used to monitor health parameters.
3. Review the required electronic components for the system and the programming integration.
4. Conduct experimental testing of the sensors and gather data based on the results.
5. Conceptualise potential designs that incorporate all required components.
6. Design a prototype based on the most viable design.
7. Conduct testing under mining conditions and constraints.
8. Determine the effects of different mining conditions on the performance of the system such as dust and varying humidity and temperature ranges.
9. Analyse gathered data based on the testing and compare it against the theoretical results.
10. Adjust and modify the design based on results.
11. Draw conclusions based on the data concerning efficacy and practicality.

Chapter 2 – Literature Review

2.1 Chapter Overview

This literature review consists of information relating to the monitoring of health parameters in mining scenarios, identifies the knowledge gap within the experimental side and challenges addressed by the technology.

2.2 Dangerous Gases and Exposure Standards

The safety of mining workers poses a significant challenge due to the nature of the activities conducted under harsh conditions. Air contamination poses a major threat to a labourer in a mining situation due to the geological area most commonly being confined with minimal to zero airflow. This causes an issue as the emission particulate matter fails to dissipate and disperse, therefore building up and becoming a combustible, toxic threat (Porselvi et al., 2021). The most common gases found in underground mining areas are CH4, CO2, CO, NO2, H2S and SO2 (Jo & Khan, 2018). These gases either pose a direct toxic threat or a combustible threat to worker's health. The exposure standards for these chemicals are measured in parts per million (ppm) at time-weighted average (TWA) and short-term exposure (STEL).

- TWA: Concentration levels over an 8-hour working day
- STEL: Concentration levels averaged over a period of 15 minutes

2.2.1 *Methane*

Methane (CH4) is a flammable, colourless, non-toxic gas with no odour in its pure state. CH4 is found in varying levels in coal deposits as natural gas and causes asphyxiating due to the displacement of oxygen from the air. Oxygen deficiency can cause headaches, dizziness and nausea and is lethal when the concentration falls below 6%. Methane mixtures ranging from 5% to 15.4% are flammable with the range of 9.46% being the most explosive (Queensland Department of Natural Resources and Mines, 2020). “Under the Coal Mine Safety and Health Act 1999 and the Coal Mining Safety and Health Regulation 2017, if methane concentration is equal to or greater than 2.5% then the underground mine is dangerous and workers must be withdrawn from the mine,” (Department of Natural Resources, Mines and Energy, 2019).

A document by (the Queensland Government, Department of Natural Resources, Mines and Energy, 2019), contains information on methane management in coal mines. The document states that "In February 2017 the Chief Inspector of Mines issued a letter to all underground site senior executives (SSEs) and underground mine managers (UMMs) advising them that if a roadway in a mine contains an atmosphere where the methane concentration is equal to or greater than 2.5% it is taken to be dangerous under section 366 of the Coal Mining Safety and Health Regulation 2017. If this occurs, coal mine workers must be withdrawn to a place of safety under section 273 of the Coal Mining Safety and Health Act 1999." By using this information, the short-term exposure limits can be derived to 2.5% (25000 ppm).

2.2.2 Carbon Dioxide

Carbon dioxide (CO_2) is a colourless gas and at low concentrations acts as a central nervous (CNS) and respiratory system stimulant. However, at high concentrations, the gas depresses the CNS and can cause narcosis and unconsciousness.

The current exposure standards are:

- TWA of 12500ppm (in coal mines)
- TWA of 5000ppm (in all other industrial applications)
- STEL of 30000ppm (in all applications).

(Queensland Department of Natural Resources and Mines, 2020)

2.2.3 Carbon Monoxide

Carbon monoxide (CO) is a tasteless, colourless, odourless gas with a flammable limit in the air of 12.5% to 74% with the most explosive concentration being 29%. Due to the inability to detect CO by taste or smell, this gas is the most dangerous gas found in coal mines. When exposed to CO, the body absorbs the gas into the bloodstream and prevents oxygen transportation to the required organs and cells resulting in death at prolonged exposure times.

The current exposure standards are:

- TWA of 30ppm
- There is no STEL or peak limitation specified for carbon monoxide.

(Queensland Department of Natural Resources and Mines, 2020)

2.2.4 *Nitrogen Dioxide*

Nitrogen dioxide (NO2) is an oxide of nitrogen with an acrid smell and acidic taste. The gas is non-flammable and incombustible but acts as a support to combustion. NO is produced by diesel exhaust because of detonation and explosive burning. The gas is highly poisonous and irritating to the respiratory system. The symptoms from inhalation typically arise several hours later rather than immediately. Concentrations of 100 ppm can severely irate the respiratory system and concentrations of 200 ppm breathed for minutes are life-threatening.

The current exposure standards are:

- TWA of 3ppm
- STEL of 5ppm

(Queensland Department of Natural Resources and Mines, 2020)

2.2.5 *Hydrogen Sulphide*

Hydrogen Sulphide (H2S) is a colourless gas with a pungent odour detectable by smell as low as 1ppm. Due to the nasal sensitivity decreasing with exposure, the ability to detect the gas using this method is unreliable. H2S is highly toxic and irritates the ayes and mucous membranes with a narcotic effect on the CNS. The resulting symptoms are dizziness, headaches and in acute doses produce an absence of oxygen in arterial blood and tissue. An exposure concentration of 500ppm can be fatal and paralysis occurs at higher levels of 1000ppm.

The current exposure standards are:

- TWA of 10ppm
- STEL of 15ppm

(Queensland Department of Natural Resources and Mines, 2020)

2.2.6 *Sulphur Dioxide*

Sulphur dioxide (S02) is a reactive, colourless gas with a strong odour and is a common combustion product in the process of burning oil and coal (Jain et al., 2016). Exposure to S02 irritates the eyes and dysfunction of the respiratory system. This increases the risk of tract infections and causes mucus secretion and coughing, leading to the possibility of lung infections such as bronchitis (Queensland, 2017).

S02 is measurable by using portable gas detectors with an electrochemical cell and Concentrations of SO2 greater than 500ppm are dangerous to health and life after short exposures.

The current exposure standards are:

- TWA of 2ppm
- STEL of 5ppm

(Queensland Department of Natural Resources and Mines, 2020)

Gas	Methane (CH4)	Carbon Dioxide (CO2)	Carbon Monoxide (MO)	Nitrogen Dioxide (NO2)	Hydrogen Sulphide (H2S)	Sulphur Dioxide (SO2)
TWA (ppm)	-	12500	30	3	10	2
STEL (ppm)	25000	30000	-	5	5	5

Table 1: Exposure standards for dangerous gases in coal mines

2.3 Communications

The problem with using multiple sensors and acquiring data simultaneously is due to the difficulty of connecting to an external network. This is especially true in underground mining scenarios where the connection to existing networks isn't feasible. Therefore, to ensure the data is tracked accurately, the sensors must be paired with a capable communication system (Lee et al., 2022). Communication between workers and the host to transfer monitored data and the location is a critical part of ensuring a safe environment to conduct work. For mining sites on the surface, GNSS/GPS is the preferred technology that provides the most accurate data. Due to the nature of sub-surface mines, GNSS/GPS tracking methods are incapable due to the needed direct line of site with GPS satellites. However, existing technologies provide the capability of tracking through Wi-Fi, Bluetooth, and Radio Frequency Identification (RFID).

2.3.1 Bluetooth and Wi-Fi

Bluetooth is a short-range technology with a range of up to 10m with a low power consumption. Recently the developed Bluetooth 5.0 is capable of up to a range of 40m with a transmission speed of 2 Mbps. Due to the range constraints, Bluetooth in mining for communication isn't optimal as the range required for mining is much higher (Lee et al., 2022). Bluetooth Low Energy (BLE) provides a different performance metric over classic Bluetooth systems by allowing a lower energy consumption contributing to a higher battery life. This benefit comes at the cost of data transfer where BLE is used for low amounts of data transfer (Proctor, 2021). Wi-Fi is useful for monitoring health parameters and communicating to a home base as the communication range is widespread and the data transmission speed is fast. Although this is the case, the cost to implement routers to build

Wi-Fi networks is extensive and isn't optimal for a small company without the financial backing and support (Lee et al., 2022)

2.3.1.1 *ESP8266 Node MCU*

The ESP8266 designed by Espressif systems allows for microcontroller connectivity to the Wi-Fi network using universal asynchronous receiver/transmitter (UART) or Serial Peripheral Interference (SPI). The module is also capable of working as a standalone application without the need for a microcontroller host. The ESP8266 contains elements of the modern computer such as CPU, RAM, networking (Wi-Fi) and an operating system (OS) (Sai Phani Gopal et al., 2019). The microchip module operates at 80 mA (Table 2) and features a deep sleep mode which consumes 60 mA and is useful for prolonging battery life when in minimal use These specifications make the module an optimal choice for communication of a health monitoring system.

Table 1-1. Specifications

Categories	Items	Parameters
Wi-Fi	Certification	Wi-Fi Alliance
	Protocols	802.11 b/g/n (HT20)
	Frequency Range	2.4 GHz ~ 2.5 GHz (2400 MHz ~ 2483.5 MHz)
	TX Power	802.11 b: +20 dBm
		802.11 g: +17 dBm
		802.11 n: +14 dBm
	Rx Sensitivity	802.11 b: –91 dbm (11 Mbps)
		802.11 g: –75 dbm (54 Mbps)
		802.11 n: –72 dbm (MCS7)
	Antenna	PCB Trace, External, IPEX Connector, Ceramic Chip
Hardware	CPU	Tensilica L106 32-bit processor
	Peripheral Interface	UART/SDIO/SPI/I2C/I2S/IR Remote Control
		GPIO/ADC/PWM/LED Light & Button
	Operating Voltage	2.5 V ~ 3.6 V
	Operating Current	Average value: 80 mA
	Operating Temperature Range	–40 °C ~ 125 °C
	Package Size	QFN32-pin (5 mm x 5 mm)
	External Interface	-
Software	Wi-Fi Mode	Station/SoftAP/SoftAP+Station
	Security	WPA/WPA2
	Encryption	WEP/TKIP/AES
	Firmware Upgrade	UART Download / OTA (via network)
	Software Development	Supports Cloud Server Development / Firmware and SDK for fast on-chip programming
	Network Protocols	IPv4, TCP/UDP/HTTP
	User Configuration	AT Instruction Set, Cloud Server, Android/iOS App

Table 2: Specifications of the ESP8266 Node MCU by Espressif Systems (Espressif Systems, 2023)

2.3.1.2 *Radio Frequency Identification (RFID)*

RFID is a short-range wireless technology that uses radio waves to communicate to a host station. An RFID system utilises RFID tags comprised of small electronic circuitry that store a specific set of data that are read by a reader and transmitted to a host station. There are 2 types of tags used: passive tags and active tags. The difference in performance relates to the signal range where active tags are capable of 100m and passive 6-8 metres (Ashutosh Patri et al., 2013). A key advantage of RFID is the ability of the signal to penetrate many obstacles without losing the signal strength required to transmit data. The power required by the process is also low, ranging from a few milliwatts to a few watts depending on operation frequency. This gives the option to provide a long battery life of 3-5 years and potentially a battery-free system depending on the signal range needed due to the correlation between higher frequency and higher required power (Smiley, 2019).

2.3.1.3 *Zigbee*

Zigbee is a low-cost, low-power wireless technology that enables communication to IoT and Machine to Machine networks (Rosencrance, 2017). In contrast to Wi-Fi, Zigbee has the advantage of a single node being connected to 255 devices and capable of extending to 65000 devices (Table 2). The technology is built for control and sensor networks and is highly applicable in a mining environment. The ability to consume little power over a few years with a small-capacity battery puts Zigbee in a strong position to be utilised in a worker monitoring situation.

Wireless Technical Standards	ZigBee/802.15.4	Bluetooth	Wi-Fi	GSM [1]/GPRS [2]
System resource requirements	4 KB–32 KB	>250 KB	>1 MB	>16 MB
Power waste	Low	Common	Common	High
Battery life (days)	100–1000+	1–7	1–5	1–7
Number of nodes in local network	65,000+	7	30	1000+
Data rate (Kbps)	20–250	1000	11,000+	64–128
Communication distance	1–3200	1–10+	1–100	1000+
Advantage	Reliability, low cost, low power consumption	Low cost and easy to operate	High speed and adaptability	Good transmission quality and large coverage range
Applications	Wireless detection and control	Short-distance data transmission	A lot of data transmissions such as Web access and video.	Voice and data transmission

[1] GSM: global system for mobile communications. [2] GPRS: general packet radio service.

Table 3: Comparison of wireless communication technologies (Lee et al., 2022)

A Zigbee network is comprised of modes configured as coordinators, routers, or end nodes. The coordinator node is responsible for allowing other nodes to connect to the network as a gateway. Every node in the network can receive data from the coordinator and their configurations can be changed using over-the-air programming (OTA). The data is routed from the coordinator to the end node by the router node and vice-versa. The function of the end nodes is to acquire data generally from sensors from the surroundings. In the application of a health monitoring system, the end nodes would have the required sensors equipped to obtain the needed measurements (Haque et al., 2022). The Wireless sensor network (WSN) can be configured in different topologies depending on the needed application. For instance, adding multiple routers as part of a mesh can increase the overall range of the system by the number of modules present and the distance apart (Appendix 1).

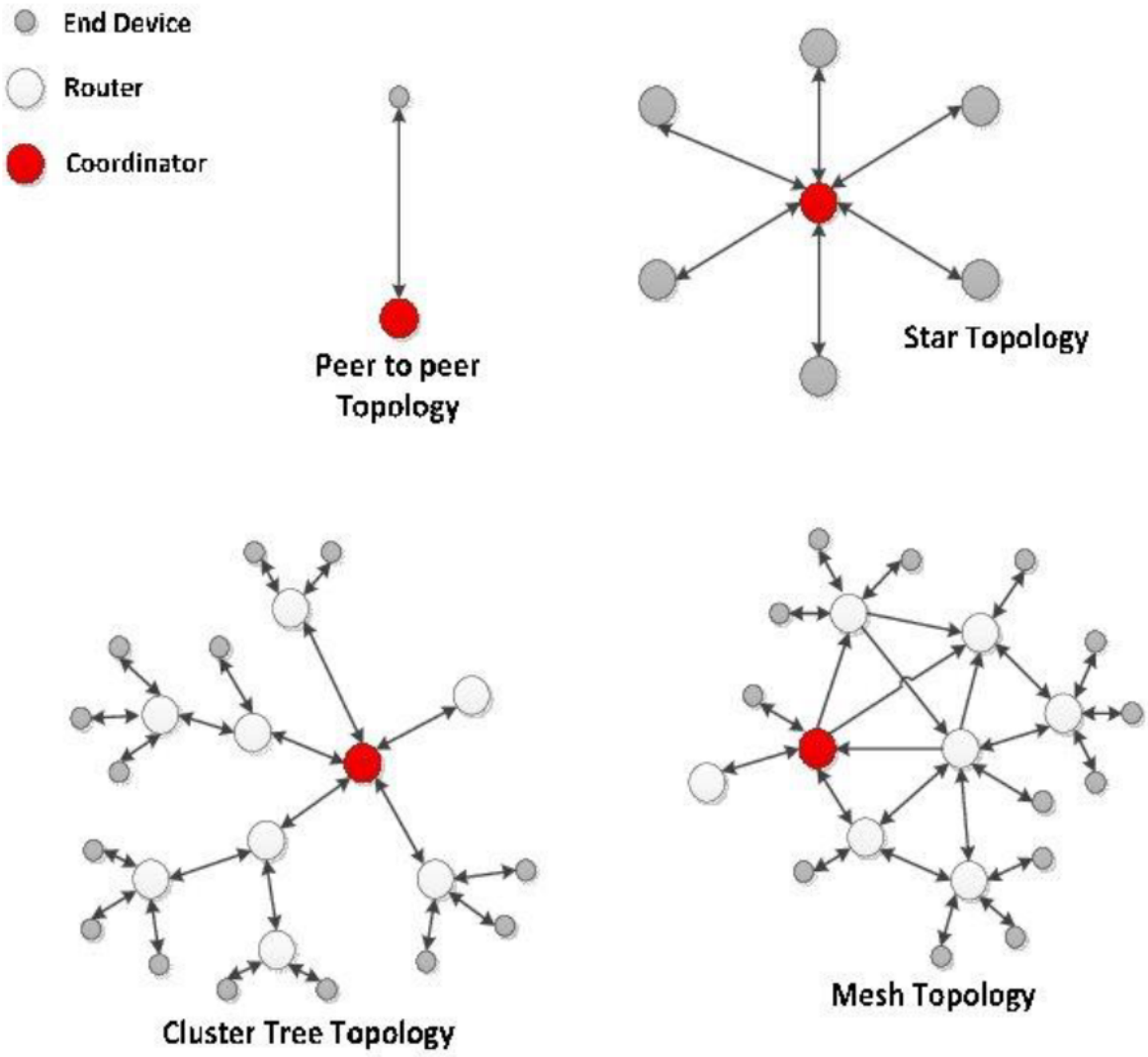

Appendix 1: Classification of ZigBee topology (Buthelezi et al., 2018)

2.4 Existing Arduino Monitoring Systems

Recently, the Arduino platform has been adopted for use in many different monitoring and control applications. Specifically, In the mining industry in the divisions of autonomous system control, geotechnical, environmental and health monitoring applications Arduino systems have been used.

2.4.1 Arduino Field Monitoring Systems

A case study by (Jo & Khan, 2018) investigated the use of IoT for underground coal mines in the use of an event reporting and early warning safety system. The author used principal component analysis (PCA) to identify the most common gases found in the underground Shangwan coal mine in China. The investigation used the following sensors: DHT11, MQ4, MQ9, MG811, MQ136, and MiCs2714, connected to an Arduino UNO board and communicated using a ZigBee module to the Azure machine learning (AML) platform (Appendix 2). The results were used as part of an artificial neural network to predict future air pollution and compared to the exposure standards and a developed "Mine Warning Index" contingency table. The testing of the effectiveness of the proposed system proved suitable with an accuracy of more than 95% efficiency using the system. However, some limitations of the system were found involving the harsh environmental conditions of underground mines and the integration of multi-sensor outputs and were to be further investigated.

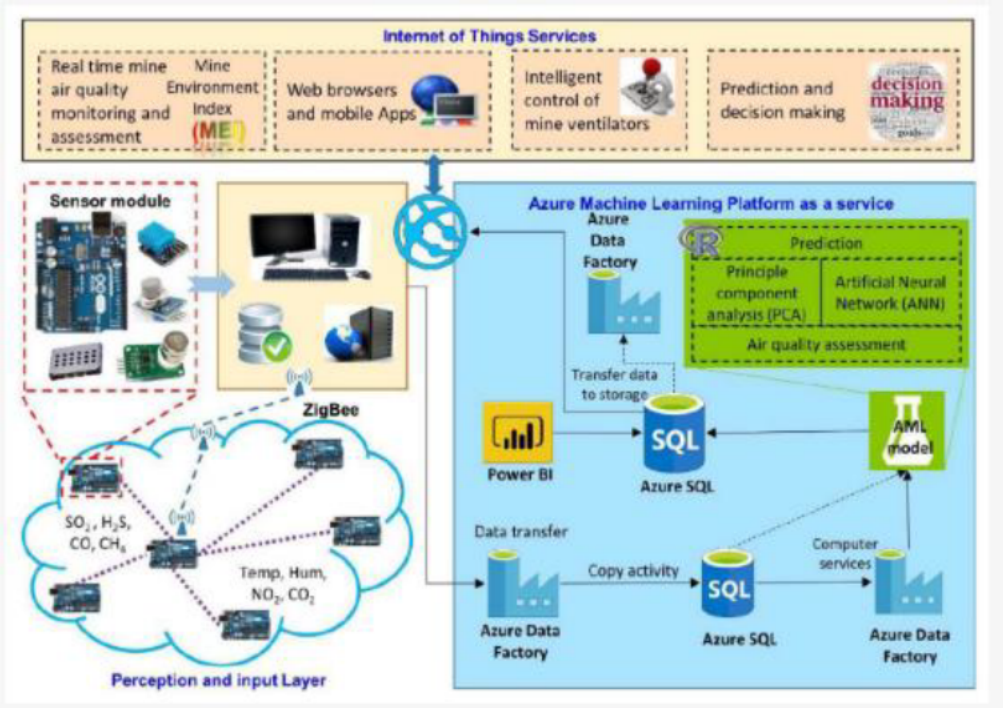

Appendix 2: System Architecture comprising Arduino as a microcontroller for air quality monitoring in mines, based on Azure Machine Learning (AML), for air quality prediction (Jo & Khan, 2018).

Another study by (Jo & Khan, 2017) established a system to track miner position and monitor gas for the Hassan Kishore coal mine in Punjab, Pakistan. The system consisted of an Arduino Mega with a BLE shield for communication and sensors DTH11, MQ135, MQ9, and MQ4. The system was capable of monitoring temperature, humidity, CO, CO2 and CH4 and uploading to the cloud (Appendix 3). The Data was relayed through router nodes connected to a base station capable of internet connection. By doing so the miner was able to send an emergency signal to the base station with the location being acquired. The previous safety system in the mine was a simple telephone communication between surface and underground stations with a manual entry of mining accidents.

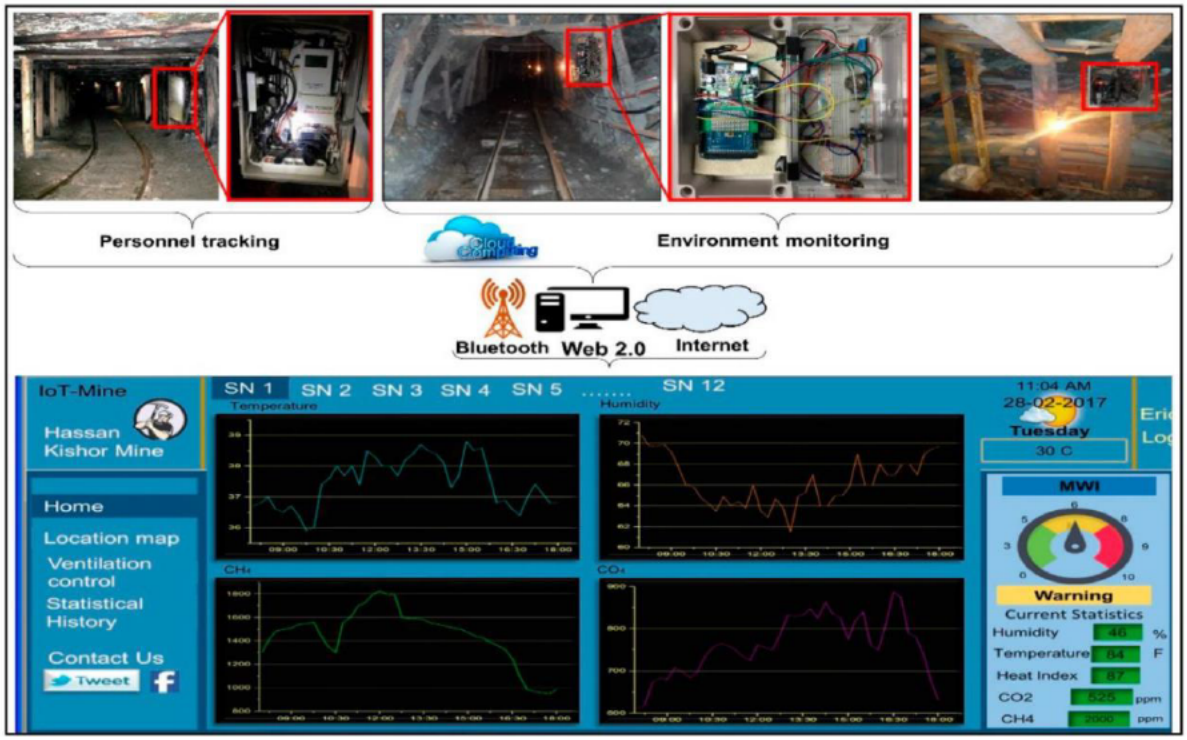

Appendix 3: An early warning IoT System for the Hassan Kishor Mine (Jo & Khan, 2017).

The system was tested in the underground mine by placing several nodes across different areas of the mine. A major challenge encountered was the topology management of the network due to the uneven and irregular mine openings and bends/curves. The experiment found the optimum topology of the BLE node network was 17m and was determined through repetitive hit and trial methods. The temperature, humidity, CH4 and CO2 were taken at two locations within the mine, the mine face and midway using the Arduino system. The measurements at these points were also taken by using the Fluke CO-220 for CO2 measurement, HOBO U12-012 fir temperature and humidity measurement and the Telaire7000 for CH4 measurement. The results of the Arduino system were then compared against the commercial instruments to find the accuracy of the system (Appendix 4). From the graph, the observed results for CO, temperature, and humidity result in a standard error of <5% which is fairly accurate whereas the results of CH4 and CO2 are much higher.

The paper concluded that the experiment was a success with accuracies of detection of 95% to 99% and provided a safer environment for the mining workers compared to the previous safety management system. The staff of the mine were interviewed after the implementation of the system and showed positive responses on the benefits of the system and a significant decrease in mining accidents. However, a few challenges were holding back the system from full implementation involving the impacts of harsh environmental conditions on the system and autonomous sensing capabilities.

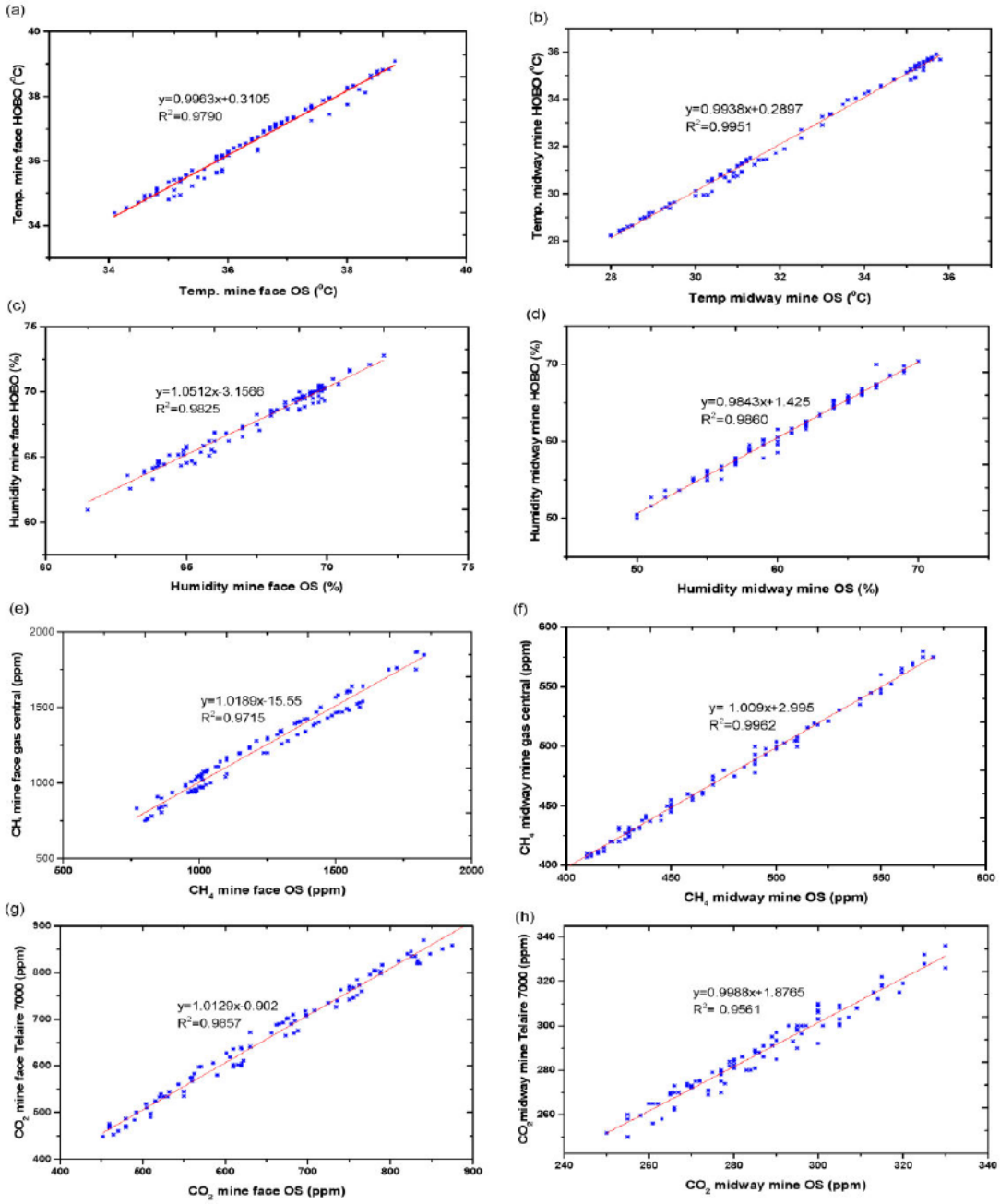

Appendix 4: (**a**) Correlation between readings of temperature at mine face 1 by our system and HOBO U12-012; (**b**) correlation of temperature readings at midway mine between our system and HOBO U12-012; (**c**) correlation of humidity at mine face 1 between our system and HOBO U12-012; (**d**) correlation of humidity at midway mine between our system and HOBO U12-012; (**e**) correlation at mine face 1 between CH_4 concentrations provided by our system and Telaire 7000; (**f**) correlation at midway mine between CH_4 concentrations provided by our system and Telaire 7000; (**g**) correlation of CO_2 concentrations at mine face 1 between our system and Fluke CO-220; (**h**) correlation of CO_2 concentrations at mine face 1 between our system and Fluke CO-220. (Jo & Khan, 2017)

2.4.2 Arduino Heart Rate Monitoring System

Underground mine fires are difficult to put out once they've been ignited due to the combustible materials and gases present in critical spots. These spots combined with the humidity levels and air pressure variations can impact the working environment and compromise equipment operation leading to downtime. The ability to detect fires in underground mining sites is a crucial part of ensuring miner's health and safety (Fire detection for underground mining, 2021). The combination of heat, smoke and flame measuring capabilities may be used to detect a fire. Due to the smoke detection capacity of the MQ-2 gas sensor, a sensor to detect a flame can be partnered with the sensor to develop a system to alert mining workers of a fire hazard.

1. (Anitha & Seshagiri, 2019) Developed a monitoring system based on the use of Zigbee communication protocol partnered with an LM35 temperature sensor, an MQ6 gas detection sensor and a fire detection sensor capable of detection within 1m. The measure values were relayed and displaced on a liquid crystal display to alert the user of the results and sound a buzzer if the data reached a specific threshold. The applicability of this system was unknown as the experimentation wasn't conducted under mining circumstances.

In this example, the MQ-6 sensor is used to primarily detect natural gas with the addition of Propane, Butane and LPG. The flame sensor is the detection solution for fire but cannot detect smoke. Therefore, a pairing of the flame sensor with a smoke measuring sensor such as the MQ-2 sensor would be suitable for creating a more robust system in the case of a fire hazard within the mining area.

2.4.3 Arduino Wearable Monitoring Systems

1. (Viswasmayee et al., 2018) created a real-time heart rate monitoring equipment for coal miners using LabVIEW. They linked an AD8232 ECG sensor to an Arduino UNO board with an ATmega328 processor to examine the heart's electrical activity. The electrocardiogram (ECG) sensor pad was connected to a human body part, such as the wrist or elbow, and it monitored the biopotentials generated by the heart. Using LabVIEW software, the system tracked the workers' heart rates and examined their health. With the use of LabVIEW, the raw signal was sampled and filtered therefore reducing the hardware requirement The study's data was collected, processed, and sent using LabVIEW as an integration platform. The control station's authorities had the option to always keep an eye on the analysed data. A website would quickly appear if a worker was suffocating due to an unusual mining environment. The paper states that the developed system has fast execution speed and the AD8232 is efficient in sensing the electrical behaviour of the heart however minimal evidence is provided.

2. another study by (Richa et al., 2021), developed a health care monitoring system for patients during the COVID-19 epidemic. The system comprised of an Arduino Uno collected real-time health data from a pulse sensor and a temperature sensor to measure the heart rate and temperature of the patient's body. The data was relayed from the machine to the internet using an ESP8266 IoT module for data storage and monitoring. The paper concluded as a success and mentioned that the device may be integrated with computer computing to share information across intensive care and treatment hospitals.

3. (Maheswari et al., 2019) developed a system an advanced communication device based on the nRF24L01 transceiver to transmit and receive data run from an Arduino Mega and Uno. The system was comprised of two parts, the transmitter side, and the receiver side and were communicated using the SPI protocol. The system was paired with a heart rate sensor, water sensor, gas sensor and an LM35 temperature sensor, however, the models and types of sensors weren't given. The system featured the use of a GSM module to transfer data and alerts to a mobile device when a specific threshold was exceeded (Appendix 5). Two LCD screens were equipped on the transmitting and receiving side of the system to display the parameters measured and warning signals from the output of the sensors (Appendix 6). The paper concluded by claiming the wireless sensor network (WSN) had better perceptive function over a wired network however the only evidence that was given was in the format of photos, and no testing was conducted on the performance of the system under mining environment circumstances.

Appendix 5: Output to mobile using GSM module, (Maheswari et al., 2019).

Appendix 6: Output of LCD based on sensor readings for receiving side (Left) and transmitting side (Right), (Maheswari et al., 2019).

2.4.4 An Investigation of Battery Life of Arduino System

The battery life of a health monitoring system is an important factor in the design as the working life of each sensor node depends on the battery lifespan. The power consumption of the circuitry and battery type selection play key roles in the efficacy of the system over large periods. The selection of battery type and arrangement should be able to operate at low and high temperatures, store high power and be resistant to voltage changes (Unsal et al., 2016). The analyse of battery life when a connection of MQ4, MQ7, MQ9 and DHT22 were connected to an Arduino UNO was conducted by (Unsal et al., 2016) The outcome of this experiment was to propose a method for optimising the battery life for the largest possible lifespan of the system. The study explored the use of different sensors to measure H_2, N_2 and CH_4 gases through the wireless use of a Wi-Fi module node MCU ESP8266.

The study found that the selection of Lithium and metal hydride batteries was the most suitable for mining applications due to the high voltage (3.6V) and high energy storage capabilities. The lifespan of the system was increased by utilising the different state options for the communication module and reducing the sampling frequency to lower the energy consumption when data transmission isn't occurring.

2.5 Arduino Microcontrollers

Arduino is an opensource electronics platform featuring a microcontroller and a circuit board that is programmable in the C language. The Arduino is capable of converting input data to a specific output desired by the function of the board. The software itself is versatile and can be run on Windows, Macintosh, OSX and Linux and is inexpensive compared to other microcontrollers of the same calibre. Due to the extensibility of the package, researchers have constructed low-cost devices suited to their needs (Kim et al., 2020). The microcontrollers can control physical functions using electrical components such as actuators. The selection of Arduino boards ranges from Entry level boards such as the most common Arduino Uno and Arduino Nano to more advanced boards that provide faster performance and higher functionality. The optimal selection of the board revolves around the required function for inputs, outputs, and processing power.

Through research of different Arduino boards and their applications, it was found that the Arduino Uno, Arduino Nano and the Arduino Mega were the most popularly used (Appendix 7). The Arduino Uno was the most used board is powered by the ATmega328 processor and is compatible with most development board shields. The Arduino Mega is powered by the Atmega2560 processor and features more I/O pins than the Uno with a larger memory space however is more expensive and physically larger. This can be an issue when the physical dimensioning of the board needs to meet a requirement such as fitting into a small area. The Arduino Nano was used in some situations as it has the same performance as the Uno but lacks the support of adding shields to the board (Kim et al., 2020).

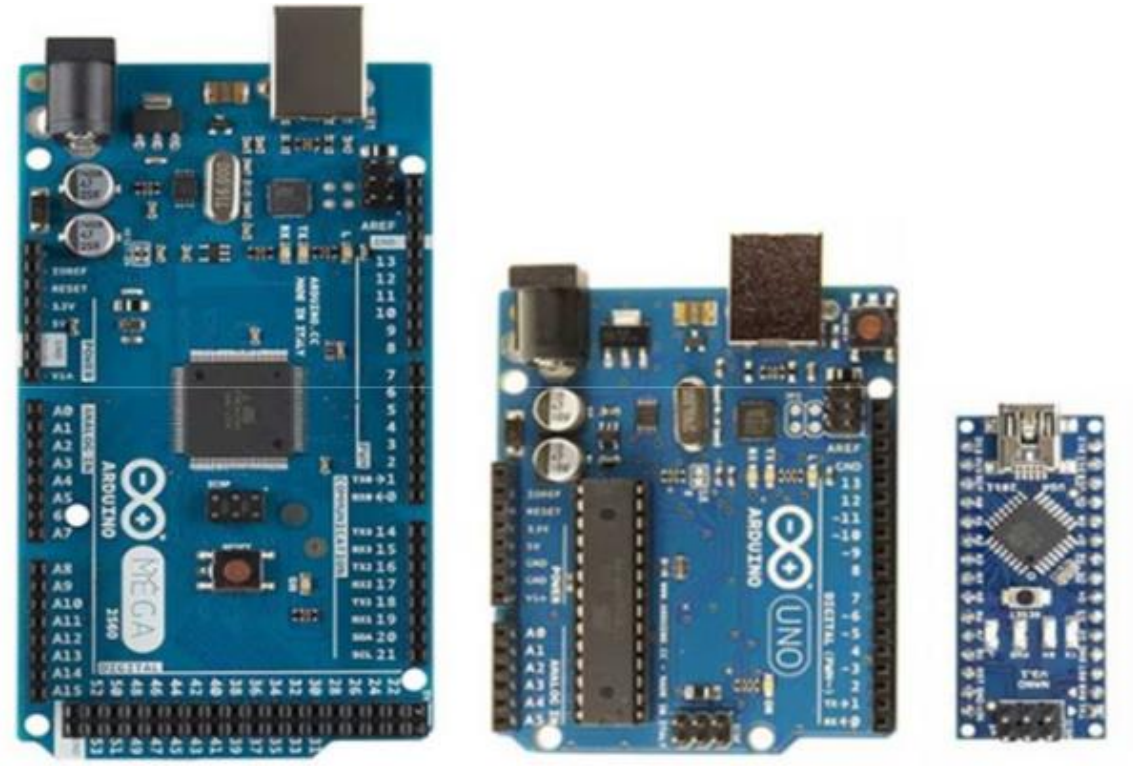

Appendix 7: Arduino Mega, UNO and NANO (Kumar, 2022)

2.5.2 *Arduino Shields*

Arduino shields provide the capability of attaching commercially available plug-and-play add-ons to the Arduino microcontroller board. The shields add functionalities to the board such as Ethernet, Wi-Fi, GPS, LCD and allowing for an easier wiring process and simplifying the complexity of the board (Velders et al., 2018). The hardware shields typically have programming libraries associated with them, aiding in the implementation of the hardware features straight to the microcontroller. A selection of shields provides the option to stack multiple together which is useful for a project that requires multiple features.

2.5.2.1 *Xbee Shield*

Shields such as the Xbee shield (Appendix 8), provide a compliant solution to meet a low-cost, low-power, wireless method to communicate using Zigbee-compatible modules (The Arduino Team, 2023). The Xbee shield module supports multiple communication protocols such as ZigBee, Wi-Fi, and specific radio frequencies. The module is used in two parts with a receiver being the endpoint for communication created by using an Arduino or Node MCU, and a coordinator to send the data using another Arduino (Karthik et al., 2021).

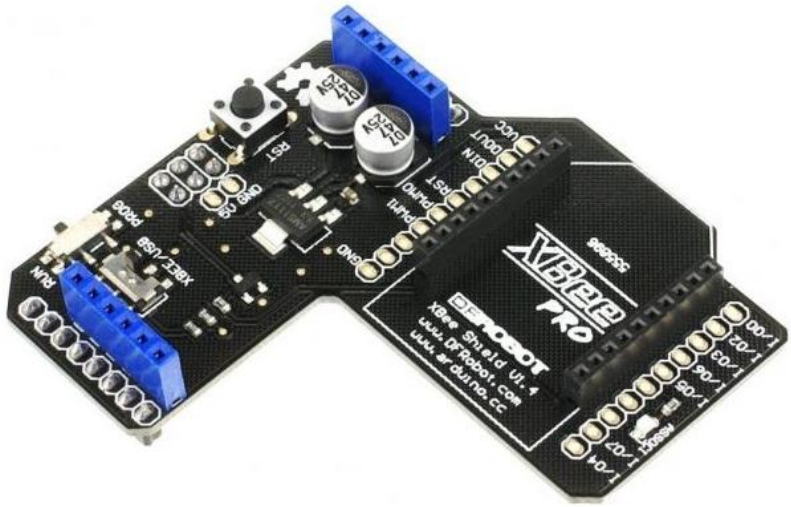

Appendix 8: Xbee Shield for Arduino (Core Electronics, 2023)

2.6 Electronic Sensors

Arduino-compatible sensors can be used to monitor different characteristics throughout an underground mining site. Sensor nodes provide the function to measure air quality parameters within the environment and typically relay information through transmission to a microcontroller device (Jo & Khan, 2018). A variety of sensor types are used in wearable technology depending on the intended application. Sensor types such as environmental sensors, location and position tracking sensors and biometric sensors provide vital information to the user and external viewer under specific conditions.

2.6.2 *Gas and Temperature/Humidity Sensors*

The ability to measure concentrations of gas and temperature change in mining environments is an important capability of a health monitoring device as stated under the Mining Safety Concerns section. Several different gas sensor modules can measure varying gas types in the mining environment. The temperature in underground mining sites can vary from 15˚C to 45˚C.

Generally, the relationship between the gas concentration and sensor resistance can be expressed by the following:

$$R_s = A(c) - \alpha$$

"Where R_s is the sensor resistance, A is a constant, c is the gas concentration and α is the slope of the R_s curve, (Jo & Khan, 2018)."

2.6.2.1 *Digital Temperature and Humidity Sensors*

The DHT11 is a digital temperature and humidity sensor typically used in applications for testing and inspection equipment, automation, data logging and weather stations. The module is low cost with a long-term stability rating of <±1% relative humidity per year and a temperature range of 0˚C to 50˚C with an accuracy of ±5% RH and ±2 ˚C (Table 3). The sampling rate of the DHT11 is 1 Hz and operates in a working voltage of 3V to 5V. The DHT22 is a more expensive version of its predecessor the DHT11 with superior characteristics. The DHT22 features a higher temperature range of -40˚C to 80˚C with a precision of ±0.5 ˚C accuracy.

Parameters	Conditions	Minimum	Typical	Maximum
Humidity				
Resolution		1%RH	1%RH	1%RH
			8 Bit	
Repeatability			±1%RH	
Accuracy	25℃		±4%RH	
	0-50℃			±5%RH
Interchangeability	Fully Interchangeable			
Measurement Range	0℃	30%RH		90%RH
	25℃	20%RH		90%RH
	50℃	20%RH		80%RH
Response Time (Seconds)	1/e(63%)25℃, 1m/s Air	6 S	10 S	15 S
Hysteresis			±1%RH	
Long-Term Stability	Typical		±1%RH/year	
Temperature				
Resolution		1℃	1℃	1℃
		8 Bit	8 Bit	8 Bit
Repeatability			±1℃	
Accuracy		±1℃		±2℃
Measurement Range		0℃		50℃
Response Time (Seconds)	1/e(63%)	6 S		30 S

Item	Measurement Range	Humidity Accuracy	Temperature Accuracy	Resolution	Package
DHT11	20-90%RH 0-50 ℃	±5%RH	±2℃	1	4 Pin Single Row

Table 4: Parameters of DHT11 Digital Temperature and Humidity Sensor (OSEPP Electronics)

Model	DHT22
Power supply	3.3-6V DC
Output signal	digital signal via single-bus
Sensing element	Polymer capacitor
Operating range	humidity 0-100%RH; temperature -40~80Celsius
Accuracy	humidity +-2%RH(Max +-5%RH); temperature <+-0.5Celsius
Resolution or sensitivity	humidity 0.1%RH; temperature 0.1Celsius
Repeatability	humidity +-1%RH; temperature +-0.2Celsius
Humidity hysteresis	+-0.3%RH
Long-term Stability	+-0.5%RH/year
Sensing period	Average: 2s
Interchangeability	fully interchangeable
Dimensions	small size 14*18*5.5mm; big size 22*28*5mm

Table 5: Parameters of DHT22 Digital Temperature and Humidity Sensor ((Aosong Electronics Co.,Ltd))

2.6.2.2 *MQ Series Gas Sensors*

The majority of the MQ series Gas sensors are more dependable and effective for monitoring gas because they are based on metal oxides and react well to erratic gas molecules (Jo & Khan, 2018). Table 4 shows that the accuracy of all sensors is ±5% and the response time lays between 20s to 30s. Each sensor has a different sensitivity to certain chemicals making the range of sensors suitable for different measuring applications.

Table 1. Sensors used for experimentation and their characteristics.

Characteristics	Sensor Module					
	MQ9	**MQ4**	**MQ811**	**DTH11**	**MQ136**	**MiCs2714**
Sensor type	MOS	MOS	MOS	Negative Temperature coefficient (NTC) sensor	Metal Oxide Semiconductor (MOS)	MOS and Microelectro-mechanical systems (MEMS)
Target gas	CO	CH_4	CO_2	Temperature and humidity	SO_2 and H_2S	NO_2
Typical detection range	10–1000 ppm	200–1000 ppm	350–10,000 ppm	20–90% RH *, 0–50 °C	0–100 ppm (SO_2 and H_2S)	0.05–5 ppm
Accuracy	±5%	±5%	±5%	±5% RH, ±2 °C temperature	±5%	±5%
Sensitive material	SnO_2	SnO_2	SnO_2	–	SnO_2	–
Sensitivity	High	High	High	±0.7 °C	3 ppm	0.25 ppm
Respond time	20 s	20 s	20 s	6 s (hum) and 10 s (temp)	30 s	30 s
Manufacturer	Hanwei electronic Co.	Hanwei electronics Co.	Hanwei electronics Co./Sandbox electronics	Aosong electronics Co.	Microelectr-onics Ltd.	SGX sensor Tech.

* Relative humidity.

Table 6: Characteristics of MQ Series Gas Sensors (Jo & Khan, 2018)

The MQ2 gas sensor is a robust sensor due to its capability to detect H2, LPG, CH4, CO, Alcohol, Smoke or Propane. The sensor is one of the most widely used sensors in the series for use in air quality monitoring and smoke detection systems (Heyasa & Galarpe, 2017). The MQ-2 consumes ≤ 900mW of power through heating consumption and operates on 5V DC or AC with a detection range of 300-10000ppm (Table 6).

Technical Parameters **Stable.1**

Model			MQ-2
Sensor Type			Semiconductor
Standard Encapsulation			Bakelite, Metal cap
Target Gas			Flammable gas, smoke
Detection range			300~10000ppm(flammable gas)
Standard Circuit Conditions	Loop Voltage	V_c	≤24V DC
	Heater Voltage	V_H	5.0V±0.1V AC or DC
	Load Resistance	R_L	Adjustable
Sensor character under standard test conditions	Heater Resistance	R_H	29Ω±3Ω（room temp.）
	Heater consumption	P_H	≤950mW
	Sensitivity	S	Ro(in air)/Rs(2000ppm C_3H_8)≥5
	Output Voltage	Vs	2.5V~4.0V（in 2000ppmC_3H_8）
	Concentration Slope	α	≤0.6($R_{3000ppm}$/$R_{1000ppm}$ C_3H_8)
Standard test conditions	Tem. Humidity		20℃±2℃; 55%±5%RH
	Standard test circuit		Vc:5.0V±0.1V; V_H:5.0V±0.1V
	Preheat time		Not less than 48 hours
	O2 content		21%（not less than 18%） O2 concentration effects initial value, sensitivity and repeatability.
Lifespan			10 years

NOTE: Output voltage (Vs) is V_{RL} in test environment.

Table 7: MQ-2 Gas Sensor Specifications

2.6.2.3 *Heart Rate Sensors*

The resting heart rate of a healthy adult ranges from 60-100 beats per minute (bpm) depending on fitness level and age. The maximum heart rate of a person can be calculated by subtracting their age from 220 e.g. For a 50-year-old, 220 – 50 = 170 bpm (Harvard Health Monitoring Harvard Medical School, 2020). As a threat to safety is encountered, the heart rate may increase drastically as a human response to danger triggers the fight or flight system. Therefore, the capability to measure the heart rate of mining workers is a critical component of a health monitoring system to alarm the needed personnel of danger.

2.7 Knowledge Gap

Throughout the literature review process, it has been found that various systems have been designed concerning health monitoring systems used in different scenarios. The knowledge gap exists within the exploring of different electrical components to complete the task efficiently and effectively. The testing of individual components and the system to find an optimal combination and solution hasn't been investigated to the full extent and allows for the development of a system that can measure each parameter needed. Further research is needed to design a lower-cost method than traditional methods of measuring the health risks of mining workers and making improvements based on the experimentation.

The testing of the system under mining circumstances must be applied to determine the effects of the environmental conditions experienced on the mining site and how the sensors react to high temperature, high humidity and dusty conditions. Many of the existing systems explored are devices that are set within the mine and aren't wearable. A wearable system would benefit the mining worker in terms of convenience and a more accessible, functional option for measuring health parameters.

3 Methodology

This project aims to explore the different methods of monitoring the health of mining workers based on the environmental factors faced by working under potentially harsh conditions. The end objective is to design and build a system capable of doing so that meets the requirements stated in the Project Brief. This research project requires using a methodological approach for acquiring initial ideas and developing them into an eventual solution by using an iterative and creative method.

The methodology used can be separated into the following parts:

1. Initial Idea Phase – This step utilises background research to produce initial ideas for a possible solution to the defined problem by considering the aim of the project, requirements, and research objectives. The initial ideas must then undergo a concept evaluation to compare the strengths and weaknesses of each idea to form a strong base to work with. For this project, each potential idea and arrangement of circuitry elements will be investigated to determine the most optimal setup to meet the requirements of the system.

2. Preliminary Design Phase – This phase builds the general framework for the project and the overall system configuration is defined using schematics, diagrams, and layouts. This phase allows an idea of the materials and the types of components needed for the project to be built upon.

3. Detailed Design Phase – This phase further elaborates on the previous phase by investigating the individual components required for the system.

4. Prototyping Phase – This phase contains the building of a prototype to conduct testing on in the next stage of the process. The prototyping phase allows for an initial design to collect feedback to further the design. The prototyping stage is an iterative process as new problems may arise that haven't been accounted for and must be solved by repeating the methodological process.

5. Testing and Evaluation – This phase involves testing the prototype by gathering data on the outputs of the system and evaluating the data through analysis of theoretical data. The phase may be repeated multiple times depending on the results of the experimentation and undesirable results.

6. Improvements Phase – This phase involves improving the system by considering the analysis results from the previous phase to increase effectiveness for the requirements set.

It's important to know that the methodology isn't a linear process, and the different phases can be repeated multiple times due to failures and undesirable outcomes. The process has been outlined to allow the best chance of staying on track and meeting the objectives and requirements set.

3.1 Research Questions

The following broad questions have been created to guide and shape the experimentation and evaluation process:

- How do high humidity and temperature affect the ability to detect parameters and the accuracy of measurements?
- How does the effects of dust affect the accuracy of the system?
- What improvements can be made to further optimise the performance and functionality of the system?

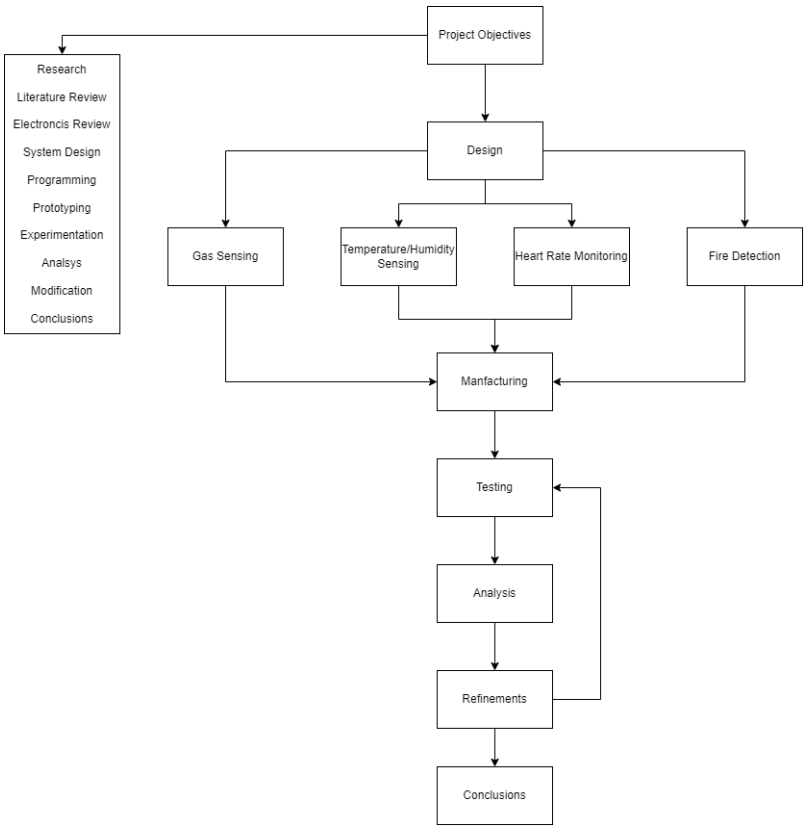

Appendix 9: Flow chart of methodology

3.2 Experimental Testing

Using a structured approach to test the system will be required to successfully obtain usable data and achieve the desired outcomes. Through an iterative process, the outcomes of the experiment will be used to refine the system and repeat the testing procedures as necessary. The testing objectives and questions of the project can be separated into the following:

- Mining Environmental Conditions – The impact of high temperature, humidity and varying dust concentrations will be tested to determine the effects on the accuracy of the sensor readings.
- Gas detection – This will be tested by using the system in a mock experiment to detect the gas selection found in mining scenarios and the ability to relay the levels to the host system.
- Heart rate monitoring – the ability to monitor the heart rate across low and high activity levels will be tested and the accuracy of these results will be verified.

The following table has been created to outline the individual experiments for the chamber testing and the variables changed in each experiment,

Table 8 – Individual Chamber Testing Experiments and Variables

Sensors	Experiment Types
Carbon Dioxide	• Baseline Accuracy • High Dust Concentration • Low Dust Concentration • High Humidity • High Temperature • Continuous Dust Concentration
Temperature/Humidity	• Baseline Accuracy • High Dust Concentration • Low Dust Concentration • Continuous Dust Concentration
Heart Rate	• Resting Baseline Accuracy • Elevated Baseline Accuracy

3.3 Temperature and Humidity Sensor Testing

The temperature and humidity sensor will be tested by conducting experimentation in a controlled stable space away from direct heat sources and humidity-generating elements. A separate thermometer and hygrometer (Ozito Digital Humidity and Temperature Meter, Appendix 10) will be used to compare the results from the sensor against and establish baseline conditions. The temperature and humidity of the testing area will be changed using a controlled method via a heater and humidifier. The experiments will be conducted using an iterative process to cover a wide range of different scenario combinations. The results will be monitored and recorded for analysis of the accuracy of the system under varying conditions.

Appendix 10: Ozito Digital Humidity and Temperature Meter

3.4 Mining Environmental Conditions Testing

The main issue in investigating whether the system will be effective in monitoring the health parameters of mining workers lays in the harsh environmental conditions during work. Therefore, experimentation on how the system as a whole and individual components react to different conditions must be tested to ensure reliability and efficiency in these types of environments. The accuracy and functionality of the system will be tested under high levels of dust, high temperatures, and high humidity.

The testing will begin by establishing baseline conditions in which the system is tested in a controlled environment without any exposure to the defined variables. This will be completed to serve as a reference point for the testing under the different mining condition variables. Due to the limited resources for testing these requirements, a mock experiment approach will be used to investigate the different variables. A chamber will be constructed to place the Arduino system into a well-ventilated area away from potential interference to prioritise safety.

3.4.1 Chamber Testing for Sensor Reactions to Environmental Conditions

The chamber will be exposed to carbon dioxide via a CO_2 gas cylinder and a regulator will be used to adjust the concentration. The test will be conducted using two different concentrations mimicking a low and high concentration of gas to simulate (Appendix 16). Fans will be added to the inside of the chamber to evenly distribute the gas and particulates inside the chamber. The same chamber will be used to simulate dusty conditions by adding a mixture of large and fine dust particulates (Appendix 12) which will be aggravated by the fan inside the chamber to increase the dust concentration (Appendix 15). To conduct the testing at different temperature levels, the chamber will be heated using a heating device and the values will be read from the temperature/humidity sensor (Appendix 13). Due to the linking between temperature and humidity, the humidity will increase as the temperature increases naturally. A humidifier will also be introduced to increase the humidity within the chamber to experiment at higher levels than the baseline (Appendix 14). The following diagram has been created to outline the experiments (Appendix 11). A continuous experiment with two increases in dust concentration will also be conducted to rule out any effect of the internal fan within the chamber on the sensor readings and to test if the readings return to the baseline before the dust concentration is introduced.

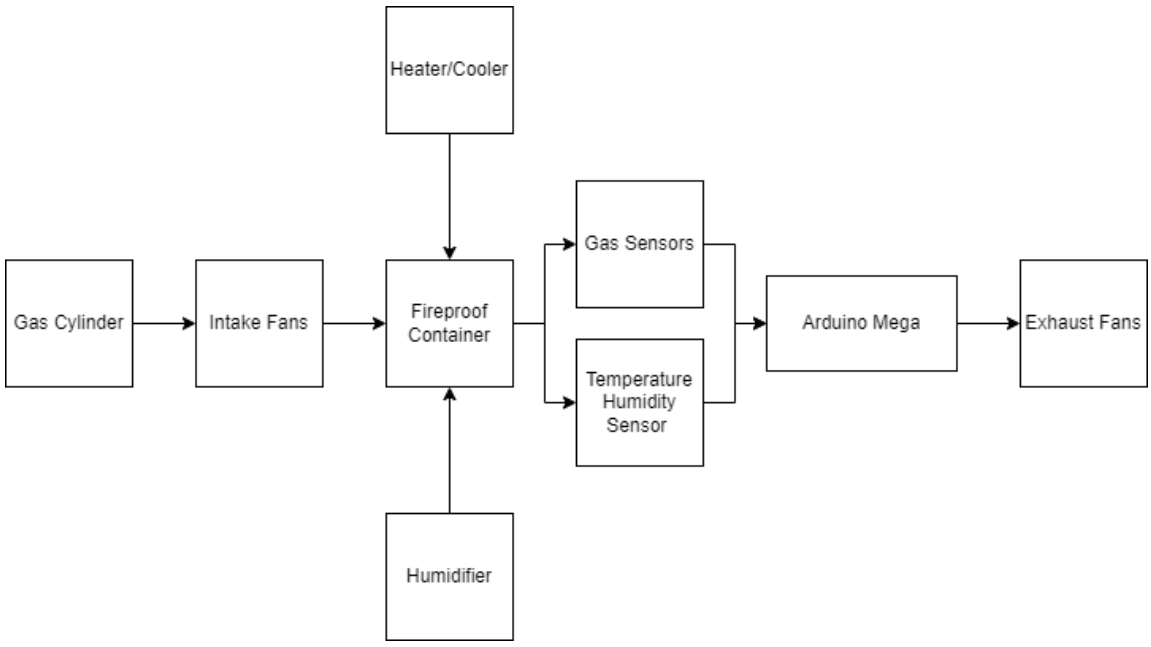

Appendix 11: Chamber Experiment Outlining the Components for Testing

From Appendix 11, the intake fans in the testing chamber are used to distribute the CO2 gas once it has been delivered into the chamber via a regulator. The heater and humidifier are used to heat and increase the humidity in the chamber, respectively. The sensors are used to read the chamber's properties, and the Arduino Mega is used to process the data. The gas is released into the atmosphere using the exhaust fans to reset the chamber.

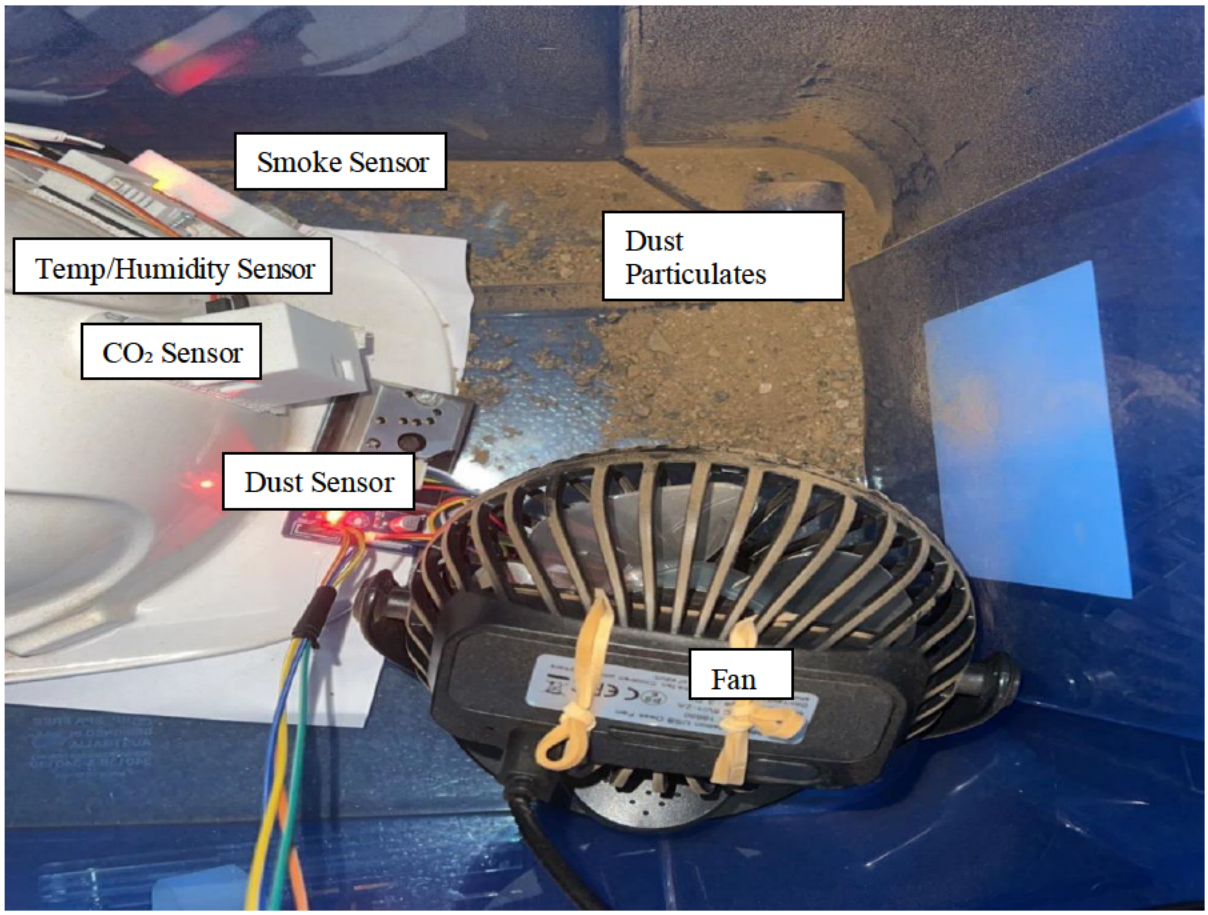

Appendix 15: Chamber Setup for the Dust Experiment

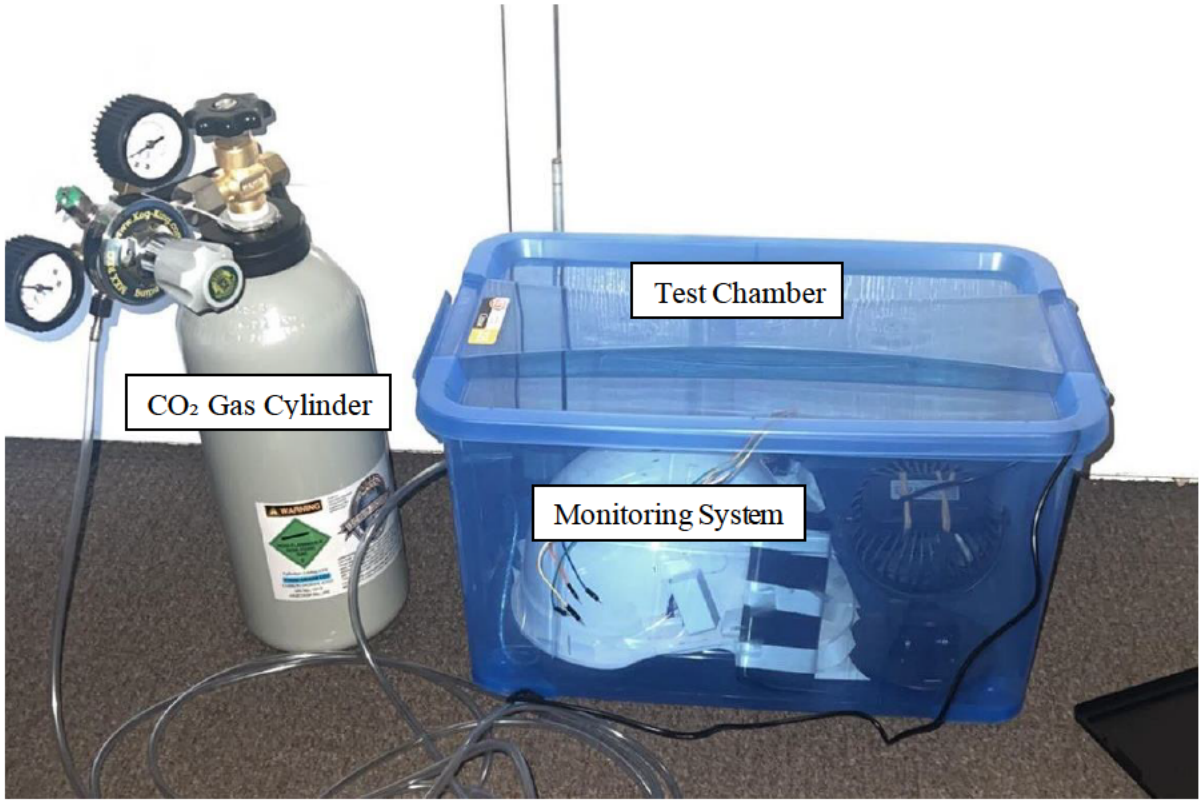

Appendix 16: Chamber Setup for the CO_2 Experiment

Appendix 12: Dust Mixture

Appendix 13: Heater

Appendix 14: Humidifier

3.4.2 Heart Rate Testing

The heart rate accuracy of the chosen sensor will be tested by equipping the Arduino-compatible heart rate sensor components to the test subject's body and measuring the heart rate over a period. The same experiment will be conducted by pairing with the Polar H10 electrocardiogram (ECG) monitoring device and the data will be compared (Appendix 17). The resting heart rate measurement of the Arduino sensor will be scrutinised against the Polar H10 measurement. To simulate a panicked scenario and an increase in heart rate for data collection purposes the test subject will be exposed to rigorous activity. The impact of sweat and varying temperature/humidity on the system will also be investigated using this approach to mimic mining practices.

Appendix 17: Polar H10 Heart Rate Monitoring Sensor

3.5 Risk Management

A risk management plan is needed to highlight the potential outcomes and risks involved throughout the project. Risk arises from an uncontrolled hazard and can pose a negative effect based on the severity of the risk. The following is a risk assessment that considers the potential hazards and consequences with steps to mitigate or eliminate the risk.

The following table has been adopted from the ‘USQ Safety Risk Management System’ (SRMS).

Table 7 – Risk Rating Matrix

	Consequences				
Probability	Insignificant	Minor	Moderate	Major	Catastrophic
Almost Certain	Moderate	High	Extreme	Extreme	Extreme
Likely	Moderate	High	High	Extreme	Extreme
Possible	Low	Moderate	High	High	High
Unlikely	Low	Low	Moderate	Moderate	Moderate
Rare	Low	Low	Low	Low	Low

Table 8 – Analysis of Hazards

Hazard	Severity	Likelihood	Consequence	Mitigation/Elimination
Soldering iron burns	Moderate	Possible	Minor	Be aware of your surroundings and turn off the soldering iron when not in use
Eye strain from computer screen	Moderate	Possible	Minor	Take breaks from the computer screen
Electrocution	Moderate	Unlikely	Catastrophic	The highest voltage used would be 5V DC for Arduino components which is a safe voltage level
Gas exposure	High	Possible	Catastrophic	Take precautions and exercise safe practice measures
Injury from testing heart rate monitoring	Moderate	Possible	Minor	Choosing a physically fit test subject with the physical requirements of a mining worker
Smoke inhalation from testing	High	Possible	Major	Conduct experiments in a controlled environment and stay clear of exhaust fans
Burns from fire testing	High	Possible	Major	Stay clear of the fire and test in a controlled environment with a fire extinguisher accessible

4 Hardware Design and Analysis

This section focuses on a review and analysis of the hardware required and the different options available for completing the project goal. If successful different options may be investigated to further the effectiveness of the system.

The required hardware can be broken down into the following categories:

- Microprocessor (Coordinator)
- PC (End node)
- Wi-Fi communications
- Gas sensors
- Smoke sensor
- Heart rate sensor
- Temperature/Humidity sensor

The ability to detect fire using the system was considered but was chosen to be omitted due to the requirement of a range of different wavelengths for various fire sources and multiple additional sensors to provide reliable detection.

The hardware design can be separated into two parts, the coordinator module, router node and end node. This combination has been adapted from the WSN topology (Appendix 1) cluster tree from the literature review and allows for a connection between all three devices across a higher range than the peer-to-peer setup.

4.1 Gas Sensor Analysis

The gas sensors analysed for this section will be the MQ series and MH-Z19-C as they can achieve the desired task for this project, are low-cost, and are compatible with the Arduino infrastructure. Sensors such as the SCD30 and MH-Z14A were considered but are out of the price range for this project. Due to the multiple different gas sensing abilities of this range of sensors, sensors must be chosen that are dedicated and provide minimal overlap of their capabilities. For example, choosing gas sensors that are highly sensitive to one gas type is optimal as the readings won't be skewed if multiple gases are present at the same point in time due to cross-sensitivity. This can also be negated to the lowest possible point through the calibration of the sensors and supporting algorithms and thresholds. For this requirement, the following sensors have been analysed in the table below.

Table 9 – Gas Sensor Electronic and Performance Requirements

	Sensors				Totals
Features	MQ-4	MQ-2	MQ-7	MH-Z19	
Gas	Methane	Smoke	Carbon Monoxide	Carbon Dioxide	
Detection Range (ppm)	300 to 10000	300 to 10000	10 to 1000	400 to 10000	
Exposure Standards (STEL) (ppm)	25000	-	30	30000	
Exposure Standards (TWA) (ppm)	-	-	-	12500	
Analogue Pins	1	1	1	0	3
Digital Pins	1	1	1	1 (PWM}	4
Ground Pins	1	1	1	1	4
VCC Pins	1	1	1	1	4
TXD Pins	0	0	0	1	1
RXD Pins	0	0	0	1	1
Voltage	5	5	5	5	NA
Current (mA)	150	150	150	150	600

The detection range of the sensors analysed for carbon dioxide and methane doesn't meet the requirement for the exposure standards. Other sensors have been considered but the cost to detect a higher range is substantially larger as the range increases. Therefore, the sensors have been chosen and the ability to detect the harmful gases will be tested concerning the detection ranges. The required pins and current consumption will be considered in the microcontroller analysis and power supply sections.

4.2 Temperature and Humidity Sensor Analysis

The following table has been developed to outline the hardware requirements and specifications of the DHT11 and DHT22 sensor modules. The temperature and humidity ranges are derived from the average maximum and minimum temperatures encountered in Australian underground mines. A study by (Donoghue, 2000) revealed that the mean psychrometric wet bulb temperature was 29.0°and the mean dry bulb temperature was 37.4°C. The dry bulb reading represents the ambient air temperature and the wet bulb reading simulates the effect of sweating which lowers the body temperature. The humidity in Australian underground mining sites reached levels of 95% to 100%.

Table 10 – DHT11 and DHT22 Specifications

Specification	DHT11	DHT22
Measurement Range	20-90%RH, 0 to 50˚C	0% to 100%RH -40 to 80˚C
Humidity Accuracy	±5%	±2%
Temperature Accuracy	±2 ˚C	±0.5°C
Response Time	2s	2s
Digital Pins	1	1
Ground Pins	1	1
VCC Pins	1	1
Operating Current	2 mA	2 mA
Temperature Ranges for Australian Mining Sites	15 to 45˚C	
Humidity Range for Australian Mining Sites	80% to 100%	

The DHT22 has been chosen to measure temperature and humidity as part of the system as the humidity range of 0% to 100% is optimal for the required range of 80% to 100%.

4.3 Heart Rate Sensor Analysis

The heart rate monitoring sensors for this section that will be analysed will be the DFRobot heart rate sensor, MAX30102 and MAX30105. The MAX range of sensors operates by measuring heart rate through optical sensing principles via red and infrared light to detect blood flow whereas the DFRobot uses electrocardiogram technology through multiple points. The ability to resist sweat, dust, and ambient light fluctuations and the hardware feature requirements and features will be analysed to decide the most optimal option for the system. The following table has been developed to analyse the different options available,

Table 11 – Heart Rate Sensor Options and Specifications

Specification	MAX30102	MAX30105	DFRobot
Communication	I2C	I2C	Analogue
Sensor Type	Optical	Optical	Optical
Operating Current	6mA	6mA	<10mA
Ambient Light Cancellation	YES	NO	NO
VCC Pins	1	1	1
Ground Pins	1	1	1
Analogue Pins	2	2	1
Digital Pins	1	1	1

From the table, the MAX30102 is the only sensor that features ambient light cancellation. Due to the mining environment being a low ambient light scenario, this feature doesn't pose any benefit for this application. The DFRobot allows for the attachment to the body through multiple electrodes rather than the optical sensing of a single photodiode (Appendix 18). This alone puts the DFRobot sensor in a more optimal position as the ability to measure heart rate without affecting the physical capabilities of the wearer is a priority.

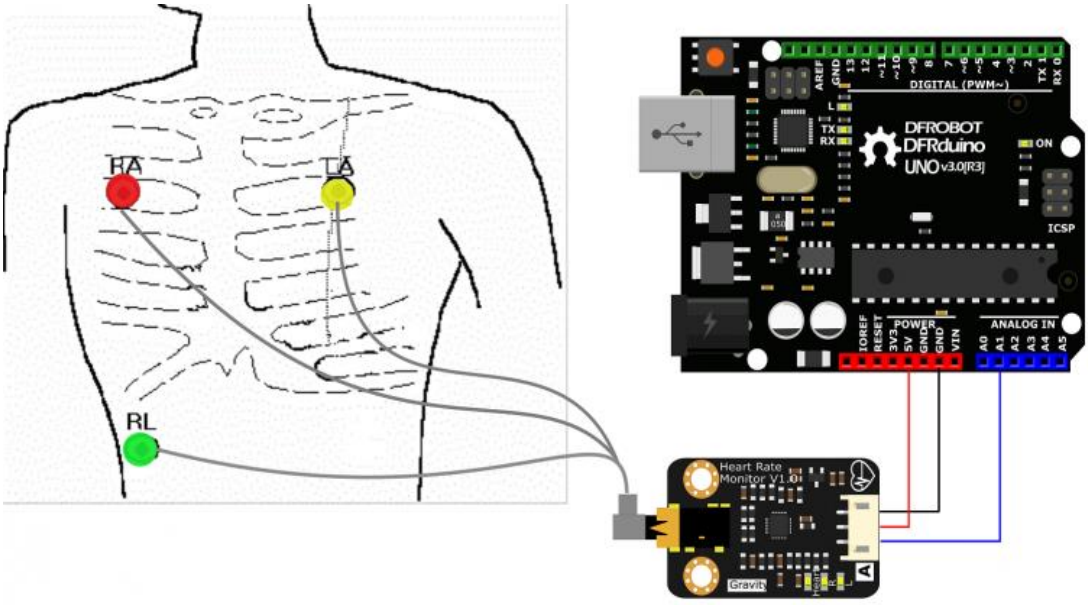

Appendix 18: ECG attachments for the DFRobot health rate monitoring sensor

4.4 Communication Protocol Analysis

The communication between the coordinator and end node microcontroller must be wireless to enable a higher range of communication in the system. Therefore, using the built-in serial or I2C communication between the two microcontrollers isn't feasible as the microcontroller would need to be hardwired. The potential options explored concerning this requirement are the Zigbee method using Xbee modules or using ESP8266 modules. The ESP8266 has been chosen over the Zigbee method as the cost of Xbee modules is very expensive with low availability of Australian stock. Therefore, considering the time constraint and the low-cost goal of this project, the ESP8266 will be used for the communication method of the health monitoring system. The ESP8266 can operate as a standalone device but for this project, the module will be paired with an Arduino microcontroller for adjustability. By using the ESP-NOW protocol the two microcontrollers can communicate wirelessly without the need for a traditional Wi-Fi network. This is especially useful for this project as the system will be able to work in a remote environment where the benefit of a Wi-Fi network may not be available.

The following table has been developed to outline the requirements and features of the ESP8266 module,

Table 12 – ESP8266-01 Module Requirements and Specification

Specification	ESP8266
Frequency Range	2.4 GHz ~ 2.5 GHz (2400 MHz ~ 2483.5 MHz)
Operating Current	80mA
Clock Speed	80 MHz
RX pins	1
TX Pins	1
VCC Pins	1
Ground Pins	1

4.5 Coordinator Microprocessor Analysis

By using the information from conducting the literature review, three options for Arduino microcontrollers were investigated. The three options consist of the Arduino UNO, Arduino Mega and the Arduino Nano. Due to the chosen configuration of the system, two Arduino microprocessors are required to act as a coordinator (Master) and an end node (Slave).

The following tables have been developed to analyse the potential options by using a ranking system for each setup and the pinout and performance requirements have been analysed,

Table 13 - Specification Table for Arduino Microcontroller Options (coordinator)

Specifications	Arduino UNO	Arduino Mega	Arduino Nano	Requirements
Digital I/O Pins	14	54	14	6
Analogue Input Pins	6	16	8	4
RX Pins	1	4	1	2
TX pins	1	4	1	2
Clock Speed	16 MHz	16 MHz	16MHz	
Flash Memory	32 KB	256 KB	16 KB	
Size	Medium	Large	Small	
Rankings				
A				
B				
C				
D				

Due to the multiple RX and TX pins required using the selection of sensors, the Arduino Mega is the only microcontroller that will be feasible for the processing task. The option to assign UART ports using software has been considered but due to the inefficiency and limited reliability of using hardware ports, the Mega has been chosen. The drawback of the size of the processor is that the size should be small enough to implement as a wearable system for comfort and fitment requirements. Therefore, the physical dimensions of the board will be considered to ensure the fitment is applicable during the prototyping stage.

4.6 Coordinator Battery Analysis

By factoring the current the current draw of all the connected sensors and modules the battery lifespan can be calculated to find the most suitable battery to power the coordinator module. By assuming the maximum current is drawn continuously from each component the following table has been developed.

Table 14 – Current Draw Requirements of Battery

Coordinator Module	Current Draw (mA)
ESP8266	80
DFRobot Heart Rate Sensor	10
DHT22	2
Gas Sensors	600
Total Current Draw	692

Assuming the system draws 692mA at 5V and is required to operate for 24 hours, the battery capacity required to power the coordinator can be calculated by using the following equations.

$$Total\ Energy\ Consumption = Current * Voltage * Time$$
$$Total\ Energy\ Consumption = 0.692 * 5\ * 24$$
$$Total\ Energy\ Consumption = 83\ Wh$$

$$Battery\ Capacity = \frac{Total\ Energy\ Consumption}{Voltage * 1000}$$

$$Battery\ Capacity = \frac{83}{5 * 1000}$$

$$Battery\ Capacity = \frac{83}{5 * 1000}$$

$Battery\ Capacity = 16600\ mAh$ for 24 hours run time

From the equation, the battery capacity required to successfully power the system for 24 hours is 16600 mAh assuming the components are operating at maximum current continuously. For a mining shift of 12 hours, the battery capacity required is 8300 mAh. This value assumes the battery efficiency is perfect which isn't true in real-world scenarios. Therefore, the battery capacity must be higher than the calculated value for use in the real-world application of the system. The aim of the system is to be powered by a battery of 10000 mAh to account for any battery inefficiency. Due to the large requirement of battery capacity and operating current, the options are limited. The following table has been developed to outline the requirements for the battery setup and the hardware required to do so.

Table 15 – Battery Options

Coordinator Battery Setup Options				
Battery Type	Voltage (V)	Ampere Hours (mAh)	Required Batteries	Rechargeable
AA (Alkaline)	1.5	2000	20	No
AAA (Alkaline)	1.5	1000	40	No
C (Alkaline)	1.5	8000	8	No
D (Alkaline)	1.5	10000	4	No
9V (Alkaline)	9	1200	9	No
18650 (Li-ion)	3.6	2600	8	Yes
26650 (Li-ion)	3.7	3400	6	Yes
Power Bank	5	10000	1	Yes

The total required batteries for each battery type can be calculated by using the following equations,

$$Number\ of\ Parralel\ Batteries\ Required = \frac{Desired\ Capacity}{Capacity\ per\ Battery}$$

$$Number\ of\ Series\ Batteries\ Required = \frac{Desired\ Voltage}{Voltage\ per\ Battery}$$

$$Total\ Batteries\ Required = \frac{Desired\ Voltage}{Voltage\ per\ Baterry}$$

From the table, the option of using alkaline batteries isn't feasible as the Capacity and voltage are very low and require a large amount of battery to be wired in series and parallel to achieve the 10000 mAh, 5V requirement. Another issue with using alkaline batteries is they aren't rechargeable and would need to be replaced after each use which isn't cost-friendly or sustainable. The 18650 and 26650 were considered but also suffer from the same problem requiring 8 and 6 batteries to meet the requirements. Therefore, a power bank has been chosen to power the system with the specifications of 5V and 10000 mAh with a rechargeable feature.

4.7 Hardware Prototype

The electrical connections between the microcontroller and the various sensors can be seen in the schematic (Schematic 1). The physical design of the system can be seen in (Appendix 19, 20, 21, 22) with each component labelled. The wearable portion of the system was chosen to be implemented into a hardhat design with the sensors on the exterior of the hardhat and circuitry on the inside to protect against damage to the microcontroller unit. Two voltage rails were created to branch the required power supply for each sensor.

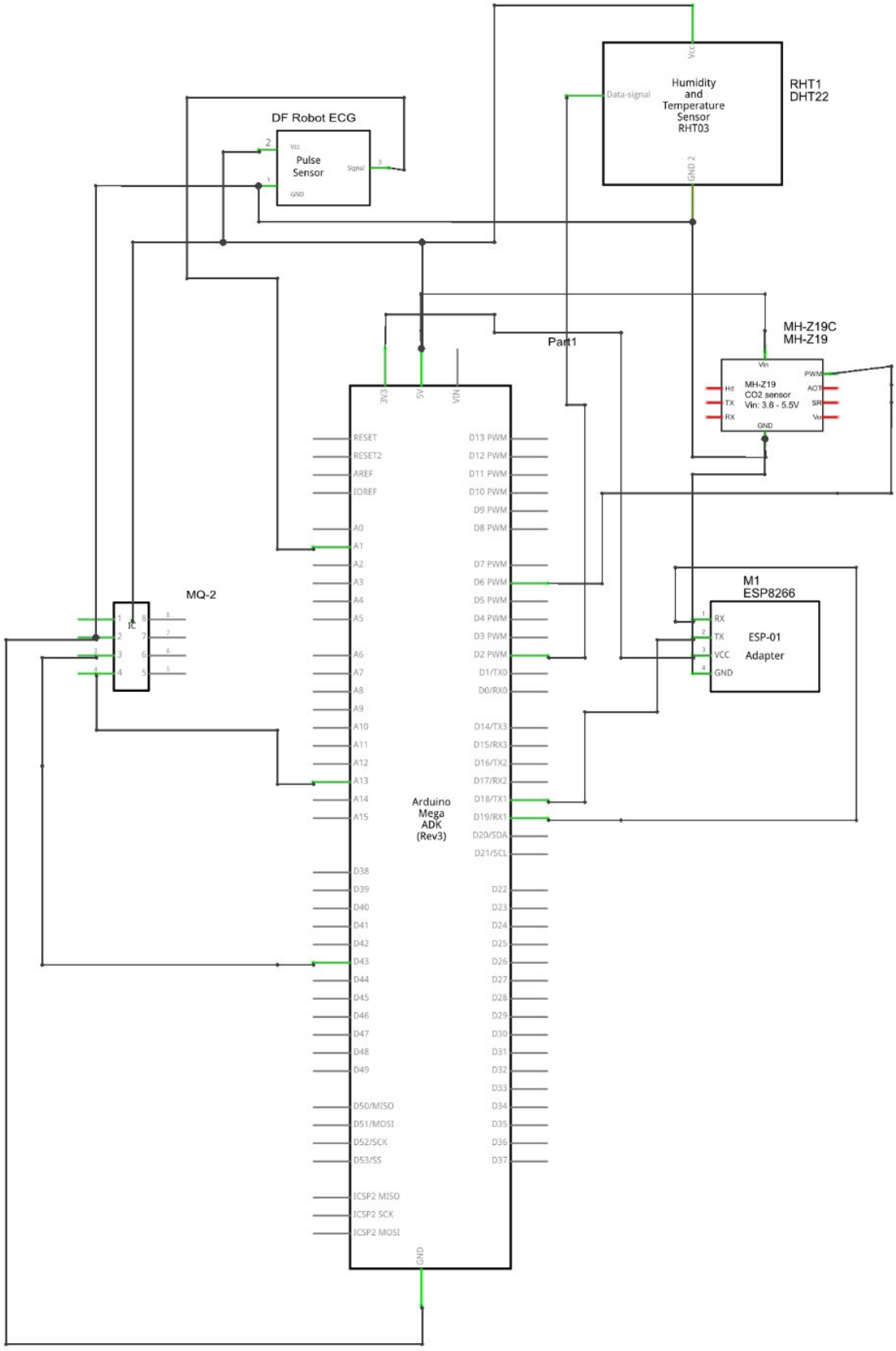

Schematic 1: Electrical Schematic of Health Monitoring System Connections

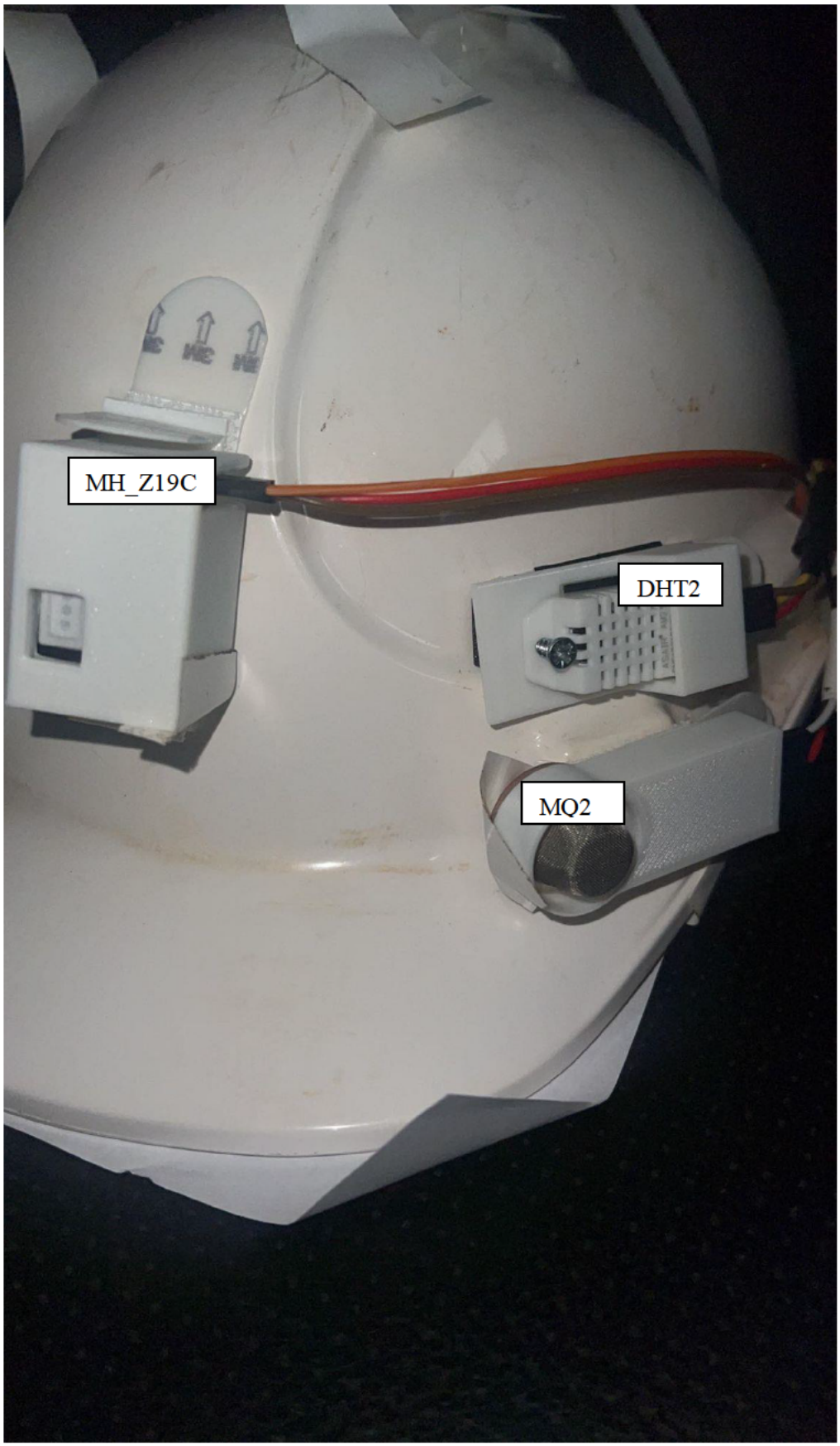

Appendix 19: Front of Prototype System

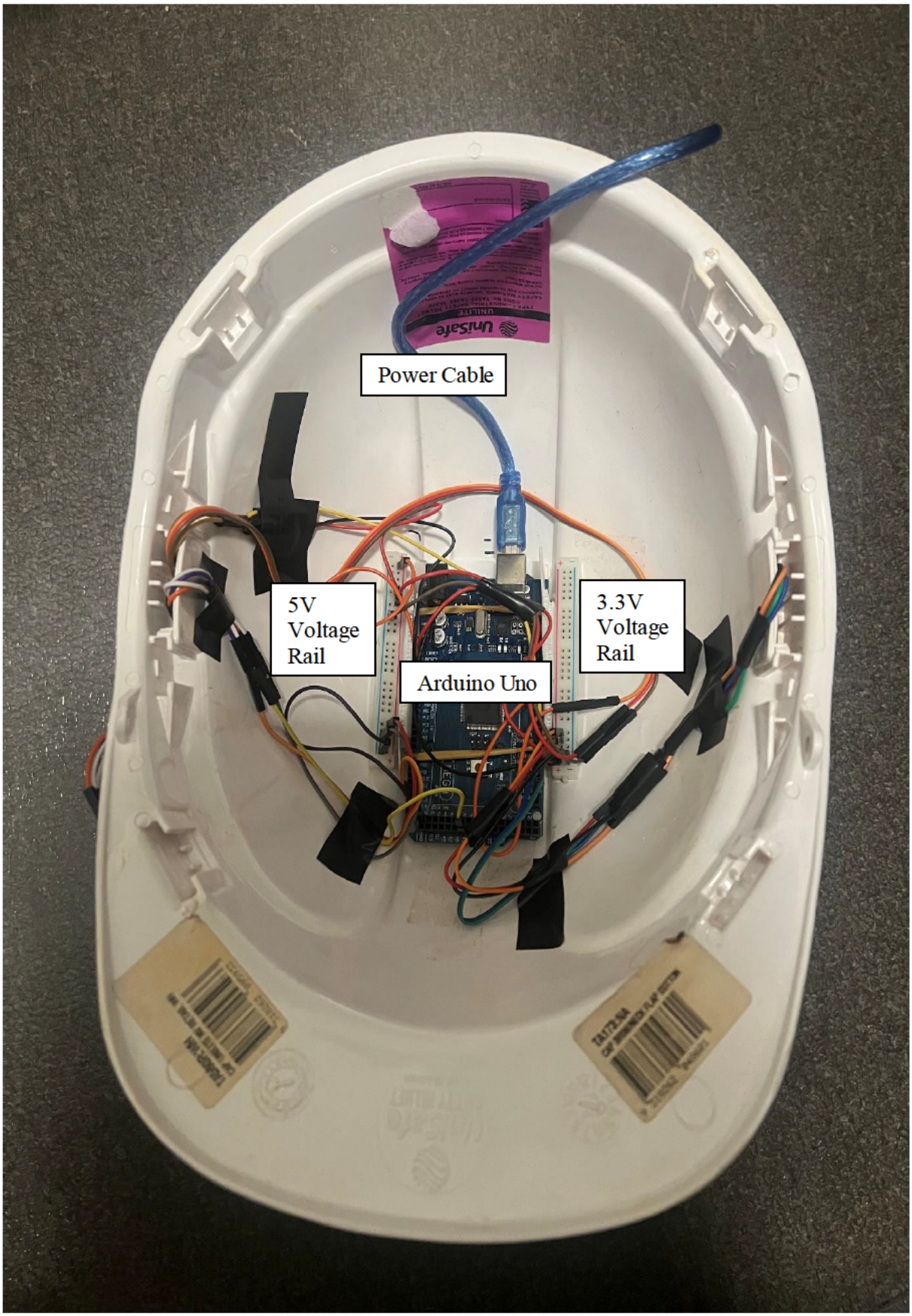

Appendix 20: Inside of Prototype System

Appendix 21: Side of Prototype System

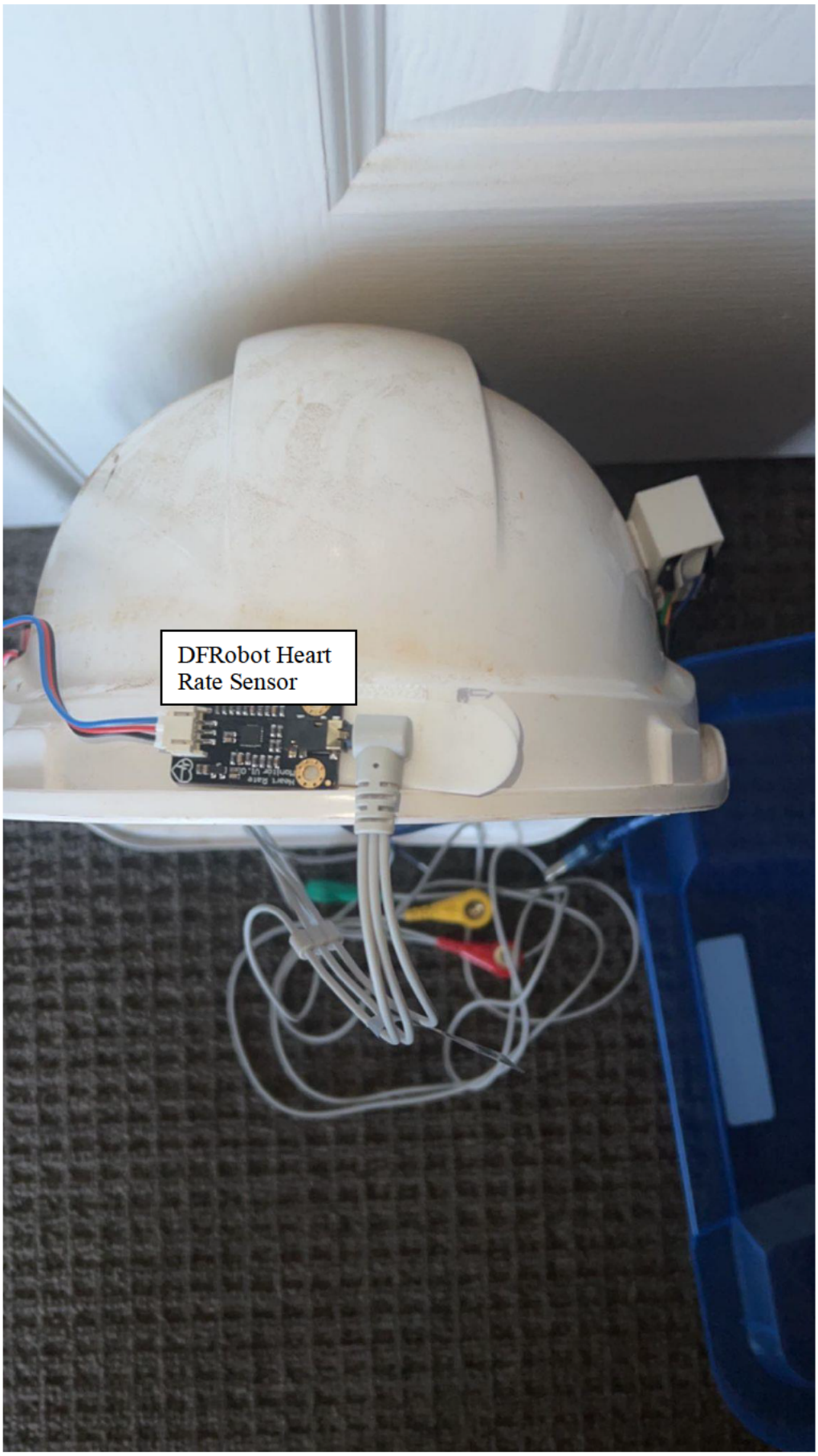

Appendix 22: Back of Prototype System

5 Code Development

The Arduino Development Environment (IDE) was used to develop code for each sensor function and the integration of the individual components to create the whole system. The Arduino IDE's comprehensive features allowed for the code to be developed, compiled, and then tested utilising the serial monitor for debugging purposes and the serial graph for data analysis. The software greatly aided in the ability to write, test, and refine the programs for a successful efficient system. ThingSpeak developed by MathWorks was chosen as the analytics platform to collect and visualise data from the connected sensor devices. The software was chosen as the features of a 1-second write time were highly suitable for the required response time of the system. The viewing features of ThingSpeak allow the sensor data to be interpreted by the viewer as the most current value which aids in the relaying of information to the safety team in the workplace. ThingSpeak also utilises MATLAB connectivity which can used to analyse the results of the experiments conducted. Several existing open-source libraries were used in the code for the system and have been credited within the code (Appendix, last).

5.1 ESP8266 Wi-Fi and ThingSpeak Connectivity

The connection of the health monitoring system to ThingSpeak requires a Wi-Fi connection which was obtained by the ESP8266 module. The ESP8266 was programmed using AT commands to connect to the Wi-Fi network using the Access point SSID and password with the connection status displayed via the serial monitor. A TCP connection to ThingSpeak was also obtained by using AT commands and the sensor data string was sent using an HTTP GET request to the required fields within the ThingSpeak channel (Appendix 23).

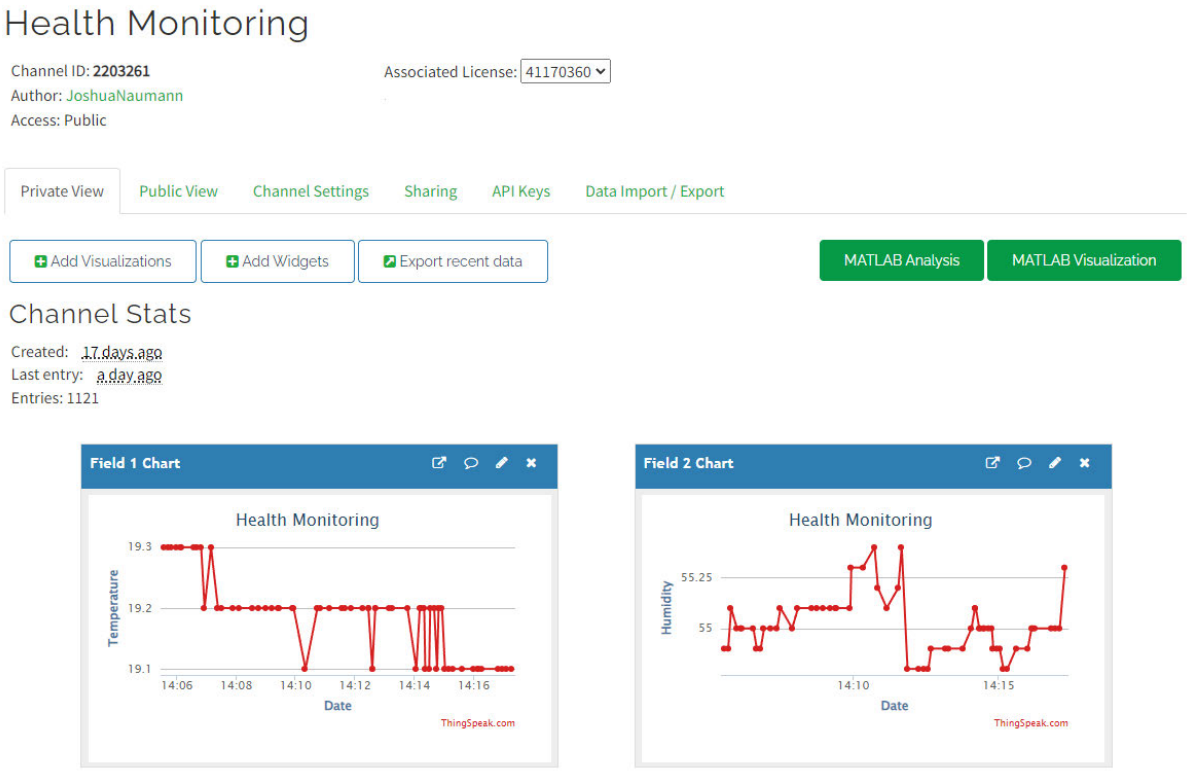

Appendix 23: ThingSpeak Channel Dashboard

6 Experimentation and Analysis

6.1 Temperature and Humidity Sensor Testing

The DHT22 temperature and humidity sensor was tested over 20 minutes whilst varying the temperature and humidity of the testing area using a humidifier and a heater. The humidity and temperature measurements were taken using the Ozito measurement device and the DHT22 via the ThingSpeak server (Appendix 24). The data was then uploaded to excel to analyse the results and draw conclusions based on the experiment (Appendix 11). The standard deviation of the humidity reading from the DHT22 when compared to the Ozito measurement device was 2.94% and the standard deviation of the temperature reading was 1.17˚C. The datasheet of the DHT22 sensor claims that the sensor provides an accuracy of ±2% RH (Relative Humidity) and ±0.5°C. From the obtained results, the humidity and standard deviation closely align with the expected accuracy. From the graphical format of both data sets (Appendix 25, Appendix 26), No outliers are present which proves the consistency of the DHT22 sensor and an accurate component for measuring the temperature and humidity of the environment.

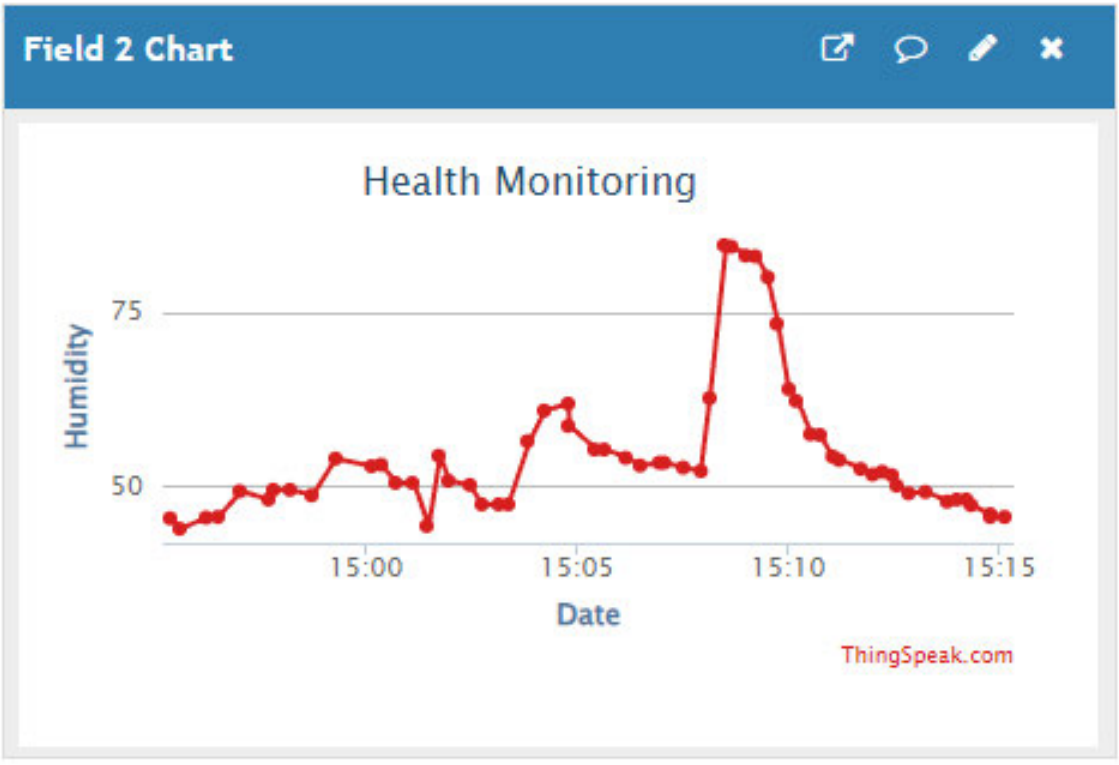

Appendix 24: ThingSpeak Humidity Channel Display

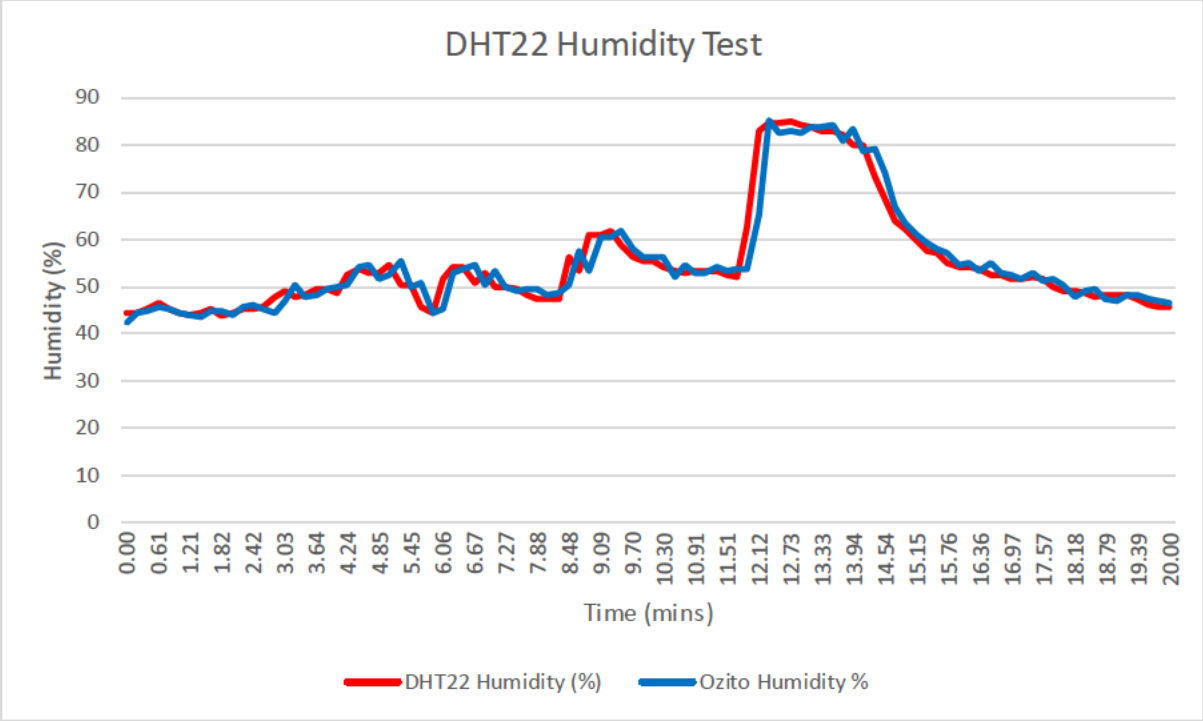

Appendix 25: DHT22 Humidity Test Against Ozito Temperature and Humidity Sensor

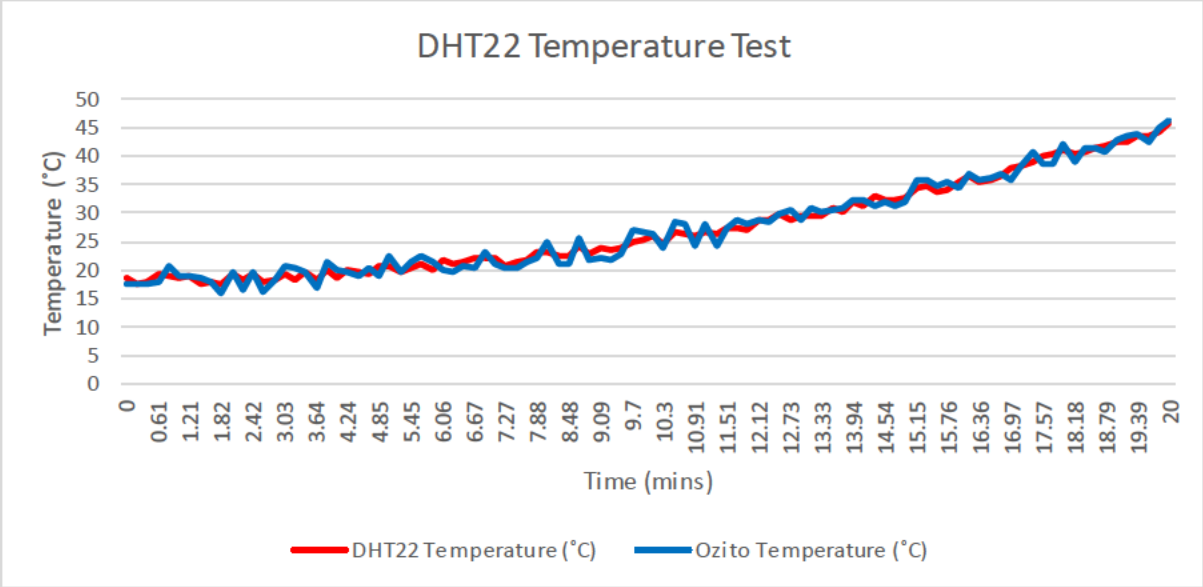

Appendix 26: DHT22 Temperature Test Against Ozito Temperature and Humidity Sensor

6.2 Heart Rate Sensor Testing

The DFRobot Heart Rate Sensor was tested over three minutes with the user being in a stationary resting state to gather data on the heart rate readings. The readings were produced in a serial format and were displayed to the PuTTY serial monitor program for data collection and visualisation (Appendix 27). During the experiment, the user's heart rate was monitored using a higher quality Polar Heart Rate Sensor Device to compare the data to establish a baseline accuracy. The Polar Sensor was assumed to be more accurate and provide the actual heart rate value to compare the DFRobot sensor against. The readings were taken every second within the range of 0s to 180s at 20˚C, 40% Humidity (Appendix 49). The data was developed into a graph to graphically display the two data sets (Appendix 28).

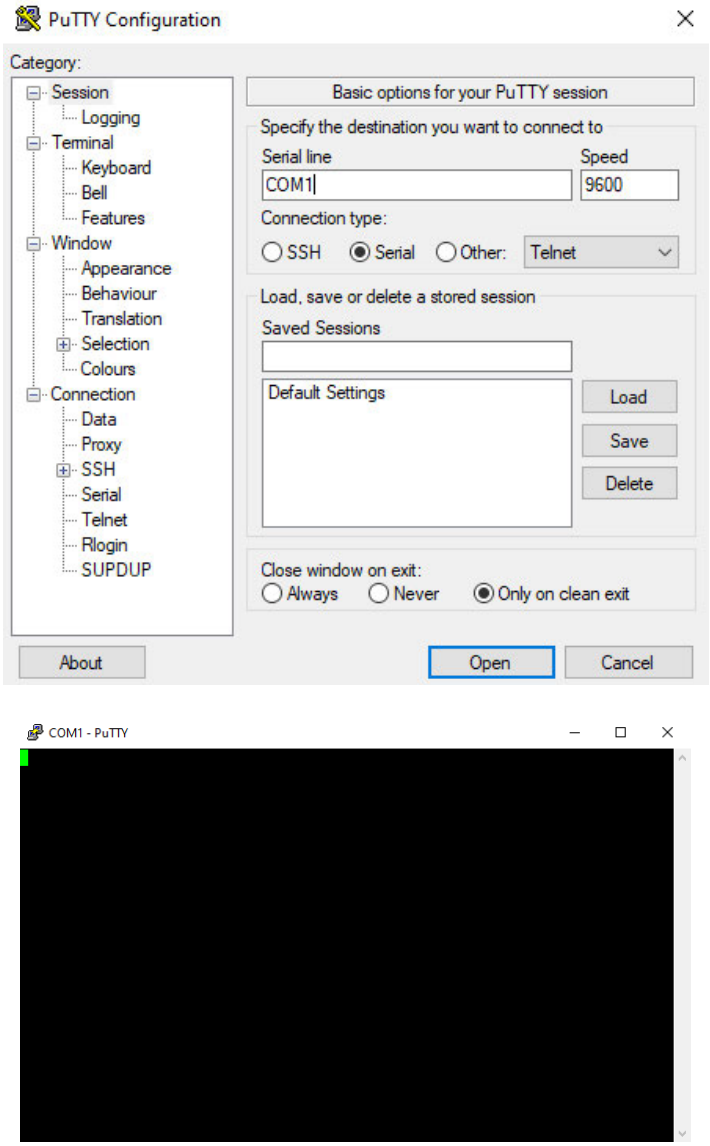

Appendix 27: PuTTY Serial Monitor and Interface

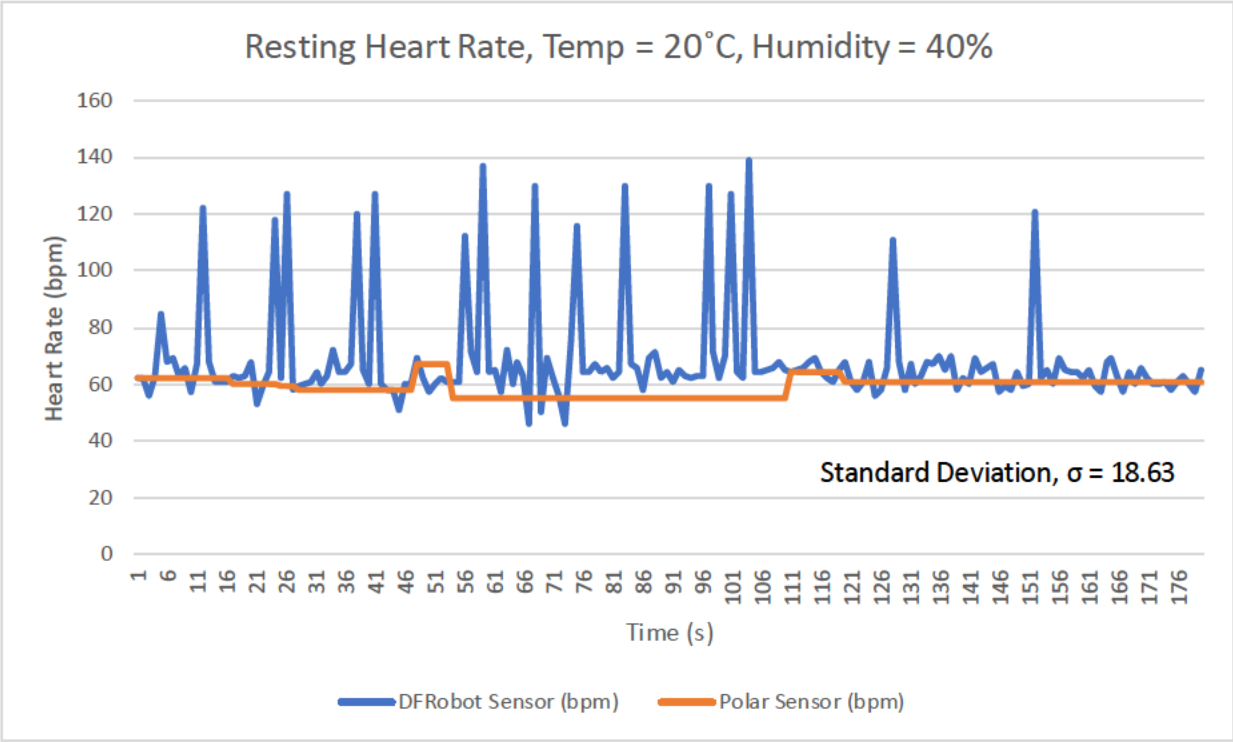

Appendix 28: Heart rate sensor data from DFRobot ECG Heart Rate Sensor and Polar Heart Rate Sensor at rest

From the graph, the DFRobot sensor has several outliers at the start of operation where the heart rate readings spikes to a much higher value than the value from the Polar Sensor. The standard deviation of the data set was 18.63 bpm which shows a high level of variance between the two measurement devices. These outliers and standard deviations were expected from the first iteration of the code as the program was an unfiltered design and didn't account for internal and external noise. From these results, the program was modified to implement the Kalman filter to reduce the errors from the raw measurements by estimating the state of the system as an average of the predicted new state using a weighted average. The following parameters have been used as part of the Kalman filtering algorithm to reduce errors and smoothen the accuracy of the system. The values of the parameters were calculated using a trial-and-error method via repetitive testing of the DFRobot sensor whilst comparing it to the Polar H10 sensor to find the variable values with the least variance in output results.

Q_angle = 0.001;
Q_gyro = 0.003;
R_angle = 0.03;
dt = 0.005;
C_0 = 1.0;

1. Q_angle: This parameter represents the covariance of the process noise for the measurement angle. A higher value results in a higher trust in the predicted state and a higher response rate to changes.

2. Q_gyro: This parameter is similar to the Q_angle variable but instead represents the covariance of the process noise for the gyro measurement.
3. R_angle: This parameter represents the covariance of the sensor noise of the angle measurement and defines the confidence in the sensor reading value rather than the predicted state. A higher value means the predicted state will be trusted more than the sensor reading.
4. dt: This parameter represents the time step between each update of the algorithm. This variable was set according to the frequency of the sensor measurements.
5. C_0: This parameter is used to calculate the Kalman filter gain. A value of 1 indicates a linear behaviour model.

The modified code can be seen in (Appendix) with the addition of the Kalman filtering method. Existing code from the public GitHub forum by Jianghao (2016) was modified to meet the requirements of the system.

The same experiment was conducted under the same conditions using the modified code to view the impact of the filtering setup on the results (Appendix 29).

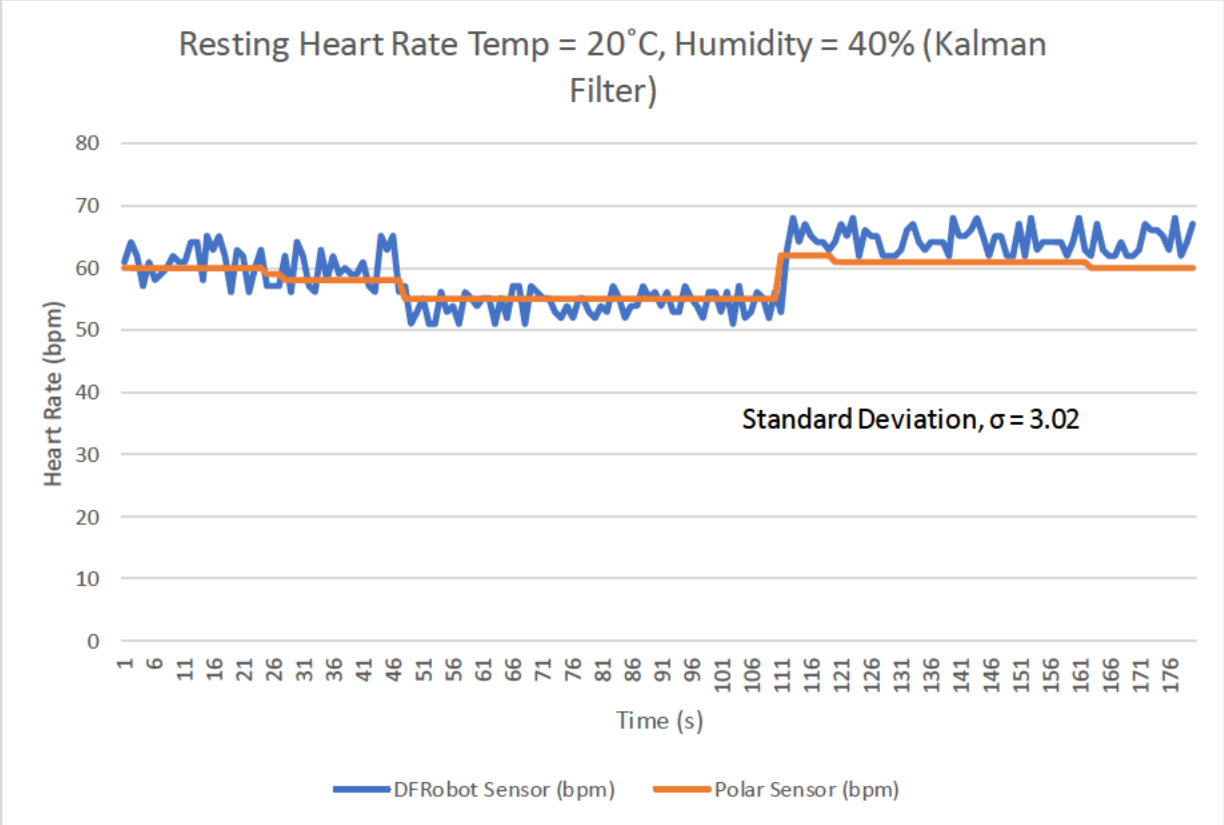

Appendix 29: Heart rate sensor data from DFRobot ECG Heart Rate Sensor and Polar Heart Rate Sensor using Kalman Filtering

From the graph, the standard deviation is 3.02 bpm which is much lower than the standard deviation of the previous test without the Kalman filter and there are also no outliers present within the graph. The results of the experiment are within the requirements for the health monitoring device as the necessity for a higher degree of precision isn't needed for the application of this system. The same experiment was conducted whilst increasing the heart rate variable through physical exertion (Appendix 51).

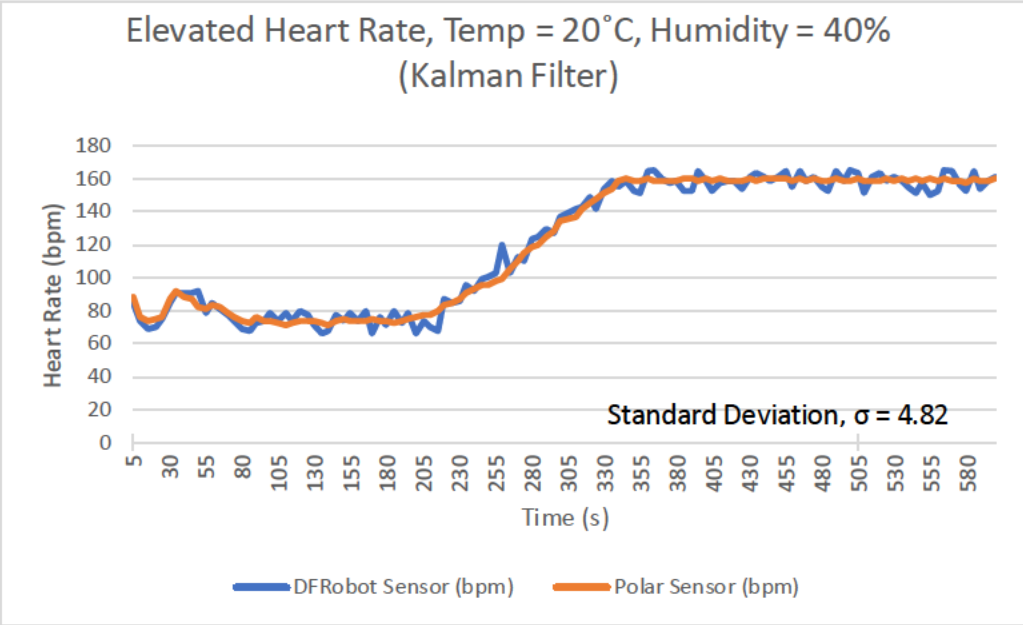

Appendix 30: Elevated Heart rate sensor data from DFRobot ECG Heart Rate Sensor and Polar Heart Rate Sensor using Kalman Filtering

The results from the experiment found the standard deviation to be 4.82 bpm and once again no outliers are present within the data set. Although the standard deviation for this elevated heart rate test is marginally higher than the resting heart rate test, this experiment can be concluded to be a success as a standard deviation of this value is low enough for the application of this system. The range of the DFRobot sensor also shows capabilities of up to 160 bpm. Higher range tests were attempted but failed at increasing the heart rate of the test subject higher than this level and weren't investigated further for injury risk prevention. Experimentation at higher humidity and temperature levels was also considered but was chosen not to be conducted due to the health risks of the test subject under such conditions.

6.3 Carbon Dioxide Sensor Testing

The MH-Z19C carbon dioxide sensor comes factory calibrated however has the option to be manually calibrated or automatically calibrated using past sensor data. To find if the sensor required manual calibration, a baseline test was implemented by testing the sensor at a known concentration of CO_2. This was achieved by gathering CO_2 data from the atmosphere outside (Appendix 52) and comparing it against the global average annual mean CO_2 of 414.4ppm in 2021 (CSIRO, 2022). From the gathered data (Appendix 31) over 15 minutes the standard deviation was 13.72 ppm, and the highest variance was 33.6 ppm. These results fall well within the claimed accuracy range of 50ppm + 5% reading value from the technical specification data sheet therefore manual calibration wasn't required.

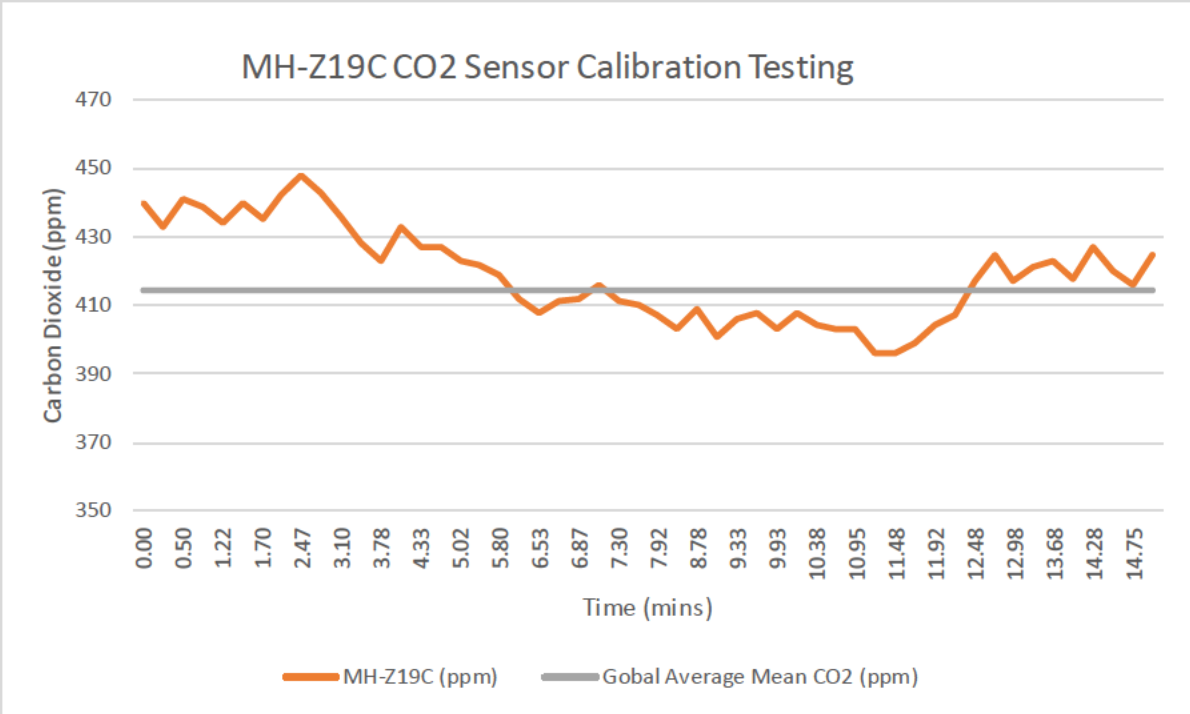

Appendix 31: Calibration Test of MH-Z19C Carbon Dioxide Sensor Using the Global Average Mean CO2 Concentration

6.3.1 Carbon Dioxide Sensor Testing at High Humidity and Temperature

Two experiments were conducted to gather data on the effects of high humidity and temperature on the MH-Z19C sensor at low and high CO_2 concentrations. The experiments were completed over an hour and the data was obtained from the ThingSpeak server. The data was uploaded to Excel for data analysis and displayed graphically to conclude from the results (Appendix 32, Appendix 33). The highest temperature and humidity obtained throughout both tests were around the 40˚C and 85% humidity mark. A more humid and heated environment was attempted to investigate the effects of a larger variance of temperature and humidity but failed and resulted in the parameters levelling off during the experiments.

6.3.2 *Carbon Dioxide Sensor Testing at Low Concentration*

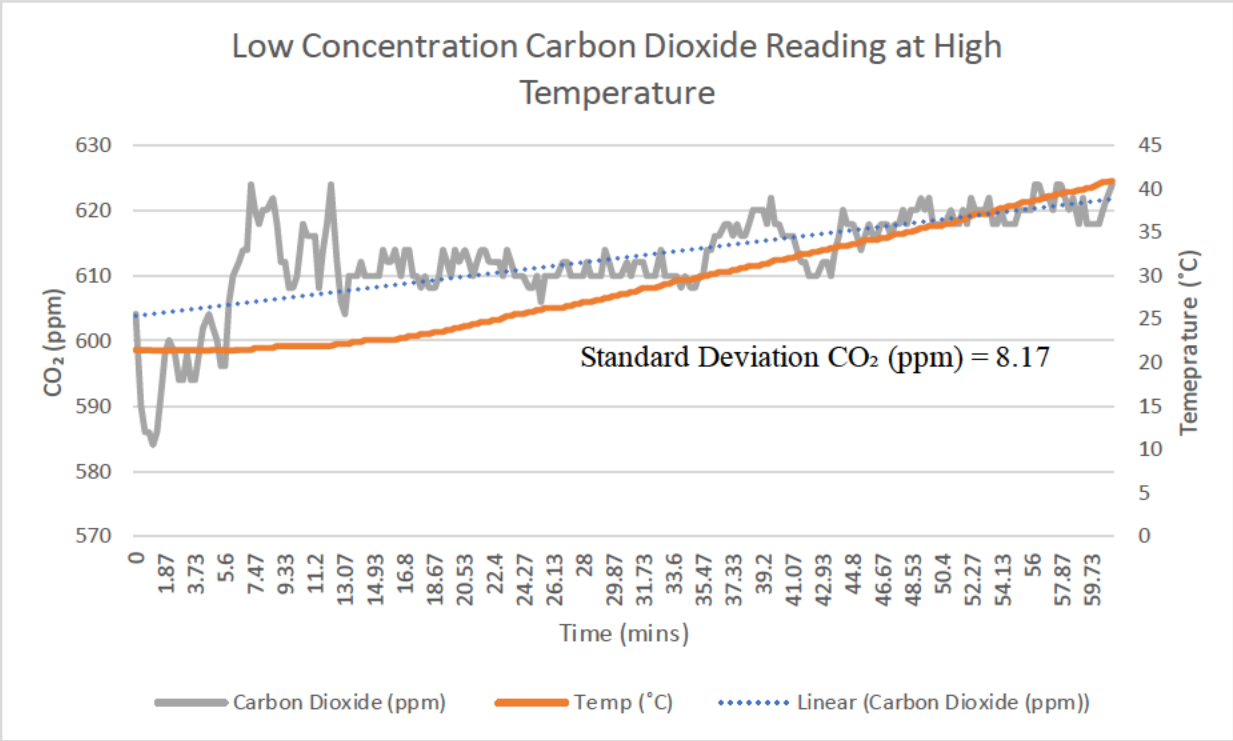

Appendix 32: Low Range Carbon Dioxide Reading at High Temperature

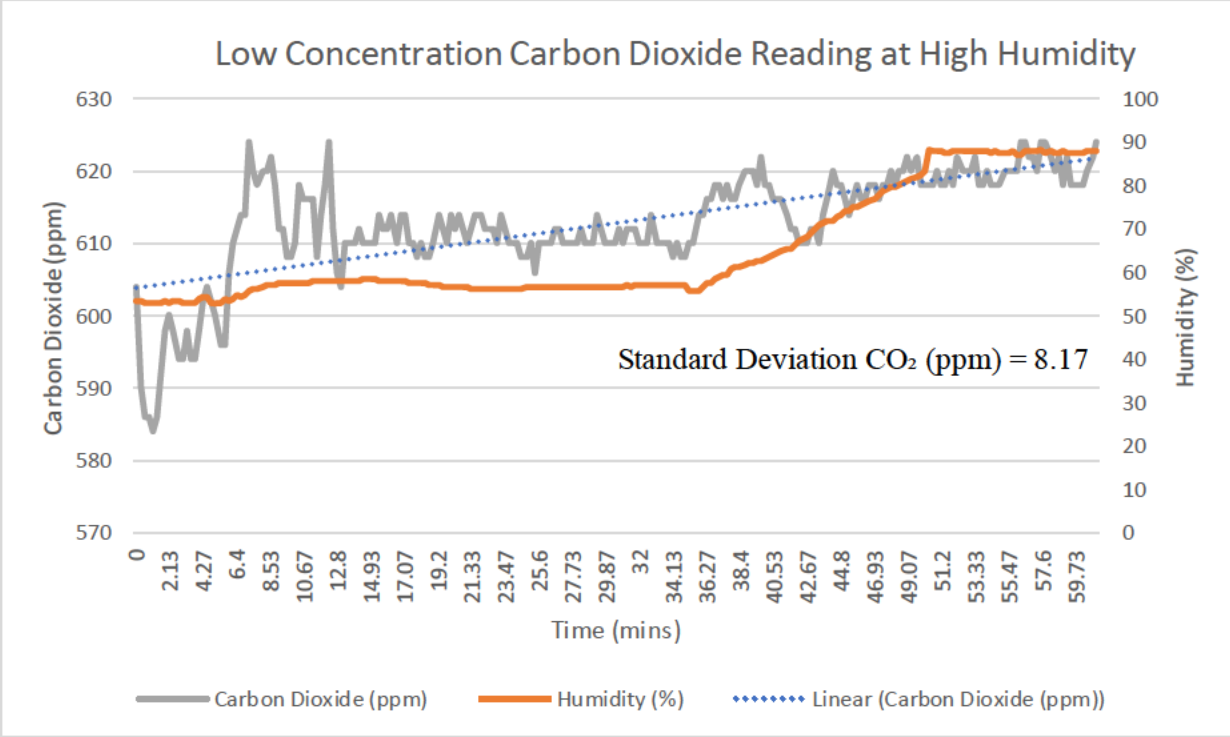

Appendix 33: Low Range Carbon Dioxide Reading at High Humidity

From the graphs, the time between 0 minutes to 15 minutes shows sporadic activity which can be explained by the sensor warming up and stabilising shortly after this period. By taking the sensor reading at the beginning of stabilisation and the final sensor reading, 16 minutes and 61 minutes, the values are 612 ppm at 22.6˚C and 58% humidity and 624 ppm at 40.9˚C and 88.1% humidity.

Time (mins)	Carbon Dioxide (ppm)	Temperature (˚C)	Humidity (%)
16	612	22.6	58
61	624	40.9	88.1

Change in Carbon Dioxide (ppm)	Change in Temperature (˚C)	Change in Humidity (%)
12	18.3	30.1

From the table, the experiment resulted in a change in CO_2 of 12ppm when the temperature increased by 18.3˚C and 30.1% humidity. This can be seen by the trendline graphically showing a gradual increase in the MH-Z19C sensor reading as the temperature and humidity increase. This means the high humidity and high-temperature environment affects the accuracy of the sensor. However, the standard deviation of the sensor reading was 7.43 ppm which is a respectable result in terms of the accuracy of the sensor under such conditions. A result of this magnitude doesn't pose any risks to the effectiveness of this sensor selection as the variance between baseline and high temperature and humidity is negligible and is within reason for the application of this sensor.

6.3.3 Carbon Dioxide Sensor Testing at High Concentration

The measurements were taken directly after the previous low-concentration test with the device still powered on which explains the low fluctuation at the start of the experiment due to the sensor already being warmed up. By taking the sensor reading measurement at the start of the increase in temperature and humidity and the measurement at the maximum, the variation and effects can be calculated and concluded.

Time (mins)	Carbon Dioxide (ppm)	Temperature (˚C)	Humidity (%)
16.2	1281	24.1	70.3
62.8	1352	44.1	86.6

Change in Carbon Dioxide (ppm)	Change in Temperature (˚C)	Change in Humidity (%)
71	20	16.3

From the table, the change in CO_2 was 71ppm over a change of 20˚C temperature and 16.3% humidity. The trendline shows a gradual increase in the sensor reading however the graph displays a stabilisation after the humidity and temperature reaches a maximum value (Appendix 34, Appendix 35). Compared to the low concentration test the standard deviation was 29.86 ppm which is much higher than the low concentration standard deviation of 7.43 ppm. This means that high temperature and humidity have a more dramatic effect on the MH-Z19C sensor reading at higher concentrations of CO_2.

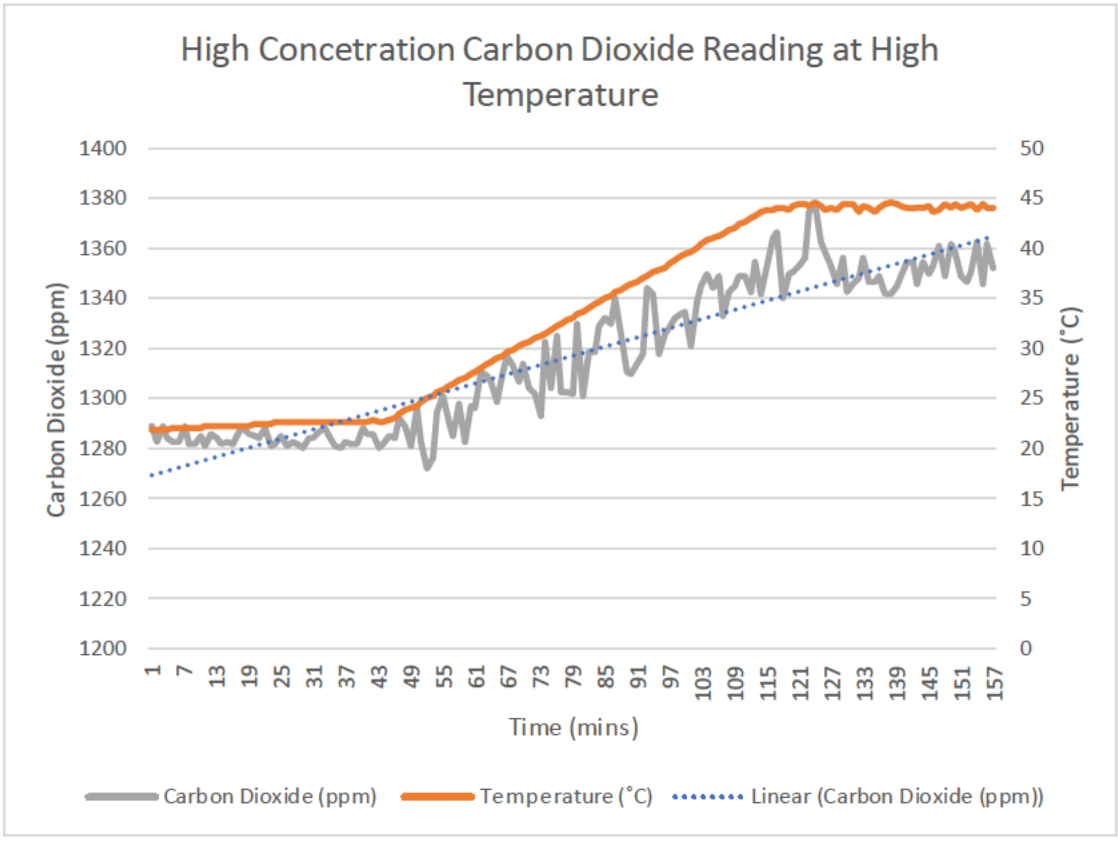

Appendix 34: High Range Carbon Dioxide Reading at High Temperature

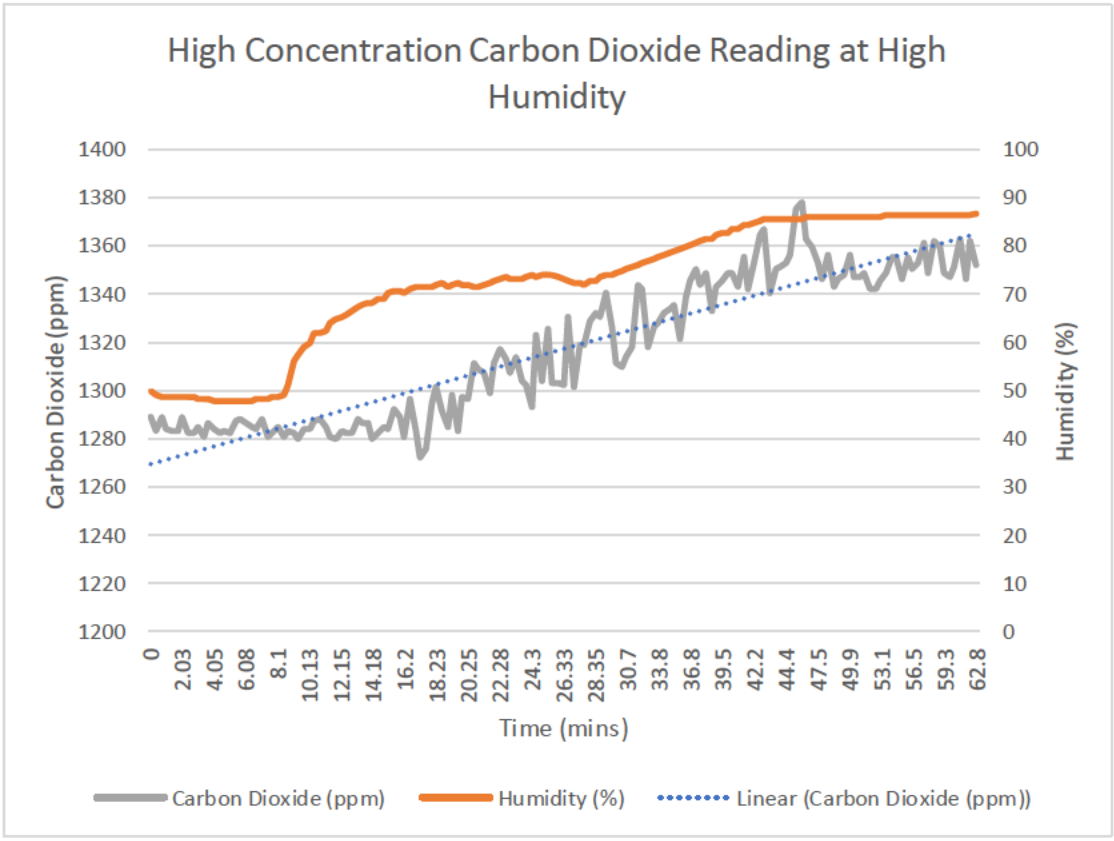

Appendix 35: High Range Carbon Dioxide Reading at High Temperature

6.4 Effects of Dust Concentrations

The effects of dust on the health monitoring system were determined through two experiments at a low dust concentration and a high dust concentration. To establish a reference point to base the results of varying dust concentrations, the chamber was allowed to equalise without a change in parameters before the dust was introduced.

6.4.1 Reference Point for Dust Testing

The following table has been prepared to find a baseline to compare the low and high dust concentrations. The results were derived from the ThingSpeak client and uploaded to Excel (Appendix 55, 57) to present the standard deviation of the sensor readings at the beginning of the experiments. Between both low and high concentrations tests, the average ambient dust concentration recorded from the SHARP GPY014AU was 39.5 µg/m^3 and 45.8 µg/m^3 respectively.

Low Dust Concentration Reference Test			
Sensor Parameters	Temperature (˚C)	Humidity (%)	Carbon Dioxide (ppm)
Standard Deviation	0.04	0.08	7.54

High Dust Concentration Reference Test			
Sensor Parameters	Temperature (˚C)	Humidity (%)	Carbon Dioxide (ppm)
Standard Deviation	0.04	0.13	4.18

6.4.2 Dust Test at High and Low Concentrations

The dust contents were added to the chamber and a maximum dust concentration of 390 µg/m^3 was achieved for the low-concentration test and 593 µg/m^3 for the high-concentration test. By taking the standard deviation from each parameter for both low and high-concentration tests, the following tables have been prepared.

Low Dust Concentration Practical Test			
Sensor Parameters	Temperature (˚C)	Humidity (%)	Carbon Dioxide (ppm)
Standard Deviation	0.13	0.40	6.29

High Dust Concentration Practical Test			
Sensor Parameters	Temperature (˚C)	Humidity (%)	Carbon Dioxide (ppm)
Standard Deviation	1.07	1.81	7.46

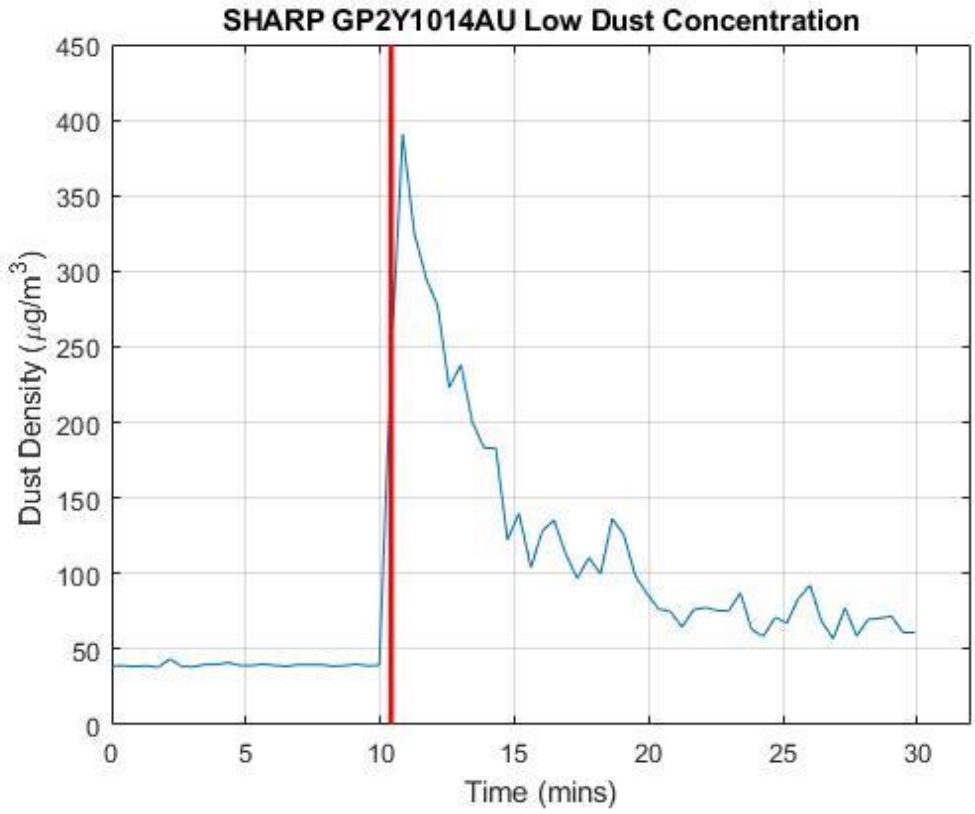

Appendix 36: Low Dust Concentration Sensor Reading

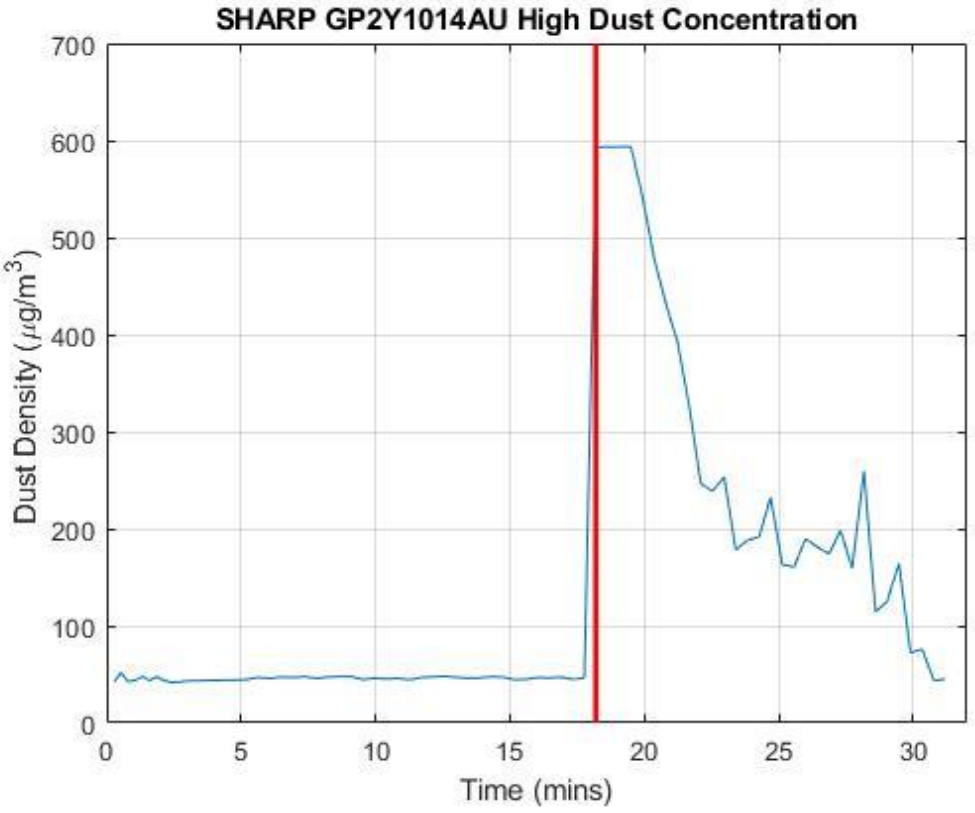

Appendix 37: High Dust Concentration Sensor Reading

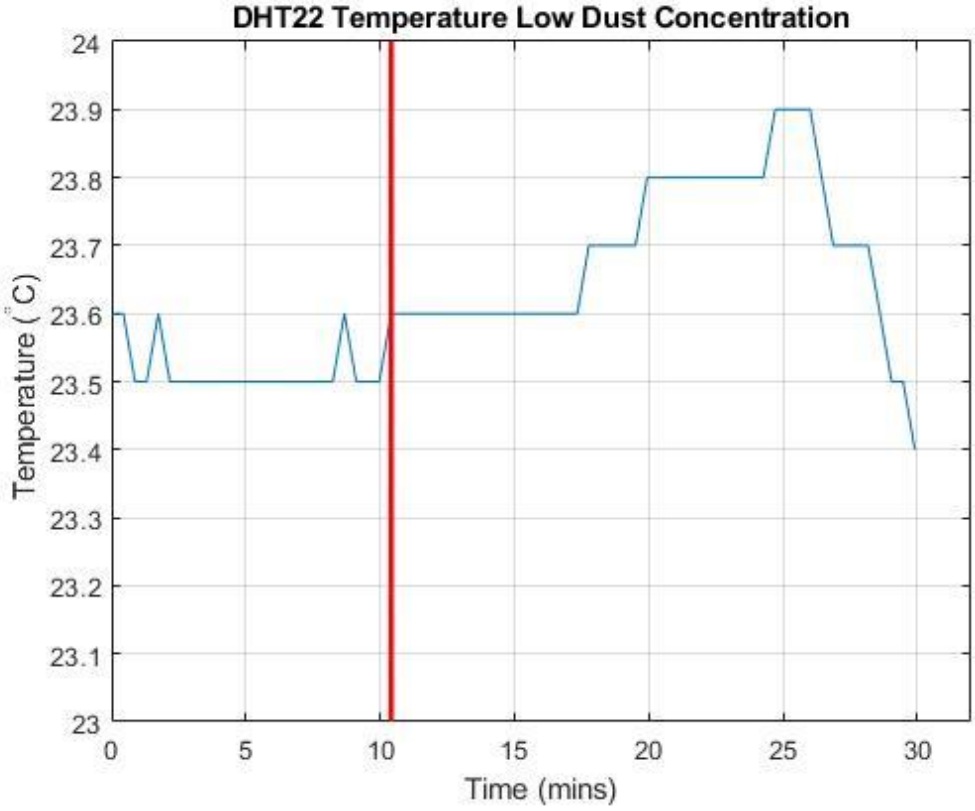

Appendix 38: Temperature Sensor Reading at Low Dust Concentration

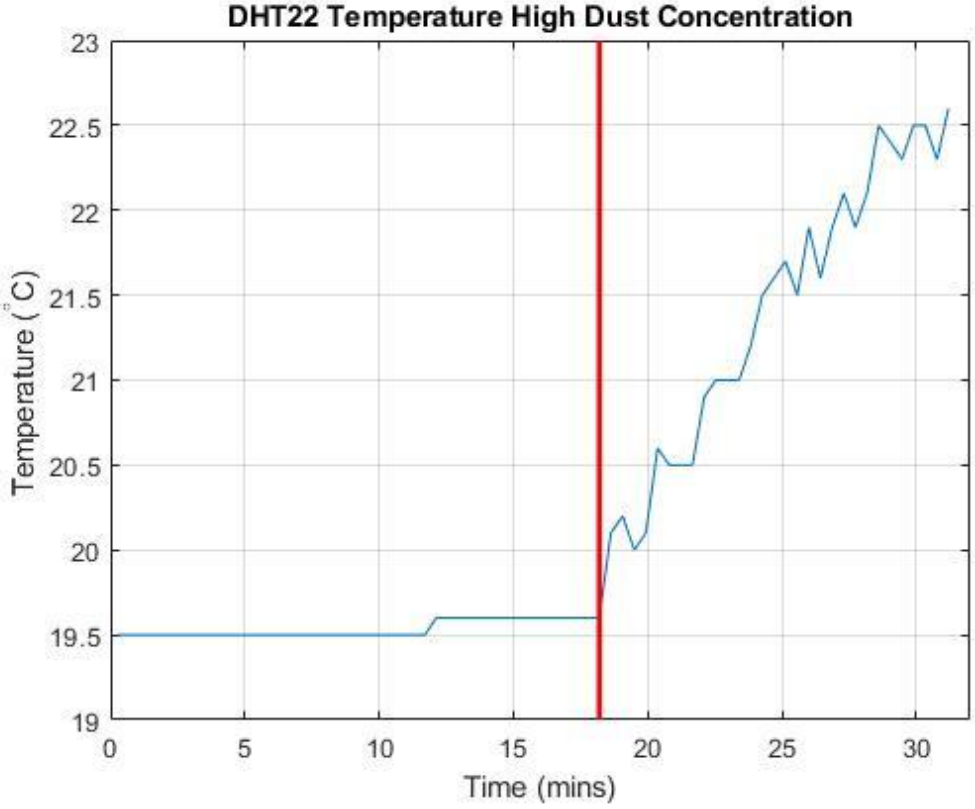

Appendix 39: Temperature Sensor Reading at High Dust Concentration

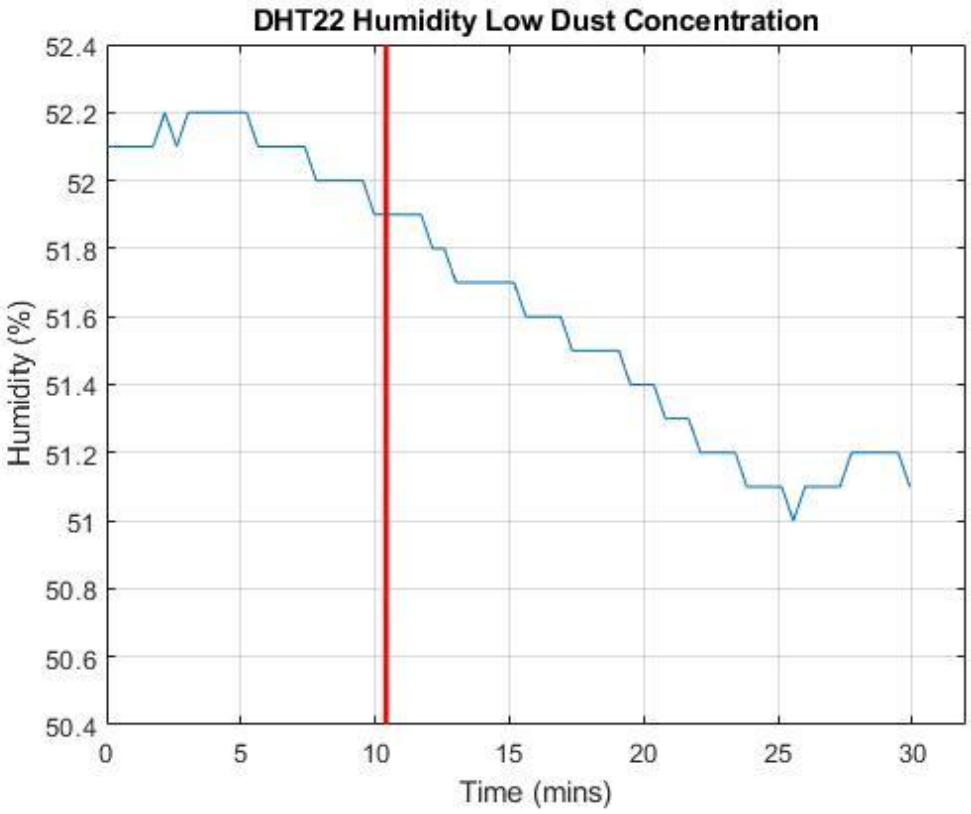

Appendix 40: Humidity Sensor Reading at Low Dust Concentration

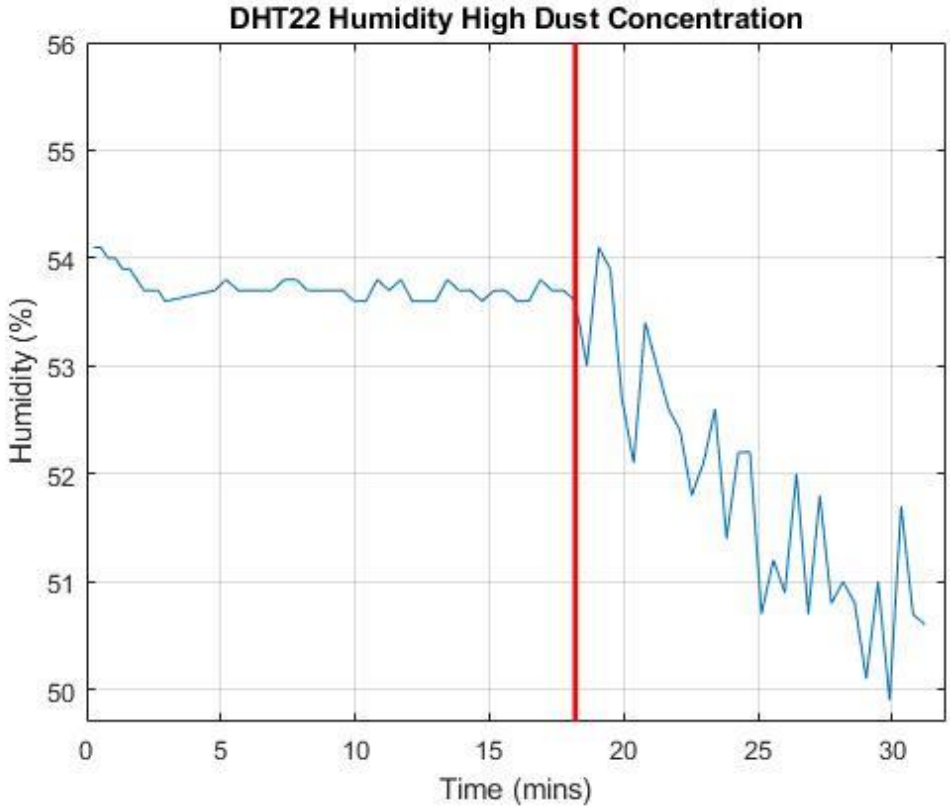

Appendix 41: Humidity Sensor Reading at High Dust Concentration

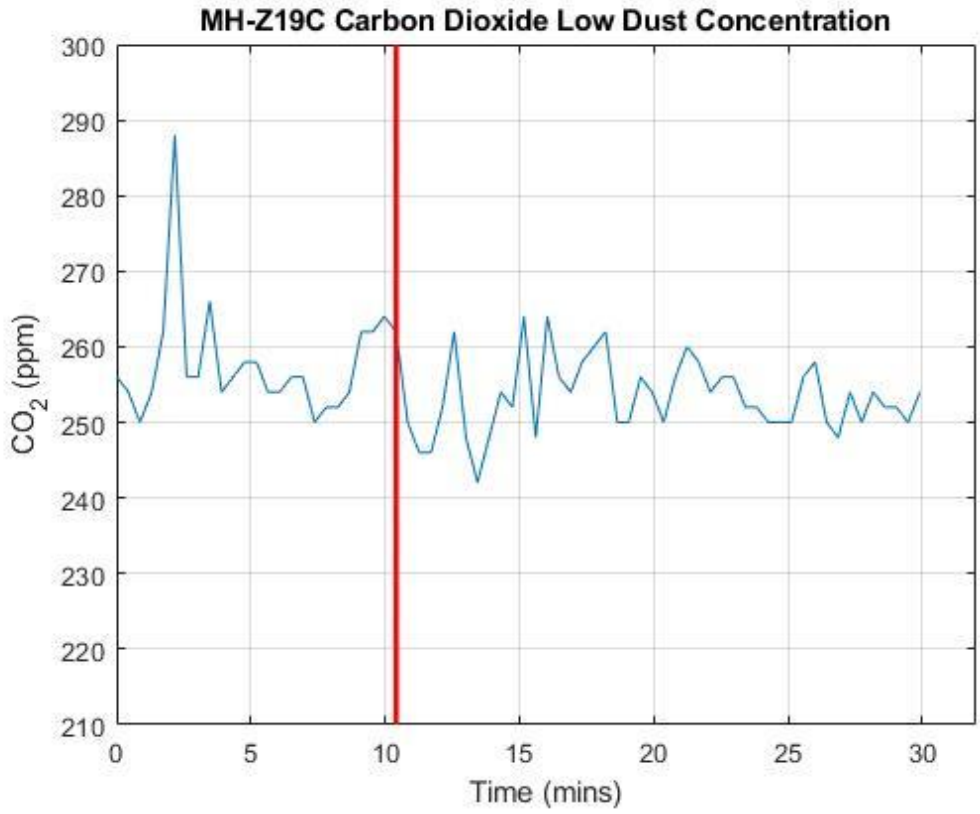

Appendix 42: Carbon Dioxide Sensor Reading at Low Dust Concentration

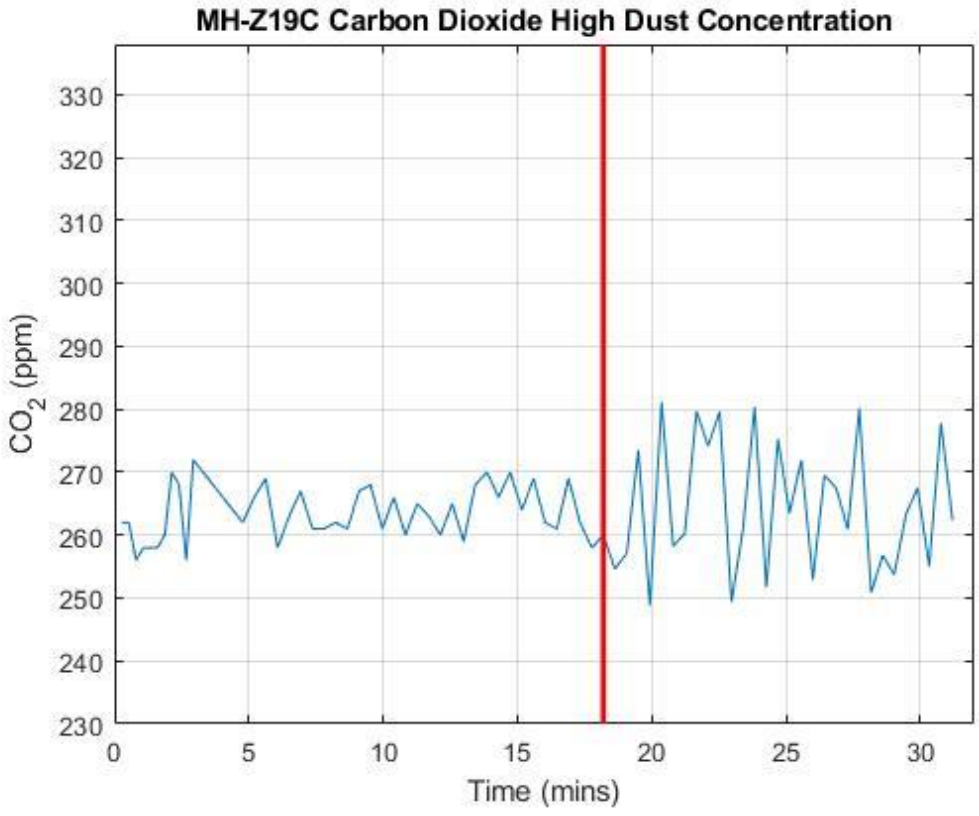

Appendix 43: Carbon Dioxide Sensor Reading at High Dust Concentration

The graphs displayed showcase the reference test up to the end of the practical test with the line in red indicating the increase in the dust concentration. Visually it can be seen that the introduction of dust into the test chamber causes a spike in the temperature reading in both scenarios. However, the higher concentration shows a higher degree of activity and variance in each parameter. This variation is also evident in the humidity reading resulting in a decrease. The carbon dioxide reading appears to align with the reference test at low concentrations however becomes more sporadic as the dust concentration is increased. To analyse and better understand the obtained data, the following tables have been developed to outline the variance in the measurement readings of the practical tests from the reference tests.

Standard Deviation of Variance in Measurement Readings from Dust Concentration Tests		
Parameters	Low Concentration	High Concentration
Temperature	0.09	1.03
Humidity	0.32	1.68
Carbon Dioxide	1.25	3.28

From the table, the data shows that there is an overall correlation between higher dust concentrations affecting the accuracy of the measurement readings. However, these variations of standard deviation are relatively small concerning the application of the health monitoring system and an accuracy error of these values wouldn't affect the purpose of the system. To better understand the highest variance, the maximum value of the practical test when compared to the average of the reference test can highlight the degree of error of the system. The following table has been created to analyse this result.

Highest Variance in Measurement Readings from Dust Concentration Tests		
Parameters	Difference in Variation (Low)	Difference in Variation (High)
Temperature	0.3	3
Humidity	0.9	4.18
Carbon Dioxide	0	9.12

From the table, the results showcase the variance seen from the graphs in a numerical format. The low dust concentration test has a low variance for both the temperature and humidity readings and the CO_2 reading remains unaffected. This is different to the high dust concentration test where the variance is much higher and influences the CO_2 reading. This can also be seen from the graphs, where there is a higher activity and variance after the dust concentration reaches a high level.

6.4.3 Continuous Dust Test

From the previous experiments conducted, the results show that the effects of low and high concentrations of dust affect the measurement readings of the tested sensors. To rule out the potential effect of the fan itself skewing the data due to the heat output within the chamber, the test was repeated without the fan implementation. The experiment was also conducted by aggravating the dust multiple times to determine if the sensor readings returned to the same baseline once the dust concentration settled down. The following graphs were prepared using the data from (Appendix 59, 60) in MATLAB.

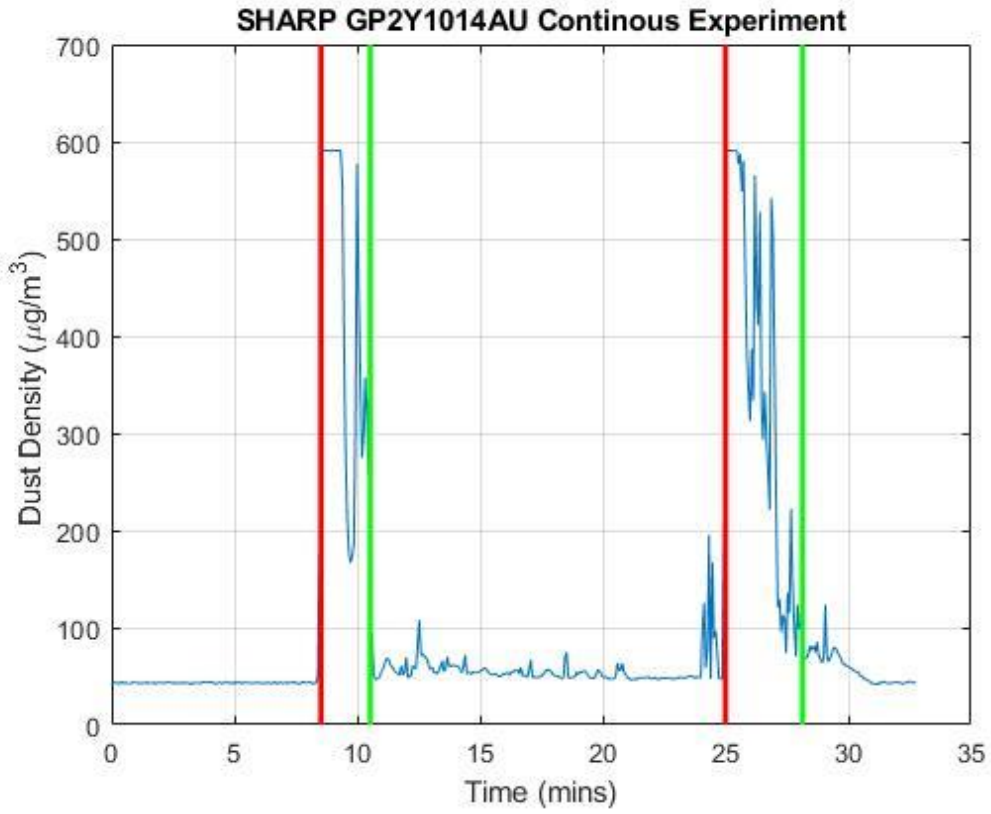

Appendix 44: Dust Concentration Reading during Continuous Experiment

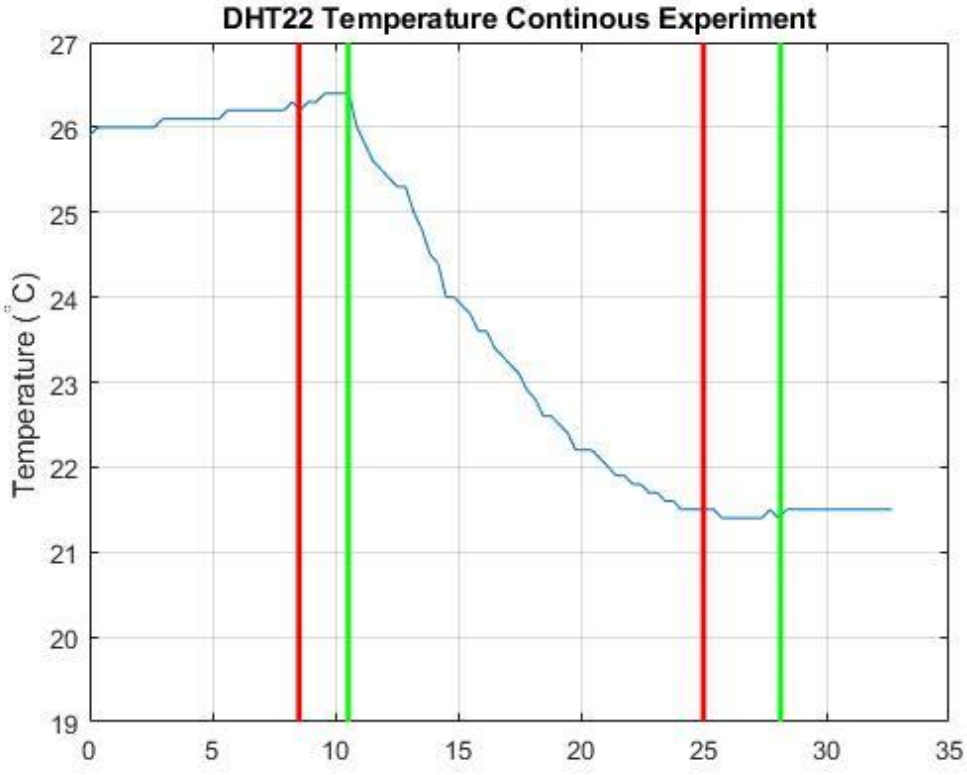

Appendix 45: Temperature Reading during Continuous Experiment

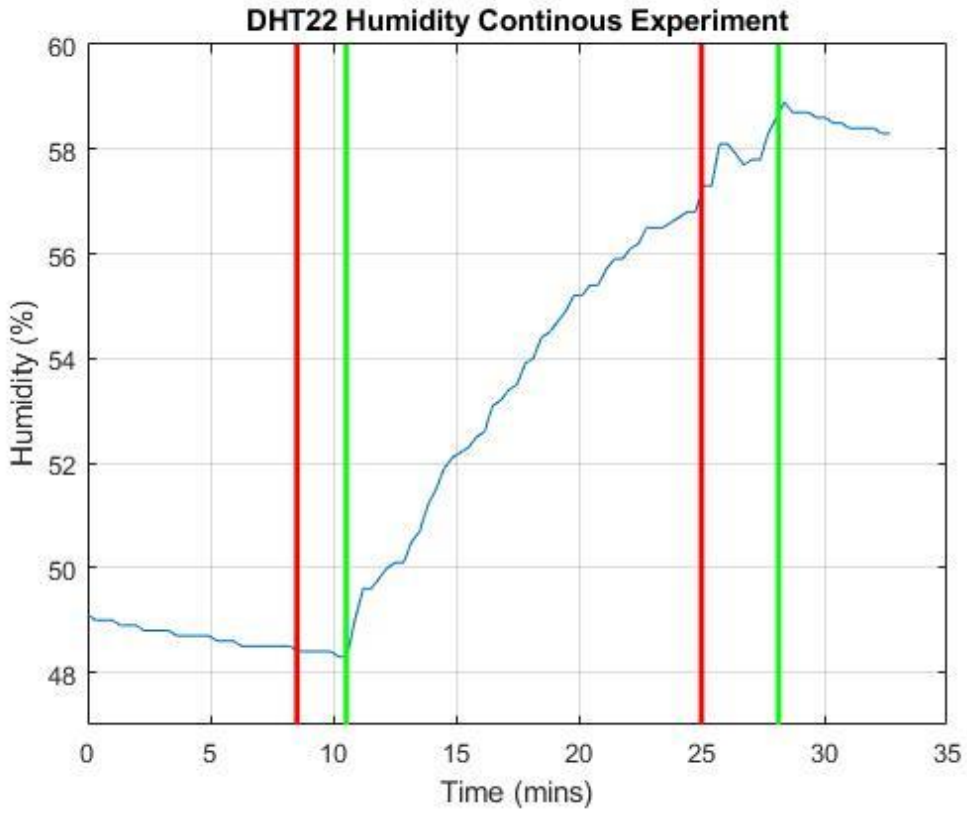

Appendix 46: Humidity Reading during Continuous Experiment

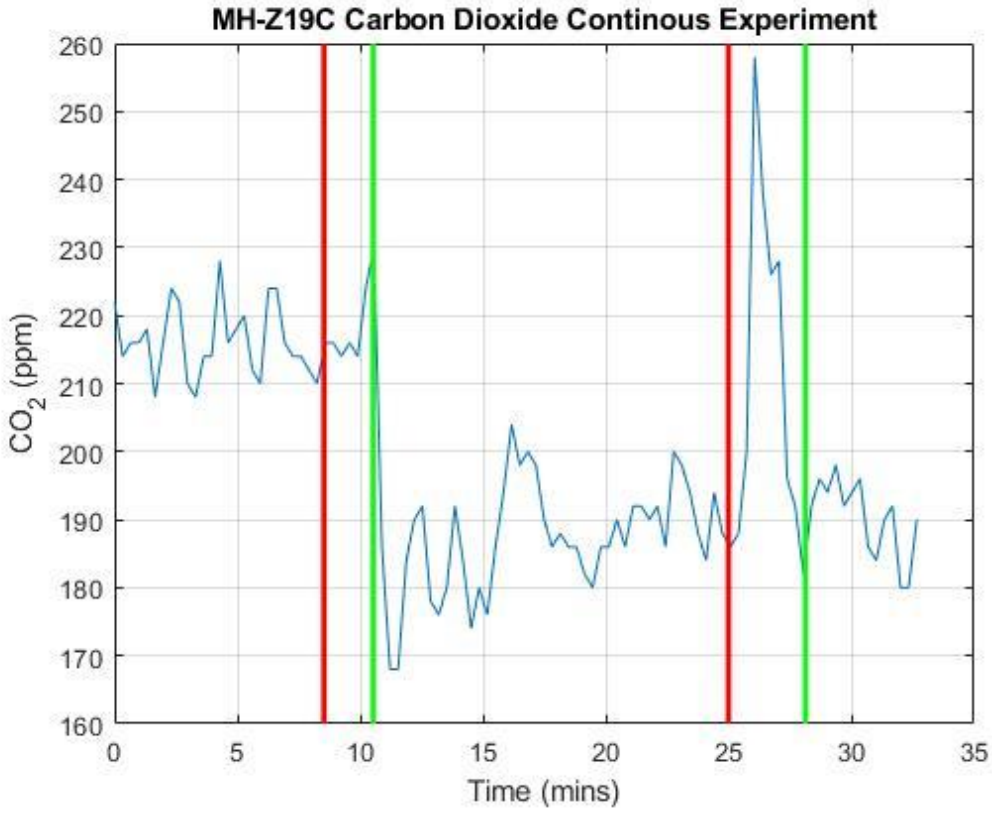

Appendix 47: Carbon Dioxide Reading during Continuous Experiment

From the dust density graph (Appendix 44), the experiment starts with an average stable dust density of 43 $\mu g/m^3$ and increases after aggravation to 590 $\mu g/m^3$. The dust concentration then settles back down to the starting baseline concentration until the concentration is increased a second time. From (Appendix 44), the temperature reading starts to decrease after the chamber experiences an increase in dust concentration. As the dust concentration falls back down to the starting concentration the temperature continues to decrease before levelling out. The second increase in dust concentration appears to not affect the temperature reading however ends with a reading lower than the reading at the start of the test and remains constant to the end of the experiment.

The humidity reading spikes after the same concentration of dust within the chamber is reached and continues to climb at a linear rate as the concentration settles back down to baseline (Appendix 46). Once the second increase in concentration is applied, a second spike can be seen and returns to a slight decline after the second high dust concentration settles.

The CO2 reading decreases dramatically after the first high dust concentration is introduced and fluctuates with the same activity level at the start of the experiment at a lower baseline (Appendix 47). Once the second high dust concentration is applied, the reading spikes to a value 58ppm higher than the previous reading. The value then decreases to the starting value before the second high dust concentration and continues to fluctuate around the same point.

From these results, the impact of the previous fan usage in the experiment impacting the sensor readings has been ruled out as the sensor readings are still impacted by the high dust concentrations.

6.5 Conclusion

This chapter examined the results from the experiments conducted and explored the validity and accuracy of the sensor readings. It identified the effects of harsh conditions that the system would encounter in real-world application and the efficacy of the design on the requirements sought out to meet.

7 Conclusions

7.1 Introduction

The purpose of this research project was to design a health monitoring system for use in the mining industry to potentially create a safer monitored environment for affected workers. The objective of this research was to investigate the limiting factors of existing health monitoring devices and conduct experimentation on the effectiveness of the proposed system under harsh mining conditions. The literature review reflected this knowledge gap with several systems existing as a concept and limited testing on the effects of a mining environment on the accuracy of the sensor readings.

7.2 Findings and Evaluation

The design proved to be successful in most areas experimented upon and would be a benefit to mining workers' health, especially in areas with limited technology. The heart rate detection portion of the system was fairly accurate and adjusted correctly to an increase in heart rate from physical exertion. The effects of high temperature and high humidity on each sensor tested were within reason and didn't provide a degree of error that affected the efficacy of the system. The greatest design restriction was the impact of dust on the system. However, from the tests conducted, the results showed that the variation was small considering the application of the system and would be adequate for providing an early warning detection for potential risks. However, if a high-accuracy reading was needed, the proposed system would be inadequate for providing such a reading.

7.3 Further Work and Recommendations

The initial design included the implementation of various sensors to measure carbon monoxide, methane, and smoke in the environment. After considering the health risks involved in testing such sensors, it was chosen to avoid testing such sensors. Commercial-grade instruments capable of testing these gas types were also proven costly and exceeded the budget for this project. It's recommended that if the finances allowed for acquiring such instruments, the data gathered would provide a more robust system and a greater understanding of the accuracy and efficacy of these sensors.

The design was also tested using a mock experiment scenario which was limited to exploring higher ranges of humidity and carbon dioxide. To further the research into whether the system is effective in a real-world scenario, field testing would prove beneficial to gather real-world data for analysis.

The heart rate sensor was only tested at the current humidity and temperature of the room the experiment was conducted. Testing at higher temperature and humidity ranges was considered but due to the potential harm inflicted on the test subject under such conditions, testing was avoided. With the correct safety procedures, this may be a feasible experiment and would provide a better understanding of the efficacy of this sensor in a real-world scenario.

The battery life of the system although mathematically calculated, wasn't tested to determine if the system was capable of being run over the required time of a working shift. Further experimentation on this issue would provide a better conclusion on the usability of the design.

Overall, the experiments were limited to a time constraint and provided data in a limited window of time. Further work would be beneficial to extend this time constraint and provide a larger amount of data to analyse the sensor readings over time.

7 References

Cortes-Ramirez, J. *et al.* (2022) "Mapping the morbidity risk associated with coal mining in Queensland, Australia," *International Journal of Environmental Research and Public Health*, 19(3), p. 1206. Available at: https://doi.org/10.3390/ijerph19031206.

Porselvi, T. *et al.* (2021) "IOT based Coal Mine Safety and Health Monitoring System using Lorawan," *2021 3rd International Conference on Signal Processing and Communication (ICPSC)* [Preprint]. Available at: https://doi.org/10.1109/icspc51351.2021.9451673.

The Arduino Team (2023) *The Arduino Guide to Lora® and LoRaWAN®: Arduino Documentation*, *Arduino Documentation | Arduino Documentation*. Available at: https://docs.arduino.cc/learn/communication/lorawan-101 (Accessed: March 20, 2023).

Rudrawar, M. *et al.* (2022) "Coal Mine Safety Monitoring and alerting system with smart helmet," *ITM Web of Conferences*, 44, p. 01005. Available at: https://doi.org/10.1051/itmconf/20224401005.

Queensland Government, Department of Natural Resources, Mines and Energy, (2019) *Methane management in underground coal mines Best practice and recommendations*. Available at: https://www.resources.qld.gov.au/__data/assets/pdf_file/0004/1449121/methane-management-in-underground-coal-mines.pdf (Accessed: 02 June 2023).

Queensland Department of Natural Resources and Mines (2020) *Flammable and toxic gases in open cut coal mines*, *Resources Safety and Health Queensland*. Queensland Department of Natural Resources and Mines. Available at: https://www.rshq.qld.gov.au/safety-notices/mines/flammable-and-toxic-gases-in-open-cut-coal-mines (Accessed: April 23, 2023).

Department of Natural Resources, Mines and Energy (2019) *Methane management in underground coal mines - resources.qld.gov.au*. Available at: https://www.resources.qld.gov.au/__data/assets/pdf_file/0004/1449121/methane-management-in-underground-coal-mines.pdf (Accessed: April 23, 2023).

The Arduino Team (2018) *What is Arduino?*, *Arduino*. Available at: https://www.arduino.cc/en/Guide/Introduction (Accessed: March 2, 2023).

Kumar, E.S. (2022) "Arduino working principle and it's use in Education," *International Journal for Research in Applied Science and Engineering Technology*, 10(4), pp. 2314–2319. Available at: https://doi.org/10.22214/ijraset.2022.41784.

Velders, A.H., Schoen, C. and Saggiomo, V. (2018) "Loop-mediated isothermal amplification (LAMP) shield for Arduino DNA detection," *BMC Research Notes*, 11(1). Available at: https://doi.org/10.1186/s13104-018-3197-9.

The Arduino Team (2023) *Arduino Xbee Shield*, *Arduino Documentation*. Available at: https://docs.arduino.cc/retired/shields/arduino-xbee-shield (Accessed: May 1, 2023).

Core Electronics (2023) *Xbee Shield for Arduino, Core Electronics*. Available at: https://core-electronics.com.au/xbee-shield-for-arduino.html?gclid=CjwKCAjwjMiiBhA4EiwAZe6jQwDNEFJUC7QF3LTIAsVwV5kj_-JjfPMiAYuV1NlFolwbu4cWsbrRARoCchMQAvD_BwE (Accessed: May 4, 2023).

Karthik *et al.* (2021) *Setting up zigbee communication to transfer data between Arduino and NODEMCU using XBee modules, IoT Design Pro - IoT Projects, Articles & News*. Available at: https://iotdesignpro.com/projects/setting-up-zigbee-communication-to-transfer-data-between-arduino-and-nodemcu-using-xbee-modules (Accessed: May 4, 2023).

Haque, K.F., Abdelgawad, A. and Yelamarthi, K. (2022) 'Comprehensive performance analysis of zigbee communication: An experimental approach with XBee S2C module', *Sensors*, 22(9), p. 3245. doi:10.3390/s22093245.

Buthelezi, B.E. *et al.* (2018) 'A new tree routing protocol for Zigbee Healthcare Monitoring Systems', *2018 International Conference on Intelligent and Innovative Computing Applications (ICONIC)* [Preprint]. doi:10.1109/iconic.2018.8601221.

Sai Phani Gopal, B.V., Akash, P. and Sri, P.S.G.A. (2019) "Design Of Iot Based Coal Mine Safety System Using Nodemcu," *International Journal of Innovative Technology and Exploring Engineering (IJITEE)* [Preprint].

Jain, R.K., Cui, Z."C. and Domen, J.K. (2016) "Environmental impacts of Mining," *Environmental Impact of Mining and Mineral Processing*, pp. 53–157. Available at: https://doi.org/10.1016/b978-0-12-804040-9.00004-8.

Queensland;, c=A.U.o=T.S.of (2017) *Sulfur dioxide, Queensland Government*. corporateName=The State of Queensland; jurisdiction=Queensland. Available at: https://www.qld.gov.au/environment/management/monitoring/air/air-pollution/pollutants/sulfur-dioxide#:~:text=Sulfur%20dioxide%20affects%20the%20respiratory,as%20asthma%20and%20chronic%20bronchitis. (Accessed: March 17, 2023).

Mardonova, M. and Choi, Y. (2018) "Review of Wearable Device Technology and its applications to the mining industry," *Energies*, 11(3), p. 547. Available at: https://doi.org/10.3390/en11030547.

Ashutosh Patri, A., Jayanthu, S. and Nayak, A. (2013) "Wireless Communication Systems For Underground Mines – A Critical Appraisal," *International Journal of Engineering Trends and Technology(IJETT)* , 4(7).

Proctor, B. (2021) *Bluetooth vs. Bluetooth Low Energy: What's the difference? [2021 update]: Blog: Link labs, Blog | Link Labs*. Available at: https://www.link-labs.com/blog/bluetooth-vs-bluetooth-low-energy#:~:text=The%20difference%20lies%20in%20how,years%20at%20a%20cheaper%20cost. (Accessed: April 2, 2023).

Smiley, S. (2019) *Active RFID vs. passive RFID: What's the difference?*, *atlasRFIDstore*. Available at: https://www.atlasrfidstore.com/rfid-insider/active-rfid-vs-passive-rfid (Accessed: April 1, 2023).

Espressif Systems (2023) "ESP8266EX Datasheet." Available at: https://doi.org/https://www.espressif.com/sites/default/files/documentation/0a-esp8266ex_datasheet_en.pdf.

Lee, W.-H. *et al.* (2022) "Development of digital device using Zigbee for environmental monitoring in underground mines," *Applied Sciences*, 12(23), p. 11927. Available at: https://doi.org/10.3390/app122311927.

Rosencrance, L. (2017) *What is zigbee?: Definition from TechTarget, IoT Agenda*. TechTarget. Available at: https://www.techtarget.com/iotagenda/definition/ZigBee (Accessed: April 7, 2023).

OSEPP Electronics (no date) *Temperature and Humidity Module DHT11 Product Manual*. OSEPP Electronics.

Aosong Electronics Co.,Ltd (no date) *Digital-output relative humidity & temperature sensor/module DHT22*. Available at: https://www.sparkfun.com/datasheets/Sensors/Temperature/DHT22.pdf (Accessed: 27 May 2023).

Heyasa, B.B. and Galarpe, V.R. (2017) "Preliminary development and testing of microcontroller-MQ2 GAS SENSORFOR University Air Quality Monitoring," *IOSR Journal of Electrical and Electronics Engineering*, 12(03), pp. 47–53. Available at: https://doi.org/10.9790/1676-1203024753.

Fire detection for underground mining (2021) *Australasian Mine Safety Journal*. Available at: https://www.amsj.com.au/fire-detection-for-underground-mining/ (Accessed: May 3, 2023).

Kim, S.-M., Choi, Y. and Suh, J. (2020) "Applications of the open-source hardware Arduino platform in the mining industry: A Review," *Applied Sciences*, 10(14), p. 5018. Available at: https://doi.org/10.3390/app10145018.

Maheswari, D.S.U. *et al.* (2019) "WIRELESS HEALTH MONITORING SYSTEM IN MINE AREAS USING nRF24L01," *International Research Journal of Engineering and Technology (IRJET)* [Preprint].

Richa *et al.* (2021) *An IOT based health monitoring system using Arduino Uno*, *International Journal of Engineering Research & Technology*. IJERT-International Journal of Engineering Research & Technology. Available at: https://www.ijert.org/an-iot-based-health-monitoring-system-using-arduino-uno (Accessed: April 22, 2023).

Anitha, K. and Seshagiri, T. (2019) "Implementation of Wireless Sensor in Coal Mine Safety System using ZigBee," *International Research Journal of Engineering and Technology (IRJET)* [Preprint].

Jo, B.W. and Khan, R. (2018) "An internet of things system for underground mine air quality pollutant prediction based on Azure Machine Learning," *Sensors*, 18(4), p. 930. Available at: https://doi.org/10.3390/s18040930.

. Jo, B. and Khan, R. (2017) "An event reporting and early-warning safety system based on the internet of things for underground coal mines: A case study," *Applied Sciences*, 7(9), p. 925. Available at: https://doi.org/10.3390/app7090925.

VISWASMAYEE, P. *et al.* (2018) 'LabVIEW based real time monitoring system for coal mine worker', *i-manager's Journal on Digital Signal Processing*, 6(4), p. 1. doi:10.26634/jdp.6.4.16096.

Harvard Health Monitoring Harvard Medical School; (2020) *What your heart rate is telling you, Harvard Health*. Available at: https://www.health.harvard.edu/heart-health/what-your-heart-rate-is-telling-you (Accessed: 23 May 2023).

Unsal, E. *et al.* (2016) 'Power management for wireless sensor networks in underground mining', *2016 24th Signal Processing and Communication Application Conference (SIU)* [Preprint]. doi:10.1109/siu.2016.7495924.

Donoghue, A.M. (2000) 'Heat exhaustion in a deep underground metalliferous mine', *Occupational and Environmental Medicine*, 57(3), pp. 165–174. doi:10.1136/oem.57.3.165.

TKJElectronics (2012) *TKJElectronics/kalmanfilter: This is a Kalman filter used to calculate the angle, rate and bias from from the input of an accelerometer/magnetometer and a gyroscope., GitHub*. Available at: https://github.com/TKJElectronics/KalmanFilter (Accessed: 03 July 2023).

CSIRO (2022) *Greenhouse gases, CSIRO*. Available at: https://www.csiro.au/en/research/environmental-impacts/climate-change/state-of-the-climate/greenhouse-gases (Accessed: 22 August 2023).

8 Appendices

Appendix 48: Humidity and Temperature Test of DHT22 Sensor

DHT22 Humidity and Temperature Test					
Time (s)	Time (mins)	DHT22 Humidity (%)	Ozito Humidity %	DHT22 Temperature (˚C)	Ozito Temperature (˚C)
0	0	44.5	42.28	18.66	17.50
12.12	0.2	44.5	44.2	17.68	17.39
24.24	0.4	45.1	44.76	17.84	17.56
36.36	0.61	46.5	45.65	19.10	17.71
48.48	0.81	45.3	45.42	19.03	20.56
60.6	1.01	44.2	44.36	18.74	19.01
72.72	1.21	44.1	44.09	18.92	19.03
84.84	1.41	44.4	43.72	17.64	18.70
96.96	1.62	45.3	44.66	17.88	17.95
109.08	1.82	43.8	44.74	17.45	15.88
121.2	2.02	44.2	44.05	19.34	19.47
133.32	2.22	45.4	45.68	18.09	16.49
145.44	2.42	45.2	46.18	19.27	19.45
157.56	2.63	45.5	45.26	17.92	15.93
169.68	2.83	47.6	44.54	18.37	18.15
181.8	3.03	49.2	46.86	19.44	20.75
193.92	3.23	47.8	50.29	18.31	20.22
206.04	3.43	48	47.65	19.64	19.77
218.16	3.64	49.4	48.37	18.13	16.80
230.28	3.84	49.4	49.4	19.99	21.37
242.4	4.04	48.6	49.93	18.40	19.88
254.52	4.24	52.5	50.16	19.86	19.49
266.64	4.44	53.9	54.04	19.54	18.97
278.76	4.65	52.8	54.44	19.33	20.49
290.88	4.85	53	51.68	20.60	18.76
303	5.05	54.4	52.53	20.71	22.58
315.12	5.25	50.4	55.21	19.60	19.67
327.24	5.45	50.4	49.8	20.35	21.21
339.36	5.66	45.6	50.92	21.16	22.30
351.48	5.86	44.2	44.33	20.00	21.47
363.6	6.06	51.6	45.22	21.62	19.87
375.72	6.26	54.3	53.05	21.18	19.49
387.84	6.46	54.3	53.87	21.33	20.78
399.96	6.67	50.7	54.65	22.00	20.44
412.08	6.87	53	50.26	21.95	23.07
424.2	7.07	50.1	53.49	22.25	21.18
436.32	7.27	50.1	50	20.80	20.35
448.44	7.47	49.4	49.16	21.39	20.32
460.56	7.68	48.2	49.66	21.63	21.43
472.68	7.88	47.3	49.37	23.11	22.23
484.8	8.08	47.3	48.15	23.11	24.96
496.92	8.28	47.3	48.72	22.42	20.96

509.04	8.48	56.4	50.14	22.43	21.10
521.16	8.69	53.1	57.41	24.26	25.45
533.28	8.89	60.8	53.37	22.75	21.83
545.4	9.09	60.8	60.44	23.84	22.25
557.52	9.29	61.8	60.63	23.34	21.71
569.64	9.49	58.6	61.77	23.67	22.76
581.76	9.7	56.2	57.88	25.06	27.06
593.88	9.9	55.2	56.11	25.21	26.58
606	10.1	55.2	56.41	26.08	26.27
618.12	10.3	54	56.07	24.66	23.96
630.24	10.5	53.2	52.22	26.55	28.35
642.36	10.71	52.9	54.63	26.21	28.06
654.48	10.91	53.1	52.94	26.00	24.12
666.6	11.11	53.3	52.82	26.79	28.10
678.72	11.31	53.3	54.15	26.14	24.24
690.84	11.51	52.6	53.27	27.36	27.39
702.96	11.72	52.1	53.55	27.47	28.90
715.08	11.92	62.6	53.82	26.89	27.89
727.2	12.12	83.1	65.03	28.59	28.90
739.32	12.32	84.6	85.24	28.68	28.54
751.44	12.52	84.6	82.4	29.72	29.72
763.56	12.73	85	82.82	28.58	30.48
775.68	12.93	84.4	82.5	29.59	28.68
787.8	13.13	84	83.98	29.51	30.71
799.92	13.33	83.1	83.65	29.50	30.32
812.04	13.53	83	84.24	30.73	30.39
824.16	13.74	82.2	80.85	30.11	30.83
836.28	13.94	80	83.4	31.77	32.42
848.4	14.14	80	78.88	31.13	32.41
860.52	14.34	73.3	79.01	32.96	31.32
872.64	14.54	68.6	73.94	32.42	31.90
884.76	14.75	63.9	66.98	32.16	31.22
896.88	14.95	62.2	63.56	32.70	32.02
909	15.15	59.5	60.81	34.43	35.81
921.12	15.35	57.4	59.31	34.77	35.91
933.24	15.55	57.3	58.07	33.77	34.74
945.36	15.76	54.9	56.95	34.15	35.55
957.48	15.96	54.2	54.43	35.53	34.46
969.6	16.16	54.2	54.85	36.53	36.96
981.72	16.36	53.7	53.45	35.28	35.76
993.84	16.56	52.4	54.83	35.82	36.20
1005.96	16.77	52.3	53.01	36.44	36.73
1018.08	16.97	51.6	52.47	37.73	35.92
1030.2	17.17	51.6	51.5	38.13	38.28
1042.32	17.37	52	52.81	39.00	40.58
1054.44	17.57	51.5	51.07	39.97	38.44
1066.56	17.78	50	51.4	40.44	38.69
1078.68	17.98	48.9	50.38	40.89	42.10
1090.8	18.18	49.1	47.77	40.51	38.78
1102.92	18.38	48.6	49.1	40.64	41.48
1115.04	18.58	47.7	49.48	41.47	41.55

1127.16	18.79	48	47.19	41.73	40.72
1139.28	18.99	48	46.94	42.60	42.88
1151.4	19.19	48	48.29	42.44	43.53
1163.52	19.39	47.2	48.13	43.39	43.96
1175.64	19.59	45.9	47.23	43.68	42.57
1187.76	19.8	45.5	46.74	44.22	45.01
1199.88	20	45.5	46.59	45.78	46.26

S.D Humidity	2.94
S.D Temperature	1.17

Appendix 49: Resting Heart Rate Test of DFRobot Heart Rate Sensor

Resting Heart Rate, Temp = 20˚C, Humidity = 40% (First Test)			
Time (s)	DFRobot Sensor (bpm)	Polar Sensor (bpm)	Difference (bpm)
1	62	62	0
2	62	62	0
3	56	62	-6
4	63	62	1
5	85	62	23
6	68	62	6
7	69	62	7
8	63	62	1
9	66	62	4
10	57	62	-5
11	67	62	5
12	122	62	60
13	68	62	6
14	61	62	-1
15	61	62	-1
16	61	62	-1
17	63	60	3
18	62	60	2
19	63	60	3
20	68	60	8
21	53	60	-7
22	59	60	-1
23	64	60	4
24	118	60	58
25	62	59	3
26	127	59	68
27	58	59	-1
28	59	58	1
29	60	58	2
30	61	58	3
31	64	58	6
32	60	58	2
33	63	58	5
34	72	58	14
35	64	58	6
36	64	58	6
37	67	58	9
38	120	58	62
39	65	58	7

40	60	58	2
41	127	58	69
42	60	58	2
43	58	58	0
44	58	58	0
45	51	58	-7
46	60	58	2
47	60	58	2
48	69	67	2
49	62	67	-5
50	57	67	-10
51	60	67	-7
52	62	67	-5
53	61	67	-6
54	61	55	6
55	61	55	6
56	112	55	57
57	71	55	16
58	64	55	9
59	137	55	82
60	64	55	9
61	65	55	10
62	57	55	2
63	72	55	17
64	60	55	5
65	68	55	13
66	63	55	8
67	46	55	-9
68	130	55	75
69	50	55	-5
70	69	55	14
71	62	55	7
72	56	55	1
73	46	55	-9
74	75	55	20
75	116	55	61
76	64	55	9
77	64	55	9
78	67	55	12
79	64	55	9
80	66	55	11
81	62	55	7
82	64	55	9
83	130	55	75
84	67	55	12

85	66	55	11
86	58	55	3
87	69	55	14
88	71	55	16
89	62	55	7
90	64	55	9
91	61	55	6
92	65	55	10
93	63	55	8
94	62	55	7
95	63	55	8
96	63	55	8
97	130	55	75
98	71	55	16
99	62	55	7
100	70	55	15
101	127	55	72
102	64	55	9
103	62	55	7
104	139	55	84
105	64	55	9
106	64	55	9
107	65	55	10
108	66	55	11
109	68	55	13
110	65	55	10
111	64	64	0
112	65	64	1
113	66	64	2
114	68	64	4
115	69	64	5
116	64	64	0
117	62	64	-2
118	61	64	-3
119	65	64	1
120	68	61	7
121	61	61	0
122	58	61	-3
123	61	61	0
124	68	61	7
125	56	61	-5
126	58	61	-3
127	66	61	5
128	111	61	50
129	68	61	7

130	58	61	-3
131	67	61	6
132	60	61	-1
133	63	61	2
134	68	61	7
135	67	61	6
136	70	61	9
137	65	61	4
138	70	61	9
139	58	61	-3
140	62	61	1
141	60	61	-1
142	69	61	8
143	64	61	3
144	66	61	5
145	67	61	6
146	57	61	-4
147	59	61	-2
148	58	61	-3
149	64	61	3
150	59	61	-2
151	60	61	-1
152	121	61	60
153	62	61	1
154	65	61	4
155	60	61	-1
156	69	61	8
157	65	61	4
158	64	61	3
159	64	61	3
160	62	61	1
161	65	61	4
162	59	61	-2
163	57	61	-4
164	68	61	7
165	69	61	8
166	63	61	2
167	57	61	-4
168	64	61	3
169	60	61	-1
170	66	61	5
171	62	61	1
172	60	61	-1
173	60	61	-1
174	61	61	0

175	58	61	-3
176	61	61	0
177	63	61	2
178	60	61	-1
179	57	61	-4
180	65	61	4

Standard Deviation (bpm)	3.28

Appendix 50: Resting Heart Rate Test of DFRobot Heart Rate Sensor with Filtering

Resting Heart Rate Temp = 20˚C, Humidity = 40% (Kalman Filter)			
Time (s)	DFRobot Sensor (bpm)	Polar Sensor (bpm)	Difference (bpm)
1	61	60	1
2	64	60	4
3	62	60	2
4	57	60	-3
5	61	60	1
6	58	60	-2
7	59	60	-1
8	60	60	0
9	62	60	2
10	61	60	1
11	61	60	1
12	64	60	4
13	64	60	4
14	58	60	-2
15	65	60	5
16	63	60	3
17	65	60	5
18	62	60	2
19	56	60	-4
20	63	60	3
21	62	60	2
22	56	60	-4
23	60	60	0
24	63	60	3
25	57	59	-2
26	57	59	-2
27	57	59	-2
28	62	58	4
29	56	58	-2
30	64	58	6
31	62	58	4
32	57	58	-1
33	56	58	-2
34	63	58	5
35	58	58	0
36	62	58	4
37	59	58	1
38	60	58	2
39	59	58	1

40	59	58	1
41	61	58	3
42	57	58	-1
43	56	58	-2
44	65	58	7
45	63	58	5
46	65	58	7
47	56	58	-2
48	57	55	2
49	51	55	-4
50	53	55	-2
51	55	55	0
52	51	55	-4
53	51	55	-4
54	56	55	1
55	53	55	-2
56	54	55	-1
57	51	55	-4
58	56	55	1
59	55	55	0
60	54	55	-1
61	55	55	0
62	55	55	0
63	51	55	-4
64	55	55	0
65	52	55	-3
66	57	55	2
67	57	55	2
68	51	55	-4
69	57	55	2
70	56	55	1
71	55	55	0
72	55	55	0
73	53	55	-2
74	52	55	-3
75	54	55	-1
76	52	55	-3
77	55	55	0
78	55	55	0
79	53	55	-2
80	52	55	-3
81	54	55	-1
82	53	55	-2
83	57	55	2
84	55	55	0

85	52	55	-3
86	54	55	-1
87	54	55	-1
88	57	55	2
89	55	55	0
90	56	55	1
91	54	55	-1
92	56	55	1
93	53	55	-2
94	53	55	-2
95	57	55	2
96	55	55	0
97	54	55	-1
98	52	55	-3
99	56	55	1
100	56	55	1
101	53	55	-2
102	56	55	1
103	51	55	-4
104	57	55	2
105	52	55	-3
106	53	55	-2
107	56	55	1
108	55	55	0
109	52	55	-3
110	56	55	1
111	53	62	-9
112	63	62	1
113	68	62	6
114	64	62	2
115	67	62	5
116	65	62	3
117	64	62	2
118	64	62	2
119	63	62	1
120	64	61	3
121	67	61	6
122	65	61	4
123	68	61	7
124	62	61	1
125	66	61	5
126	65	61	4
127	65	61	4
128	62	61	1
129	62	61	1

130	62	61	1
131	63	61	2
132	66	61	5
133	67	61	6
134	64	61	3
135	63	61	2
136	64	61	3
137	64	61	3
138	64	61	3
139	62	61	1
140	68	61	7
141	65	61	4
142	65	61	4
143	66	61	5
144	68	61	7
145	65	61	4
146	62	61	1
147	65	61	4
148	65	61	4
149	62	61	1
150	62	61	1
151	67	61	6
152	62	61	1
153	68	61	7
154	63	61	2
155	64	61	3
156	64	61	3
157	64	61	3
158	64	61	3
159	62	61	1
160	64	61	3
161	68	61	7
162	63	61	2
163	62	60	2
164	67	60	7
165	63	60	3
166	62	60	2
167	62	60	2
168	64	60	4
169	62	60	2
170	62	60	2
171	63	60	3
172	67	60	7
173	66	60	6
174	66	60	6

175	65	60	5
176	63	60	3
177	68	60	8
178	62	60	2
179	64	60	4
180	67	60	7

Standard Deviation (bpm)	3.016

Appendix 51: Elevated Heart Rate Test of DFRobot Heart Rate Sensor with Filtering

Elevated Heart Rate, Temp = 20˚C, Humidity = 40%		
Time (s)	DFRobot Sensor (bpm)	Polar Sensor (bpm)
5	85	88
10	74	76
15	69	74
20	70	75
25	75	76
30	85	87
35	90	92
40	91	88
45	90	87
50	92	82
55	79	81
60	84	83
65	81	82
70	77	79
75	73	76
80	69	74
85	68	72
90	72	76
95	103	74
100	78	73
105	74	72
110	78	71
115	74	72
120	80	73
125	77	74
130	71	73
135	66	72
140	68	71
145	77	74
150	74	75
155	79	74
160	73	73
165	80	74
170	66	75
175	76	73
180	71	74
185	80	72
190	72	74
195	79	75

200	66	76
205	74	77
210	70	77
215	68	80
220	87	83
225	85	85
230	86	87
235	95	90
240	92	93
245	99	95
250	100	96
255	103	98
260	120	99
265	103	105
270	112	110
275	110	115
280	123	118
285	125	120
290	129	125
295	127	128
300	137	134
305	139	136
310	141	137
315	143	141
320	149	145
325	142	148
330	154	151
335	159	154
340	155	158
345	158	160
350	153	159
355	151	158
360	164	160
365	165	159
370	160	159
375	157	158
380	159	159
385	153	160
390	152	160
395	164	159
400	159	160
405	152	159
410	157	160
415	158	159

420	159	159
425	154	159
430	161	160
435	163	159
440	161	160
445	158	160
450	161	160
455	164	160
460	155	159
465	164	160
470	158	159
475	161	160
480	155	159
485	152	158
490	164	160
495	159	158
500	165	159
505	163	160
510	151	159
515	161	159
520	163	158
525	159	160
530	161	159
535	158	160
540	155	159
545	151	160
550	157	158
555	150	160
560	152	159
565	165	160
570	164	159
575	156	158
580	153	157
585	164	160
590	154	158
595	159	159
600	161	160

Appendix 52: Calibration Test of MH-Z19C Carbon Dioxide Sensor

MH-Z19C CO_2 Sensor Calibration Testing			
Time (mins)	Time (s)	MH-Z19C (ppm)	Global Average Mean CO_2 (ppm)
0.00	0	440	414.4
0.23	14	433	414.4
0.50	30	441	414.4
0.92	55	439	414.4
1.22	73	434	414.4
1.48	89	440	414.4
1.70	102	435	414.4
2.10	126	442	414.4
2.47	148	448	414.4
2.83	170	443	414.4
3.10	186	436	414.4
3.35	201	428	414.4
3.78	227	423	414.4
4.13	248	433	414.4
4.33	260	427	414.4
4.70	282	427	414.4
5.02	301	423	414.4
5.42	325	422	414.4
5.80	348	419	414.4
6.25	375	412	414.4
6.53	392	408	414.4
6.72	403	411	414.4
6.87	412	412	414.4
7.08	425	416	414.4
7.30	438	411	414.4
7.65	459	410	414.4
7.92	475	407	414.4
8.32	499	403	414.4
8.78	527	409	414.4
8.93	536	401	414.4
9.33	560	406	414.4
9.47	568	408	414.4
9.93	596	403	414.4
10.20	612	408	414.4
10.38	623	404	414.4
10.82	649	403	414.4
10.95	657	403	414.4
11.10	666	396	414.4
11.48	689	396	414.4

11.65	699	399	414.4
11.92	715	404	414.4
12.17	730	407	414.4
12.48	749	417	414.4
12.73	764	425	414.4
12.98	779	417	414.4
13.27	796	421	414.4
13.68	821	423	414.4
13.97	838	418	414.4
14.28	857	427	414.4
14.52	871	420	414.4
14.75	885	416	414.4
15.10	906	425	414.4

Standard Deviation	13.72
Highest Variance	33.6

Appendix 53: Low Concentration MH-Z19C Carbon Dioxide Sensor Test at High Temperature and High Humidity

Low CO_2 High Humidity and Temperature				
Time (mins)	Time (s)	Temp (˚C)	Humidity (%)	Carbon Dioxide (ppm)
0	0	21.5	53.2	604
0.27	16	21.5	53.2	590
0.53	32	21.5	53	586
0.8	48	21.5	53.1	586
1.07	64	21.4	53	584
1.33	80	21.4	52.9	586
1.6	96	21.4	53	592
1.87	112	21.4	53.4	598
2.13	128	21.4	53	600
2.4	144	21.4	53.2	598
2.67	160	21.5	53.3	594
2.93	176	21.4	52.9	594
3.2	192	21.5	52.9	598
3.47	208	21.5	53	594
3.73	224	21.4	53	594
4	240	21.4	53.6	598
4.27	256	21.4	54.4	602
4.53	272	21.4	54.2	604
4.8	288	21.5	52.9	602
5.07	304	21.5	52.8	600
5.33	320	21.5	52.9	596
5.6	336	21.4	53.9	596
5.87	352	21.4	53.5	606
6.13	368	21.4	54	610
6.4	384	21.5	54.9	612
6.67	400	21.5	54.4	614
6.93	416	21.5	54.7	614
7.2	432	21.5	55.5	624
7.47	448	21.6	56.2	620
7.73	464	21.6	56.3	618
8	480	21.7	56.8	620
8.27	496	21.7	56.9	620
8.53	512	21.7	57	622
8.8	528	21.8	57.1	618
9.07	544	21.9	57.4	612
9.33	560	21.9	57.4	612
9.6	576	21.9	57.4	608
9.87	592	21.9	57.5	608

10.13	608	21.9	57.5	610
10.4	624	21.9	57.6	618
10.67	640	21.9	57.7	616
10.93	656	21.9	57.7	616
11.2	672	21.9	57.8	616
11.47	688	21.9	57.8	608
11.73	704	22.0	57.9	614
12	720	22.0	58	618
12.27	736	22.0	58	624
12.53	752	22.1	58	612
12.8	768	22.2	58	606
13.07	784	22.2	58.1	604
13.33	800	22.2	58.1	610
13.6	816	22.3	58.1	610
13.87	832	22.3	58.1	610
14.13	848	22.4	58.1	612
14.4	864	22.5	58.2	610
14.67	880	22.5	58.2	610
14.93	896	22.5	58.2	610
15.2	912	22.5	58.2	610
15.47	928	22.6	58.1	614
15.73	944	22.6	58.1	612
16	960	22.6	58	612
16.27	976	22.7	58	614
16.53	992	22.8	58	610
16.8	1008	22.8	57.9	614
17.07	1024	23.0	57.8	614
17.33	1040	23.0	57.7	610
17.6	1056	23.1	57.7	610
17.87	1072	23.3	57.4	608
18.13	1088	23.3	57.4	610
18.4	1104	23.3	57.3	608
18.67	1120	23.5	57.2	608
18.93	1136	23.5	57.1	610
19.2	1152	23.6	57	614
19.47	1168	23.8	56.8	612
19.73	1184	23.8	56.8	610
20	1200	23.9	56.6	614
20.27	1216	24.0	56.6	612
20.53	1232	24.2	56.5	614
20.8	1248	24.3	56.4	612
21.07	1264	24.4	56.4	610
21.33	1280	24.5	56.3	612
21.6	1296	24.6	56.3	614
21.87	1312	24.8	56.3	614

22.13	1328	24.9	56.3	612
22.4	1344	25.0	56.3	612
22.67	1360	25.0	56.3	612
22.93	1376	25.2	56.3	610
23.2	1392	25.3	56.2	614
23.47	1408	25.4	56.3	612
23.73	1424	25.4	56.3	610
24	1440	25.5	56.3	610
24.27	1456	25.6	56.3	610
24.53	1472	25.6	56.3	608
24.8	1488	25.7	56.4	608
25.07	1504	25.8	56.4	610
25.33	1520	25.8	56.4	606
25.6	1536	25.9	56.4	610
25.87	1552	26.0	56.5	610
26.13	1568	26.1	56.4	610
26.4	1584	26.2	56.5	610
26.67	1600	26.3	56.5	612
26.93	1616	26.4	56.5	612
27.2	1632	26.5	56.5	610
27.47	1648	26.5	56.6	610
27.73	1664	26.7	56.6	610
28	1680	26.7	56.6	610
28.27	1696	26.7	56.6	612
28.53	1712	26.8	56.6	610
28.8	1728	26.9	56.6	610
29.07	1744	26.9	56.6	610
29.33	1760	27.0	56.7	614
29.6	1776	27.0	56.6	612
29.87	1792	27.1	56.7	610
30.13	1808	27.3	56.8	610
30.4	1824	27.3	56.8	610
30.67	1840	27.4	56.8	612
30.93	1856	27.4	56.8	610
31.2	1872	27.6	56.9	612
31.47	1888	27.6	56.8	612
31.73	1904	27.8	56.9	612
32	1920	27.9	56.9	610
32.27	1936	28.0	57	610
32.53	1952	28.1	57	610
32.8	1968	28.3	57	614
33.07	1984	28.3	57	610
33.33	2000	28.4	57.1	610
33.6	2016	28.5	57.1	610
33.87	2032	28.6	57.1	610

34.13	2048	28.7	57.1	608
34.4	2064	28.8	57.1	610
34.67	2080	29.0	57.1	608
34.93	2096	29.1	57.2	608
35.2	2112	29.1	55.8	610
35.47	2128	29.2	55.7	610
35.73	2144	29.2	55.6	614
36	2160	29.3	56.5	614
36.27	2176	29.4	57.5	616
36.53	2192	29.4	57.7	616
36.8	2208	29.6	58.6	618
37.07	2224	29.6	58.7	618
37.33	2240	29.6	59.3	616
37.6	2256	29.8	59.4	618
37.87	2272	29.9	60.6	616
38.13	2288	30.1	61.1	616
38.4	2304	30.2	61.2	618
38.67	2320	30.4	61.6	620
38.93	2336	30.4	61.9	620
39.2	2352	30.5	62.2	620
39.47	2368	30.6	62.6	618
39.73	2384	30.8	62.8	622
40	2400	30.9	62.9	618
40.27	2416	30.9	63.7	618
40.53	2432	31.0	64.6	616
40.8	2448	31.0	65.5	616
41.07	2464	31.2	66.3	616
41.33	2480	31.2	66.7	614
41.6	2496	31.4	67.1	612
41.87	2512	31.6	67.4	612
42.13	2528	31.8	68.0	610
42.4	2544	31.9	68.5	610
42.67	2560	32.1	69.1	610
42.93	2576	32.3	69.3	612
43.2	2592	32.5	70.2	612
43.47	2608	32.6	71.1	610
43.73	2624	32.6	72.0	614
44	2640	32.8	73.0	616
44.27	2656	32.9	73.8	620
44.53	2672	33.0	74.7	618
44.8	2688	33.0	75.3	618
45.07	2704	33.1	75.8	616
45.33	2720	33.2	76.8	614
45.6	2736	33.2	77.3	616
45.87	2752	33.3	77.8	618

46.13	2768	33.4	78.4	616
46.4	2784	33.4	78.8	616
46.67	2800	33.5	79.6	618
46.93	2816	33.7	79.9	618
47.2	2832	33.8	80.5	616
47.47	2848	33.9	81.3	618
47.73	2864	34.1	82.1	618
48	2880	34.2	82.4	620
48.27	2896	34.2	83.2	618
48.53	2912	34.3	83.8	620
48.8	2928	34.4	84.5	620
49.07	2944	34.4	85.2	622
49.33	2960	34.5	85.6	620
49.6	2976	34.5	86.0	622
49.87	2992	34.7	86.2	618
50.13	3008	34.9	86.8	618
50.4	3024	35.0	87.4	618
50.67	3040	35.1	87.8	618
50.93	3056	35.1	87.5	620
51.2	3072	35.2	88.0	618
51.47	3088	35.3	88.2	618
51.73	3104	35.4	87.3	620
52	3120	35.6	87.6	618
52.27	3136	35.7	88.1	622
52.53	3152	35.8	88.2	620
52.8	3168	35.8	88.1	620
53.07	3184	35.9	88.0	620
53.33	3200	36.0	87.8	622
53.6	3216	36.0	88.0	618
53.87	3232	36.1	87.6	618
54.13	3248	36.3	87.3	620
54.4	3264	36.4	87.6	618
54.67	3280	36.5	87.2	618
54.93	3296	36.5	87.3	618
55.2	3312	36.7	87.8	620
55.47	3328	36.7	88.0	620
55.73	3344	36.9	88.2	620
56	3360	37.0	87.8	620
56.27	3376	37.2	87.5	624
56.53	3392	37.4	88.2	624
56.8	3408	37.6	88.1	622
57.07	3424	37.8	87.9	622
57.33	3440	37.8	87.5	620
57.6	3456	37.9	88.0	624
57.87	3472	37.9	87.8	624

58.13	3488	37.9	87.3	622
58.4	3504	38.0	87.2	620
58.67	3520	38.0	87.2	622
58.93	3536	38.1	87.8	618
59.2	3552	38.1	87.4	622
59.47	3568	38.1	88.2	618
59.73	3584	38.2	88.0	618
60	3600	38.3	88.0	618
60.27	3616	38.5	87.6	618
60.53	3632	38.6	87.8	620
60.8	3648	38.7	87.3	622
61.07	3664	38.8	87.3	624

S.D (CO_2) (ppm)	7.43

Appendix 54: High Concentration MH-Z19C Carbon Dioxide Sensor Test at High Temperature and High Humidity

High CO_2 High Humidity and Temperature			
Time (mins)	Temperature (˚C)	Humidity (%)	Carbon Dioxide (ppm)
0	21.9	49.7	1289
0.34	21.9	48.9	1283
0.68	21.9	48.6	1289
1.01	21.9	48.6	1284
1.35	22	48.5	1283
1.69	22	48.5	1283
2.03	22	48.5	1289
2.36	22.1	48.5	1282
2.7	22.1	48.4	1282
3.04	22.1	48.2	1285
3.38	22.2	48.2	1281
3.71	22.2	48	1286
4.05	22.2	47.9	1284
4.39	22.2	47.8	1282
4.73	22.3	47.8	1283
5.06	22.3	47.8	1282
5.4	22.3	47.7	1287
5.74	22.3	47.8	1288
6.08	22.3	47.9	1286
6.41	22.4	47.9	1285
6.75	22.5	48	1284
7.09	22.5	48.1	1288
7.43	22.5	48.2	1281
7.76	22.6	48.4	1282
8.1	22.6	48.6	1285
8.44	22.6	49.1	1281
8.78	22.6	51	1283
9.11	22.6	56.2	1282
9.45	22.6	57.3	1280
9.79	22.6	58.8	1284
10.13	22.6	59.6	1284
10.46	22.6	61.7	1287
10.8	22.7	61.9	1288
11.14	22.7	62.4	1285
11.48	22.7	64	1281
11.81	22.7	64.7	1280
12.15	22.7	65.1	1283
12.49	22.7	65.4	1282

12.83	22.7	66.6	1282
13.16	22.7	67.2	1288
13.5	22.7	67.7	1286
13.84	22.8	68	1286
14.18	22.7	68.1	1280
14.51	22.7	68.8	1282
14.85	22.8	69	1285
15.19	23.1	70	1284
15.53	23.4	70.4	1292
15.86	23.8	70.5	1289
16.2	24.1	70.3	1281
16.54	24.3	71.1	1296
16.88	24.6	71.4	1283
17.21	25	71.5	1272
17.55	25.3	71.6	1276
17.89	25.6	71.6	1295
18.23	25.9	71.8	1301
18.56	26.2	72.4	1291
18.9	26.5	71.2	1285
19.24	26.8	72	1298
19.58	27.1	72.2	1283
19.91	27.4	71.8	1297
20.25	27.7	71.7	1296
20.59	28.1	71.3	1311
20.93	28.4	71.5	1309
21.26	28.6	72	1307
21.6	29	72.1	1299
21.94	29.3	72.5	1311
22.28	29.7	73	1317
22.61	29.9	73.5	1313
22.95	30.2	72.9	1307
23.29	30.5	73.2	1314
23.63	30.7	73.2	1304
23.96	31.1	73.3	1302
24.3	31.3	73.7	1293
24.64	31.5	73.4	1323
24.98	31.8	73.7	1304
25.31	32.2	74	1325
25.65	32.5	73.8	1303
25.99	32.8	73.5	1303
26.33	33.1	73.1	1302
26.66	33.4	72.5	1330
27	33.7	72.4	1301
27.34	34.1	72.1	1319
27.68	34.4	71.9	1319

28.01	34.6	72.6	1329
28.35	35	72.6	1332
28.69	35.2	73.5	1330
29.03	35.6	74	1340
29.36	35.9	73.9	1326
29.6	36.2	74.3	1311
30.1	36.4	74.7	1310
30.7	36.7	75.1	1314
31.1	37.1	75.5	1318
31.5	37.3	75.9	1344
32.1	37.6	76.4	1342
32.8	37.9	76.9	1318
33.3	38.1	77.2	1326
33.8	38.5	77.5	1328
34.2	38.9	77.9	1332
34.8	39.2	78.3	1334
35.4	39.4	78.8	1335
35.7	39.7	79.3	1321
36.4	40	79.7	1339
36.8	40.4	80.1	1345
37.3	40.8	80.5	1350
37.6	41	80.8	1344
38.1	41.3	81.2	1349
38.4	41.5	81.5	1333
38.8	41.8	82	1343
39.5	42.1	82.4	1345
39.8	42.4	82.8	1349
40.3	42.7	83.3	1349
40.8	43	83.6	1343
41.5	43.3	84.1	1355
41.9	43.6	84.4	1342
42.2	43.9	84.8	1353
42.4	43.9	85.3	1364
42.7	44.1	85.6	1367
42.9	44	85.6	1340
43.2	43.8	85.6	1350
43.9	44.2	85.7	1351
44.4	44.5	85.7	1353
44.9	44.5	85.7	1356
45.4	44.3	85.7	1375
45.7	44.6	85.7	1378
46.4	44.2	85.8	1363
46.9	43.8	85.8	1359
47.5	44	85.8	1353
47.9	43.9	85.8	1346

48.1	44.5	85.9	1356
48.4	44.5	85.9	1343
48.6	44.4	85.9	1346
49.2	43.7	85.9	1348
49.9	44.3	86	1356
50.3	44	86	1347
51	43.7	86	1347
51.6	44	86.1	1349
52.2	44.5	86.1	1342
52.5	44.6	86.1	1342
53.1	44.4	86.1	1345
53.6	44.3	86.2	1349
54.2	44.1	86.2	1355
54.7	44.1	86.2	1355
55.2	44	86.2	1346
55.8	44	86.3	1355
56.5	44.3	86.3	1350
56.7	43.7	86.3	1353
57.2	43.8	86.3	1361
57.9	44.4	86.4	1349
58.5	44	86.4	1362
58.9	44.5	86.4	1359
59.3	44	86.4	1349
59.9	44.3	86.5	1347
60.4	44.4	86.5	1351
61	43.9	86.5	1363
61.6	44.4	86.5	1346
62.2	44	86.5	1362
62.8	44.1	86.6	1352

S.D (CO_2) (ppm)	29.86

Appendix 55: Low Dust Concentration Reference Test

Low Dust Concentration Reference Test					
Time (mins)	Time (s)	Temperature (˚C)	Humidity (%)	Carbon Dioxide (ppm)	Dust Density (µg/m³)
0.01	0.32857	23.6	52.1	256	39.04
0.44	26.3286	23.6	52.1	254	39.03
0.87	52.3286	23.5	52.1	250	38.59
1.31	78.3286	23.5	52.1	254	39.01
1.74	104.329	23.6	52.1	262	38.09
2.17	130.329	23.5	52.2	288	43.42
2.61	156.329	23.5	52.1	256	38.65
3.04	182.329	23.5	52.2	256	38.29
3.47	208.329	23.5	52.2	266	39.89
3.91	234.329	23.5	52.2	254	39.89
4.34	260.329	23.5	52.2	256	41.14
4.77	286.329	23.5	52.2	258	39.26
5.21	312.329	23.5	52.2	258	39.2
5.64	338.329	23.5	52.1	254	40.06
6.07	364.329	23.5	52.1	254	39.24
6.51	390.329	23.5	52.1	256	38.68
6.94	416.329	23.5	52.1	256	39.77
7.37	442.329	23.5	52.1	250	39.65
7.81	468.329	23.5	52	252	39.76
8.24	494.329	23.5	52	252	38.75
8.67	520.329	23.6	52	254	39.14
9.11	546.329	23.5	52	262	40.04
9.54	572.329	23.5	52	262	39.01
9.97	598.329	23.5	51.9	264	39.28

S.D	0.04	0.08	7.54

Appendix 56: Low Dust Concentration Practical Test

Low Dust Concentration Test					
Time (mins)	Time (s)	Temperature (˚C)	Humidity (%)	Carbon Dioxide (ppm)	Dust Density (µg/m³)
0.01	0	23.6	52.1	256	39.04
0.44	26	23.6	52.1	254	39.03
0.87	52	23.5	52.1	250	38.59
1.31	78	23.5	52.1	254	39.01
1.74	104	23.6	52.1	262	38.09
2.17	130	23.5	52.2	288	43.42
2.61	156	23.5	52.1	256	38.65
3.04	182	23.5	52.2	256	38.29
3.47	208	23.5	52.2	266	39.89
3.91	234	23.5	52.2	254	39.89
4.34	260	23.5	52.2	256	41.14
4.77	286	23.5	52.2	258	39.26
5.21	312	23.5	52.2	258	39.2
5.64	338	23.5	52.1	254	40.06
6.07	364	23.5	52.1	254	39.24
6.51	390	23.5	52.1	256	38.68
6.94	416	23.5	52.1	256	39.77
7.37	442	23.5	52.1	250	39.65
7.81	468	23.5	52	252	39.76
8.24	494	23.5	52	252	38.75
8.67	520	23.6	52	254	39.14
9.11	546	23.5	52	262	40.04
9.54	572	23.5	52	262	39.01
9.97	598	23.5	51.9	264	39.28
10.41	624	23.6	51.9	262	240.46
10.84	650	23.6	51.9	250	390.98
11.27	676	23.6	51.9	246	325.68
11.71	702	23.6	51.9	246	295.19
12.14	728	23.6	51.8	252	277.24
12.57	754	23.6	51.8	262	223.11
13.01	780	23.6	51.7	248	238.02
13.44	806	23.6	51.7	242	199.84
13.87	832	23.6	51.7	248	183.18
14.31	858	23.6	51.7	254	182.81
14.74	884	23.6	51.7	252	122.29
15.17	910	23.6	51.7	264	139.83
15.61	936	23.6	51.6	248	103.86
16.04	962	23.6	51.6	264	128.13
16.47	988	23.6	51.6	256	135.28

16.91	1014	23.6	51.6	254	112.95
17.34	1040	23.6	51.5	258	96.61
17.77	1066	23.7	51.5	260	110.53
18.21	1092	23.7	51.5	262	99.72
18.64	1118	23.7	51.5	250	136.3
19.07	1144	23.7	51.5	250	125.69
19.51	1170	23.7	51.4	256	98.15
19.94	1196	23.8	51.4	254	86.45
20.37	1222	23.8	51.4	250	76.6
20.81	1248	23.8	51.3	256	74.77
21.24	1274	23.8	51.3	260	64.68
21.67	1300	23.8	51.3	258	76.06
22.11	1326	23.8	51.2	254	77.46
22.54	1352	23.8	51.2	256	75.54
22.97	1378	23.8	51.2	256	75.28
23.41	1404	23.8	51.2	252	87.22
23.84	1430	23.8	51.1	252	62.76
24.27	1456	23.8	51.1	250	58.56
24.71	1482	23.9	51.1	250	70.98
25.14	1508	23.9	51.1	250	67.28
25.57	1534	23.9	51	256	83.46
26.01	1560	23.9	51.1	258	92.32
26.44	1586	23.8	51.1	250	68.25
26.87	1612	23.7	51.1	248	56.86
27.31	1638	23.7	51.1	254	77.23
27.74	1664	23.7	51.2	250	58.75
28.17	1690	23.7	51.2	254	69.63
28.61	1716	23.6	51.2	252	70.51
29.04	1742	23.5	51.2	252	71.71
29.47	1768	23.5	51.2	250	60.97
29.91	1794	23.4	51.1	254	60.98

S.D	0.13	0.4	6.33

Appendix 57: High Dust Concentration Reference Test

High Dust Concentration Reference Test					
Time (mins)	Time (s)	Temperature (˚C)	Humidity (%)	Carbon Dioxide (ppm)	Dust Density (µg/m³)
0.27	0	19.5	54.1	262	42.11
0.53	26	19.5	54.1	262	51.51
0.8	52	19.5	54	256	42.65
1.07	78	19.5	54	258	43.96
1.33	104	19.5	53.9	258	47.92
1.6	130	19.5	53.9	258	43.79
1.87	156	19.5	53.8	260	47.42
2.13	182	19.5	53.7	270	43.7
2.4	208	19.5	53.7	268	41.86
2.67	234	19.5	53.7	256	42.04
2.93	260	19.5	53.6	272	43.18
4.77	286	19.5	53.7	262	44.27
5.20	312	19.5	53.8	266	44.65
5.63	338	19.5	53.7	269	46.76
6.07	364	19.5	53.7	258	45.91
6.50	390	19.5	53.7	263	47.22
6.93	416	19.5	53.7	267	46.73
7.37	442	19.5	53.8	261	47.61
7.80	468	19.5	53.8	261	45.94
8.23	494	19.5	53.7	262	47.20
8.67	520	19.5	53.7	261	47.71
9.10	546	19.5	53.7	267	47.55
9.53	572	19.5	53.7	268	44.63
9.97	598	19.5	53.6	261	46.01
10.40	624	19.5	53.6	266	45.34
10.83	650	19.5	53.8	260	45.82
11.27	676	19.5	53.7	265	44.49
11.70	702	19.5	53.8	263	46.71
12.13	728	19.6	53.6	260	47.35
12.57	754	19.6	53.6	265	47.94
13.00	780	19.6	53.6	259	46.95
13.43	806	19.6	53.8	268	46.10
13.87	832	19.6	53.7	270	46.31
14.30	858	19.6	53.7	266	47.46
14.73	884	19.6	53.6	270	47.23
15.17	910	19.6	53.7	264	44.51
15.60	936	19.6	53.7	269	44.96
16.03	962	19.6	53.6	262	46.72
16.47	988	19.6	53.6	261	46.32

16.90	1014	19.6	53.8	269	47.02
17.33	1040	19.6	53.7	262	44.90
17.77	1066	19.6	53.7	258	46.21

S.D	0.04	0.13	4.18

Appendix 58: High Dust Concentration Practical Test

High Dust Concentration Test					
Time (mins)	Time (s)	Temperature (˚C)	Humidity (%)	Carbon Dioxide (ppm)	Dust Density (µg/m³)
0.27	0	19.5	54.1	262	42.11
0.53	26	19.5	54.1	262	51.51
0.8	52	19.5	54	256	42.65
1.07	78	19.5	54	258	43.96
1.33	104	19.5	53.9	258	47.92
1.6	130	19.5	53.9	258	43.79
1.87	156	19.5	53.8	260	47.42
2.13	182	19.5	53.7	270	43.7
2.4	208	19.5	53.7	268	41.86
2.67	234	19.5	53.7	256	42.04
2.93	260	19.5	53.6	272	43.18
4.77	286	19.5	53.7	262	44.27
5.2	312	19.5	53.8	266	44.65
5.63	338	19.5	53.7	269	46.76
6.07	364	19.5	53.7	258	45.91
6.5	390	19.5	53.7	263	47.22
6.93	416	19.5	53.7	267	46.73
7.37	442	19.5	53.8	261	47.61
7.8	468	19.5	53.8	261	45.94
8.23	494	19.5	53.7	262	47.2
8.67	520	19.5	53.7	261	47.71
9.1	546	19.5	53.7	267	47.55
9.53	572	19.5	53.7	268	44.63
9.97	598	19.5	53.6	261	46.01
10.4	624	19.5	53.6	266	45.34
10.83	650	19.5	53.8	260	45.82
11.27	676	19.5	53.7	265	44.49
11.7	702	19.5	53.8	263	46.71
12.13	728	19.6	53.6	260	47.35
12.57	754	19.6	53.6	265	47.94
13	780	19.6	53.6	259	46.95
13.43	806	19.6	53.8	268	46.1
13.87	832	19.6	53.7	270	46.31
14.3	858	19.6	53.7	266	47.46
14.73	884	19.6	53.60	270	47.23
15.17	910	19.6	53.70	264	44.51
15.6	936	19.6	53.70	269	44.96
16.03	962	19.6	53.60	262	46.72
16.47	988	19.6	53.60	261	46.32

16.9	1014	19.6	53.80	269	47.02
17.33	1040	19.6	53.70	262	44.9
17.77	1066	19.6	53.70	258	46.21
18.2	1092	19.6	53.60	260	593.12
18.63	1118	20.1	53.04	255	593.35
19.07	1144	20.2	54.07	257	593.51
19.5	1170	20.0	53.92	274	593.49
19.93	1196	20.1	52.75	249	542.08
20.37	1222	20.6	52.08	281	478.42
20.8	1248	20.5	53.39	258	431.92
21.23	1274	20.5	52.99	260	392.74
21.67	1300	20.5	52.59	280	326.15
22.1	1326	20.9	52.36	274	246.49
22.53	1352	21.0	51.81	280	238.66
22.97	1378	21.0	52.06	249	253.17
23.4	1404	21.0	52.63	261	178.03
23.83	1430	21.2	51.39	280	188.11
24.27	1456	21.5	52.21	252	191.63
24.7	1482	21.6	52.16	275	232.25
25.13	1508	21.7	50.74	263	163.13
25.57	1534	21.5	51.22	272	160.52
26	1560	21.9	50.89	253	189.69
26.43	1586	21.6	52.02	270	181.14
26.87	1612	21.9	50.69	267	174.05
27.3	1638	22.1	51.77	261	198.33
27.73	1664	21.9	50.84	280	159.1
28.17	1690	22.1	50.97	251	259.41
28.6	1716	22.5	50.81	257	114.33
29.03	1742	22.4	50.10	254	125.13
29.47	1768	22.3	51.05	263	164.24
29.9	1794	22.5	49.92	268	72.29
30.33	1820	22.5	51.73	255	75.97
30.77	1846	22.3	50.70	278	43.34
31.2	1872	22.6	50.60	262	45.21

S.D	1.07	1.18	7.46

Appendix 59: Continuous Dust Concentration Practical Test

Continuous Experiment Sensor Readings				
Time (mins)	Time (s)	Temperature (˚C)	Humidity (%)	Carbon Dioxide (ppm)
0	0	25.9	49.1	222
0.33	19.8	26	49	214
0.66	39.6	26	49	216
0.99	59.4	26	49	216
1.32	79.2	26	48.9	218
1.65	99	26	48.9	208
1.98	118.8	26	48.9	216
2.31	138.6	26	48.8	224
2.64	158.4	26	48.8	222
2.97	178.2	26.1	48.8	210
3.3	198	26.1	48.8	208
3.63	217.8	26.1	48.7	214
3.96	237.6	26.1	48.7	214
4.29	257.4	26.1	48.7	228
4.62	277.2	26.1	48.7	216
4.95	297	26.1	48.7	218
5.28	316.8	26.1	48.6	220
5.61	336.6	26.2	48.6	212
5.94	356.4	26.2	48.6	210
6.27	376.2	26.2	48.5	224
6.6	396	26.2	48.5	224
6.93	415.8	26.2	48.5	216
7.26	435.6	26.2	48.5	214
7.59	455.4	26.2	48.5	214
7.92	475.2	26.2	48.5	212
8.25	495	26.3	48.5	210
8.58	514.8	26.2	48.4	216
8.91	534.6	26.3	48.4	216
9.24	554.4	26.3	48.4	214
9.57	574.2	26.4	48.4	216
9.9	594	26.4	48.4	214
10.23	613.8	26.4	48.3	224
10.56	633.6	26.4	48.3	230
10.89	653.4	26	49	186
11.22	673.2	25.8	49.6	168
11.55	693	25.6	49.6	168
11.88	712.8	25.5	49.8	184
12.21	732.6	25.4	50	190
12.54	752.4	25.3	50.1	192

12.87	772.2	25.3	50.1	178
13.2	792	25	50.5	176
13.53	811.8	24.8	50.7	180
13.86	831.6	24.5	51.2	192
14.19	851.4	24.4	51.5	184
14.52	871.2	24	51.9	174
14.85	891	24	52.1	180
15.18	910.8	23.9	52.2	176
15.51	930.6	23.8	52.3	186
15.84	950.4	23.6	52.5	194
16.17	970.2	23.6	52.6	204
16.5	990	23.4	53.1	198
16.83	1009.8	23.3	53.2	200
17.16	1029.6	23.2	53.4	198
17.49	1049.4	23.1	53.5	190
17.82	1069.2	22.9	53.9	186
18.15	1089	22.8	54	188
18.48	1108.8	22.6	54.4	186
18.81	1128.6	22.6	54.5	186
19.14	1148.4	22.5	54.7	182
19.47	1168.2	22.4	54.9	180
19.8	1188	22.2	55.2	186
20.13	1207.8	22.2	55.2	186
20.46	1227.6	22.2	55.4	190
20.79	1247.4	22.1	55.4	186
21.12	1267.2	22	55.7	192
21.45	1287	21.9	55.9	192
21.78	1306.8	21.9	55.9	190
22.11	1326.6	21.8	56.1	192
22.44	1346.4	21.8	56.2	186
22.77	1366.2	21.7	56.5	200
23.1	1386	21.7	56.5	198
23.43	1405.8	21.6	56.5	194
23.76	1425.6	21.6	56.6	188
24.09	1445.4	21.5	56.7	184
24.42	1465.2	21.5	56.8	194
24.75	1485	21.5	56.8	188
25.08	1504.8	21.5	57.3	186
25.41	1524.6	21.5	57.3	188
25.74	1544.4	21.4	58.1	200
26.07	1564.2	21.4	58.1	258
26.4	1584	21.4	57.9	238
26.73	1603.8	21.4	57.7	226
27.06	1623.6	21.4	57.8	228
27.39	1643.4	21.4	57.8	196

27.72	1663.2	21.5	58.3	192
28.05	1683	21.4	58.6	182
28.38	1702.8	21.5	58.9	192
28.71	1722.6	21.5	58.7	196
29.04	1742.4	21.5	58.7	194
29.37	1762.2	21.5	58.7	198
29.7	1782	21.5	58.6	192
30.03	1801.8	21.5	58.6	194
30.36	1821.6	21.5	58.5	196
30.69	1841.4	21.5	58.5	186
31.02	1861.2	21.5	58.4	184
31.35	1881	21.5	58.4	190
31.68	1900.8	21.5	58.4	192
32.01	1920.6	21.5	58.4	180
32.34	1940.4	21.5	58.3	180
32.67	1960.2	21.5	58.3	190

Appendix 60: Continuous Practical Test Dust Concentration

Continuous Experiment Dust Concentration		
Time (mins)	Time (s)	Dust Density (µg/m³)
0	0	41.99
0.07	4	43.08
0.13	8	43.71
0.20	12	42.94
0.27	16	42.5
0.33	20	42.88
0.40	24	44.03
0.47	28	42.44
0.53	32	43.61
0.60	36	43.03
0.67	40	42.87
0.73	44	42.04
0.80	48	43.13
0.87	52	43.57
0.93	56	43.26
1.00	60	43.61
1.07	64	42.62
1.13	68	42.94
1.20	72	42.47
1.27	76	43.45
1.33	80	43.31
1.40	84	43.01
1.47	88	43.89
1.53	92	42.58
1.60	96	43.11
1.67	100	42.94
1.73	104	43.65
1.80	108	42.06
1.87	112	43.48
1.93	116	42.97
2.00	120	43.88
2.07	124	42.68
2.13	128	42.76
2.20	132	43.33
2.27	136	43.66
2.33	140	43.59
2.40	144	43.46
2.47	148	42.57
2.53	152	43.21

2.60	156	42.46
2.67	160	43.67
2.73	164	42.88
2.80	168	42.77
2.87	172	43.17
2.93	176	43.38
3.00	180	42.99
3.07	184	43.21
3.13	188	43.08
3.20	192	42.13
3.27	196	41.78
3.33	200	43.49
3.40	204	42.74
3.47	208	43.22
3.53	212	42.71
3.60	216	43.14
3.67	220	42.92
3.73	224	44.01
3.80	228	43.9
3.87	232	42.92
3.93	236	43.63
4.00	240	43.99
4.07	244	44.28
4.13	248	43.27
4.20	252	42.53
4.27	256	42.43
4.33	260	43.04
4.40	264	44.1
4.47	268	42.03
4.53	272	42.67
4.60	276	43.49
4.67	280	44.41
4.73	284	42.46
4.80	288	43.57
4.87	292	42.66
4.93	296	42.08
5.00	300	43.79
5.07	304	42.99
5.13	308	43.34
5.20	312	44.17
5.27	316	42.37
5.33	320	42.5
5.40	324	44.25
5.47	328	43.25
5.53	332	43.1

5.60	336	43.19
5.67	340	42.78
5.73	344	42.71
5.80	348	43.3
5.87	352	43.01
5.93	356	43.36
6.00	360	43.45
6.07	364	42.43
6.13	368	42.79
6.20	372	42.81
6.27	376	43.09
6.33	380	42.99
6.40	384	43
6.47	388	42.97
6.53	392	42.24
6.60	396	44.23
6.67	400	43.11
6.73	404	42.38
6.80	408	43.12
6.87	412	43.1
6.93	416	42.92
7.00	420	42.96
7.07	424	43.59
7.13	428	42.29
7.20	432	43.72
7.27	436	42.75
7.33	440	43.09
7.40	444	44.14
7.47	448	42.94
7.53	452	43.43
7.60	456	42.36
7.67	460	42.73
7.73	464	42.65
7.80	468	44.29
7.87	472	43.7
7.93	476	42.94
8.00	480	43.38
8.07	484	43.88
8.13	488	43.07
8.20	492	42.73
8.27	496	42.38
8.33	500	43.27
8.40	504	51.66
8.47	508	217.32
8.53	512	590.44

8.60	516	590.91
8.67	520	590.96
8.73	524	590.91
8.80	528	590.9
8.87	532	591.03
8.93	536	589.9
9.00	540	590.94
9.07	544	590.98
9.13	548	590.89
9.20	552	590.9
9.27	556	590.76
9.33	560	590.84
9.40	564	555.64
9.47	568	390.93
9.53	572	280.98
9.60	576	210.78
9.67	580	176.25
9.73	584	167.07
9.80	588	172.67
9.87	592	187.04
9.93	596	305.34
10.00	600	577.29
10.07	604	438.65
10.13	608	355.72
10.20	612	274.72
10.27	616	298.89
10.33	620	357.67
10.40	624	317.42
10.47	628	244.4
10.53	632	68.81
10.60	636	94.07
10.67	640	53.74
10.73	644	46.82
10.80	648	46.7
10.87	652	47.88
10.93	656	49.21
11.00	660	55.3
11.07	664	58.43
11.13	668	62.77
11.20	672	68.46
11.27	676	67.98
11.33	680	63.72
11.40	684	59.59
11.47	688	58.3
11.53	692	54.96

11.60	696	53.67
11.67	700	51.29
11.73	704	51.09
11.80	708	60.51
11.87	712	51.14
11.93	716	54.8
12.00	720	69.37
12.07	724	48.27
12.13	728	49.49
12.20	732	51.14
12.27	736	61.12
12.33	740	57.91
12.40	744	58.22
12.47	748	84.01
12.53	752	107.95
12.60	756	70.74
12.67	760	72.73
12.73	764	71.22
12.80	768	68.32
12.87	772	66.75
12.93	776	59.22
13.00	780	57.04
13.07	784	58.87
13.13	788	53.24
13.20	792	54.34
13.27	796	52.27
13.33	800	56.04
13.40	804	59.13
13.47	808	66.22
13.53	812	54.82
13.60	816	56.88
13.67	820	70.03
13.73	824	60.5
13.80	828	59.61
13.87	832	61.83
13.93	836	61.09
14.00	840	60.76
14.07	844	60.35
14.13	848	59.45
14.20	852	55.97
14.27	856	53.73
14.33	860	59.7
14.40	864	71.7
14.47	868	52.5
14.53	872	53.87

14.60	876	53.13
14.67	880	51.87
14.73	884	54.4
14.80	888	54.08
14.87	892	53.03
14.93	896	54.05
15.00	900	54.54
15.07	904	56.55
15.13	908	56.75
15.20	912	58.6
15.27	916	56.47
15.33	920	54.57
15.40	924	52.19
15.47	928	51.29
15.53	932	51.49
15.60	936	51.98
15.67	940	52.23
15.73	944	50.35
15.80	948	49.95
15.87	952	50.3
15.93	956	52.85
16.00	960	51.55
16.07	964	52.98
16.13	968	53.76
16.20	972	50.92
16.27	976	53.4
16.33	980	55.66
16.40	984	54.59
16.47	988	56.87
16.53	992	55.5
16.60	996	52.84
16.67	1000	58.98
16.73	1004	50.28
16.80	1008	50.32
16.87	1012	51.25
16.93	1016	48.43
17.00	1020	55.29
17.07	1024	66.79
17.13	1028	49.96
17.20	1032	48.27
17.27	1036	49.41
17.33	1040	48.35
17.40	1044	48.9
17.47	1048	49.63
17.53	1052	51.24

17.60	1056	52.35
17.67	1060	54.72
17.73	1064	56.61
17.80	1068	56.26
17.87	1072	55.81
17.93	1076	53.84
18.00	1080	50.78
18.07	1084	50.22
18.13	1088	50.62
18.20	1092	49.13
18.27	1096	48.95
18.33	1100	47.98
18.40	1104	47.67
18.47	1108	70.46
18.53	1112	74.47
18.60	1116	48.34
18.67	1120	47.91
18.73	1124	48.93
18.80	1128	49.14
18.87	1132	48.7
18.93	1136	54.28
19.00	1140	51.84
19.07	1144	53.7
19.13	1148	54.47
19.20	1152	54.7
19.27	1156	55.47
19.33	1160	54.01
19.40	1164	49.72
19.47	1168	48.12
19.53	1172	48.19
19.60	1176	47.2
19.67	1180	48.85
19.73	1184	51.32
19.80	1188	56.71
19.87	1192	54.58
19.93	1196	52.93
20.00	1200	49.08
20.07	1204	49.17
20.13	1208	49.41
20.20	1212	47.87
20.27	1216	47.21
20.33	1220	46.9
20.40	1224	47.42
20.47	1228	47.05
20.53	1232	49.29

20.60	1236	63.53
20.67	1240	56.34
20.73	1244	55.86
20.80	1248	63.42
20.87	1252	53.39
20.93	1256	52.3
21.00	1260	48.35
21.07	1264	48
21.13	1268	46.56
21.20	1272	46.42
21.27	1276	47.46
21.33	1280	46.28
21.40	1284	47.71
21.47	1288	47.41
21.53	1292	48.6
21.60	1296	48.21
21.67	1300	48.7
21.73	1304	48.24
21.80	1308	49.09
21.87	1312	49.17
21.93	1316	47.99
22.00	1320	47.61
22.07	1324	47.4
22.13	1328	49.12
22.20	1332	46.98
22.27	1336	46.96
22.33	1340	47.36
22.40	1344	47.85
22.47	1348	48.35
22.53	1352	48.08
22.60	1356	47.88
22.67	1360	48.07
22.73	1364	48.54
22.80	1368	46.88
22.87	1372	46.89
22.93	1376	47.61
23.00	1380	47.52
23.07	1384	48.2
23.13	1388	49.52
23.20	1392	48.57
23.27	1396	47.48
23.33	1400	48.67
23.40	1404	48.92
23.47	1408	48.92
23.53	1412	49.79

23.60	1416	50.1
23.67	1420	50.19
23.73	1424	48.09
23.80	1428	48.26
23.87	1432	49.65
23.93	1436	48.91
24.00	1440	48.7
24.07	1444	102.01
24.13	1448	125.33
24.20	1452	58.37
24.27	1456	80.62
24.33	1460	195.13
24.40	1464	47.33
24.47	1468	166.75
24.53	1472	89.04
24.60	1476	96.37
24.67	1480	72.66
24.73	1484	47.83
24.80	1488	46.96
24.87	1492	47.27
24.93	1496	222.71
25.00	1500	590.76
25.07	1504	590.85
25.13	1508	590.84
25.20	1512	590.88
25.27	1516	590.69
25.33	1520	590.6
25.40	1524	590.86
25.47	1528	590.85
25.53	1532	576.89
25.60	1536	587.4
25.67	1540	548.83
25.73	1544	580.37
25.80	1548	479.71
25.87	1552	387.4
25.93	1556	348.63
26.00	1560	312.61
26.07	1564	386.79
26.13	1568	333.33
26.20	1572	565.51
26.27	1576	439.27
26.33	1580	411.17
26.40	1584	527.49
26.47	1588	329.2
26.53	1592	292.91

26.60	1596	343.1
26.67	1600	295.7
26.73	1604	265.44
26.80	1608	221.11
26.87	1612	541.46
26.93	1616	504.75
27.00	1620	372.67
27.07	1624	211.48
27.13	1628	120.96
27.20	1632	129.09
27.27	1636	95.16
27.33	1640	112.95
27.40	1644	109.92
27.47	1648	73.69
27.53	1652	135.79
27.60	1656	115.15
27.67	1660	222.1
27.73	1664	148.19
27.80	1668	100.73
27.87	1672	70.27
27.93	1676	123.8
28.00	1680	98.02
28.07	1684	101.83
28.13	1688	76.25
28.20	1692	68.39
28.27	1696	68.95
28.33	1700	69.39
28.40	1704	75.35
28.47	1708	81.8
28.53	1712	76.99
28.60	1716	80.82
28.67	1720	74.77
28.73	1724	85.4
28.80	1728	71.55
28.87	1732	67.78
28.93	1736	63.72
29.00	1740	68.03
29.07	1744	123.48
29.13	1748	70.37
29.20	1752	64.98
29.27	1756	69.65
29.33	1760	72.35
29.40	1764	79.08
29.47	1768	79.72
29.53	1772	76.65

29.60	1776	72.4
29.67	1780	69.79
29.73	1784	65.74
29.80	1788	62.69
29.87	1792	61.75
29.93	1796	60.67
30.00	1800	59.31
30.07	1804	59.00
30.13	1808	57.83
30.20	1812	55.60
30.27	1816	55.49
30.33	1820	54.28
30.40	1824	53.57
30.47	1828	51.18
30.53	1832	49.65
30.60	1836	48.63
30.67	1840	47.19
30.73	1844	46.69
30.80	1848	45.79
30.87	1852	44.71
30.93	1856	42.90
31.00	1860	42.21
31.07	1864	41.64
31.13	1868	42.18
31.20	1872	42.16
31.27	1876	42.72
31.33	1880	43.14
31.40	1884	44.40
31.47	1888	44.33
31.53	1892	43.32
31.60	1896	42.20
31.67	1900	42.33
31.73	1904	43.84
31.80	1908	42.56
31.87	1912	43.44
31.93	1916	44.05
32.00	1920	43.76
32.07	1924	43.37
32.13	1928	42.98
32.20	1932	42.08
32.27	1936	42.54
32.33	1940	42.84
32.40	1944	43.67
32.47	1948	44.37
32.53	1952	44.27

32.60	1956	42.86
32.67	1960	44.17
32.73	1964	43.26

Appendix 61: Heart Rate Sensor Header File Code

```
#include <MsTimer2.h>

typedef void (*HEARTCBFUNC)(uint8_t rawData, int value);

class HeartRate {
  uint8_t pin;
  uint8_t rawData;
  HEARTCBFUNC cb;
  int sampleNum;
  const int sampleSize = 4;
  int sample[4];
  int sum_high;
  int num_sum_high;
  int sum_low;
  int num_sum_low;
  bool average_switch;
  bool high;
  bool low;
  int Count;
  int heartRateNum;
  int go1, go2, go3, go4;
  int heartRate[20];
  int sum;
  float heart;
  float Angle;
  float Q_bias;
  float Pdot[4];
  float PP[2][2];
  float Q_angle;
  float Q_gyro;
  float R_angle;
  float dt;
  float C_0;
  float Angle_err;
  float PCt_0, PCt_1;
  float E;
  float K_0, K_1;
  float t_0, t_1;

public:
  HeartRate(uint8_t _pin, uint8_t _rawData);
  void setCB(HEARTCBFUNC cb_);
  void begin();
  void recv();

private:
  void goInit();
```

```
  float kalmanUpdate(float Accel, float Gyro);
  int calculateSpeed();
};

HeartRate::HeartRate(uint8_t _pin, uint8_t _rawData)
  : pin(_pin), rawData(_rawData) {
  sampleNum = 0;
  sum_high = 0;
  num_sum_high = 0;
  sum_low = 0;
  num_sum_low = 0;
  average_switch = false;
  high = true;
  low = false;
  Count = 0;
  heartRateNum = 0;
  go1 = go2 = go3 = go4 = 0;
  sum = 0;
  heart = 0.0;
  Angle = 0.0;
  Q_bias = 0.0;
  Q_angle = 0.001;
  Q_gyro = 0.003;
  R_angle = 0.03;
  dt = 0.005;
  C_0 = 1.0;
  Angle_err = 0.0;
  PCt_0 = PCt_1 = 0.0;
  E = 0.0;
  K_0 = K_1 = 0.0;
  t_0 = t_1 = 0.0;
}

void HeartRate::setCB(HEARTCBFUNC cb_) {
  cb = cb_;
}

void HeartRate::begin() {
  MsTimer2::set(5,  recv);
  MsTimer2::start();
}

void HeartRate::recv() {
  int value;
  int data = analogRead(pin);
  if (rawData == 1) {
    Serial.println(data);
    cb(rawData, data);
```

Appendix 62: Health Monitoring System Main Code

```
#include <DHT.h>  // by Adrafruit (2023)
#include "HeartSpeed.h" // by [jianghao](hao.jiang@dfrobot.com)
#include "MHZ19.h" // by malokhvii-eduard (2023)

#define DHTPIN 2          // Digital pin connected to the DHT sensor
#define DHTTYPE DHT22     // DHT sensor type
#define MQ2pin 0
//#define WIFI_SSID "[redacted]"    // Wi-Fi name (SSID)
//#define WIFI_PASS "[redacted]"     // Wi-Fi password
#define WIFI_SSID "[redacted]"    // Wi-Fi name (SSID)
#define WIFI_PASS "[redacted]"     // Wi-Fi password
#define API "[redacted]"       // ThingSpeak API key
#define HOST "api.thingspeak.com"
#define PORT 80

// Co2 sensor
const int pwmpin = 6;
float MQ2Value;  //variable to store sensor value


DHT dht(DHTPIN, DHTTYPE);      // Create a DHT object
HeartSpeed heartspeed(A1);    // Create a HeartSpeed object
MHZ19 *mhz19_pwm = new MHZ19(pwmpin); // Create MHZ19 object

void setup() {
  Serial.begin(9600);
  Serial1.begin(115200);
  dht.begin();
  // Begin heartspeed calculation function
  heartspeed.setCB(mycb);
  heartspeed.begin();
pinMode(buzzer, OUTPUT); // Set buzzer pin as output


  Serial.print("MH-Z19/MQ2 now warming up...  ");
 delay(3000); // Wait 3 mins for MHZ19 to warm up
  // Connect to Wifi using AT commands
  sendCommand("AT", 5, "OK");
  sendCommand("AT+CWMODE=1", 5, "OK");
  sendCommand("AT+CWJAP=\"" + String(WIFI_SSID) + "\",\"" + String(WIFI_PASS)
+ "\"", 20, "OK");
}

void loop() {
  float tem = dht.readTemperature();
  float hum = dht.readHumidity();
```

```
  // Perform heart rate calculations using the HeartSpeed library
  int heartRate = heartspeed.calculateSpeed();
  int co2ppm = mhz19_pwm->getPpmPwm();
  MQ2Value = analogRead(MQ2pin);
   Serial.print("co2: ");
    Serial.println(co2ppm);

  }
  String getData = "GET /update?api_key=" + String(API) +
                "&field1=" + String(tem) +
                "&field2=" + String(hum) +
                "&field3=" + String(heartRate) +
                "&field4=" + String(co2ppm) +
                "&field5=" + String(MQ2Value) +
                " HTTP/1.1\r\n" +
                "Host: " + String(HOST) + "\r\n\r\n";
// Sending data to Thinspeak
  sendCommand("AT+CIPMUX=0", 5, "OK");
  sendCommand("AT+CIPSTART=\"TCP\",\"" + String(HOST) + "\"," + String(PORT),
15, "OK");
  sendCommand("AT+CIPSEND=" + String(getData.length()), 4, ">");

  Serial1.println(getData);
  delay(2000);
  sendCommand("AT+CIPCLOSE", 5, "OK");

}

void sendCommand(String command, int maxTime, char readReplay[]) {
  Serial.print(command);
  Serial1.println(command);
// Update status to serial monitor for debugging
  unsigned long timeout = millis();
  while (millis() - timeout < maxTime * 1000UL) {
    if (Serial1.find(readReplay)) {
      Serial.println(" - OK");
      return;
    }
  }

  Serial.println(" - Fail");
}

void mycb(uint8_t rawData, int value) {
  if (rawData) {
    Serial.println(value);
  } else {
   // Serial.print("HeartRate Value = ");
```

```
   // Serial.println(value);
  }
}
```